UFP ZS 2024

SV UFP 2024 XA 3C

UFP 2024 3C dokoncenie 09. 12.

# Ionization

**The Townsend (symbol Td) is a physical unit of the reduced electric field (ratio E/N), where E is electric field and N is concentration of neutral particles.**
**It is named after John Sealy Townsend, who conducted early research into gas ionization.**

# Energy levels He

## Grotrian diagram He
## Ionization energy He

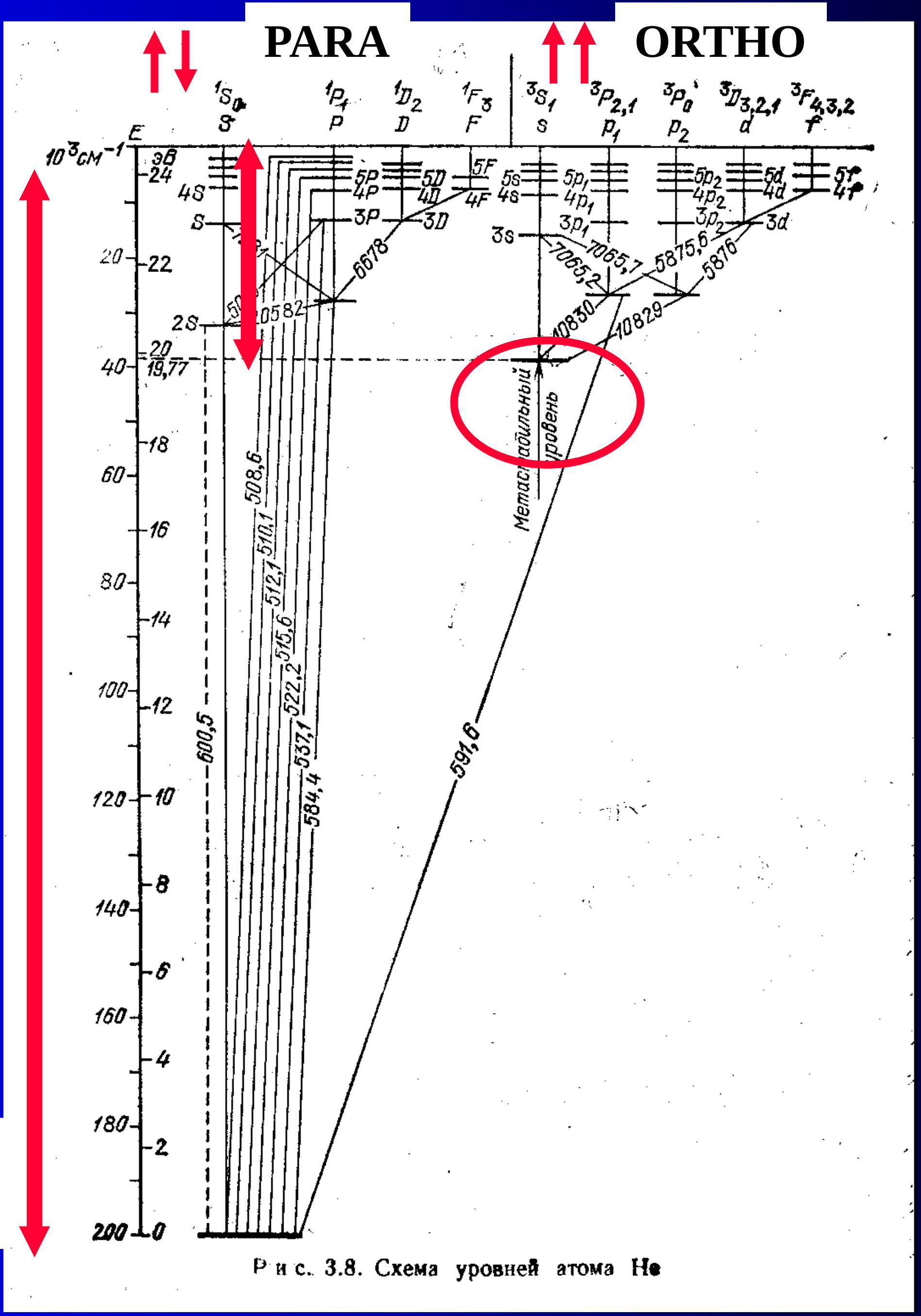


24.46eV → ~198400 cm$^{-1}$ → ~50nm
vacuum ultraviolet

**Ionization cross section**

# Ionization by electron impact

## Atoms

$$Ar + e^-(\varepsilon_0) \rightarrow Ar^+ + e_1^-(\varepsilon_1) + e_2^-(\varepsilon_2)$$

## Molecules

$$N_2(\nu,j) + e^-(\varepsilon_0) \rightarrow N_2^+(\nu,j) + e_1^-(\varepsilon_1) + e_2^-(\varepsilon_2)$$

$$\rightarrow N^+(\varepsilon_{KIN}) + N(\varepsilon_{KIN}) + e_1^-(\varepsilon_3) + e_2^-(\varepsilon_4)$$

$NH_3 + e^-(\varepsilon_0) \rightarrow$ …..to many channels

# Ionization energies

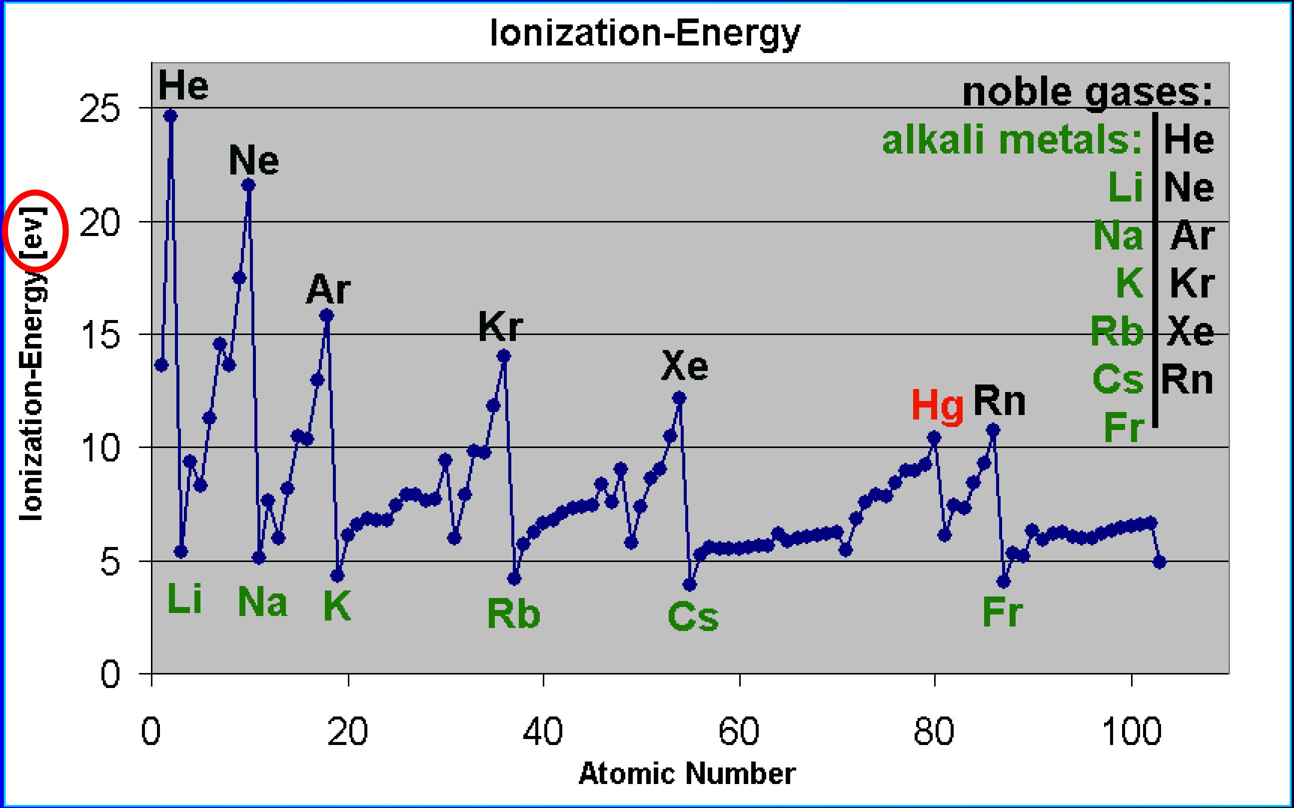


$$Ar + e^-(\varepsilon_0) \rightarrow Ar^+ + e_1^-(\varepsilon_1) + e_2^-(\varepsilon_2)$$

$$N_2 + e^-(\varepsilon_0) \rightarrow \text{ion} \ldots$$

# Ionization energies

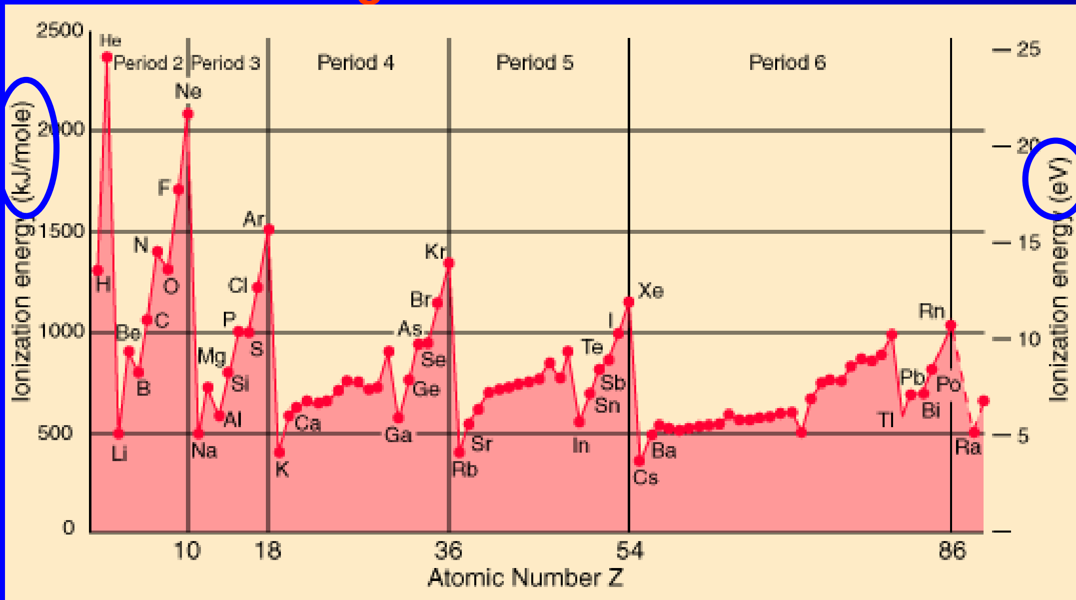


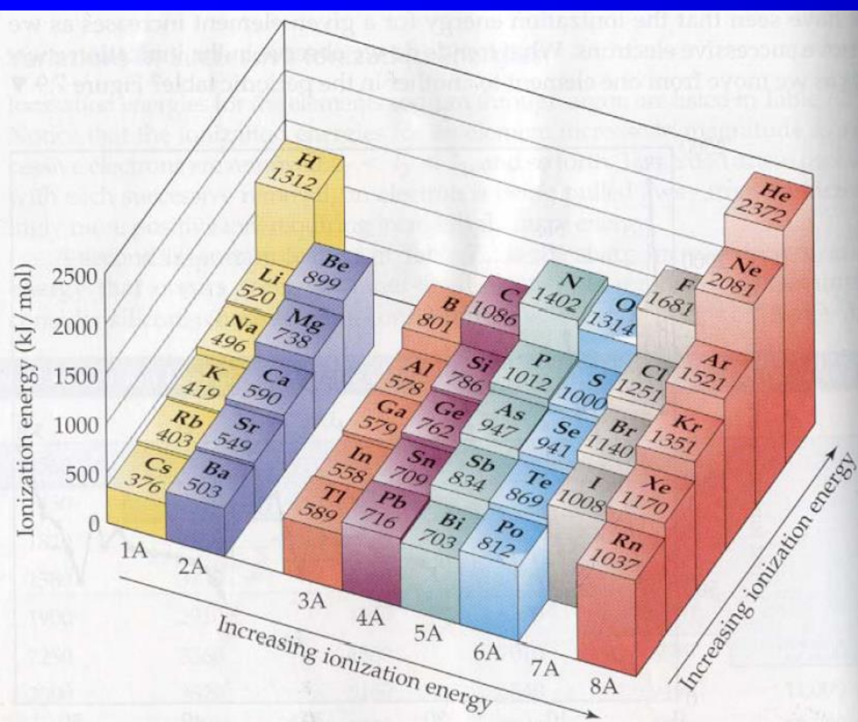


## Ionization Energy

- **First ionization energy ($IE_1$)**

The minimum amount of energy required to remove the most loosely bound electron from an isolated gaseous atom to form a 1+ ion.

$$\text{atom}_{(g)} + \text{energy} \rightarrow \text{ion}^{+}_{(g)} + e^{-}$$

| Element/Compound | Ionization Potential (Volts or eV) |
|---|---|
| He | 24.6 |
| Ar | 15.8 |
| $H_2$ | 15.4 |
| $N_2$ | 15.6 |
| $O_2$ | 12.1 |
| $CO_2$ | 13.8 |
| CO | 14.1 |
| C | 11.3 |
| Si | 8.2 |
| Fe | 7.9 |
| Ni | 7.6 |
| Na | 5.1 |
| K | 4.3 |
| Cs | 3.9 |

# Ionization cross section – idea of experiment

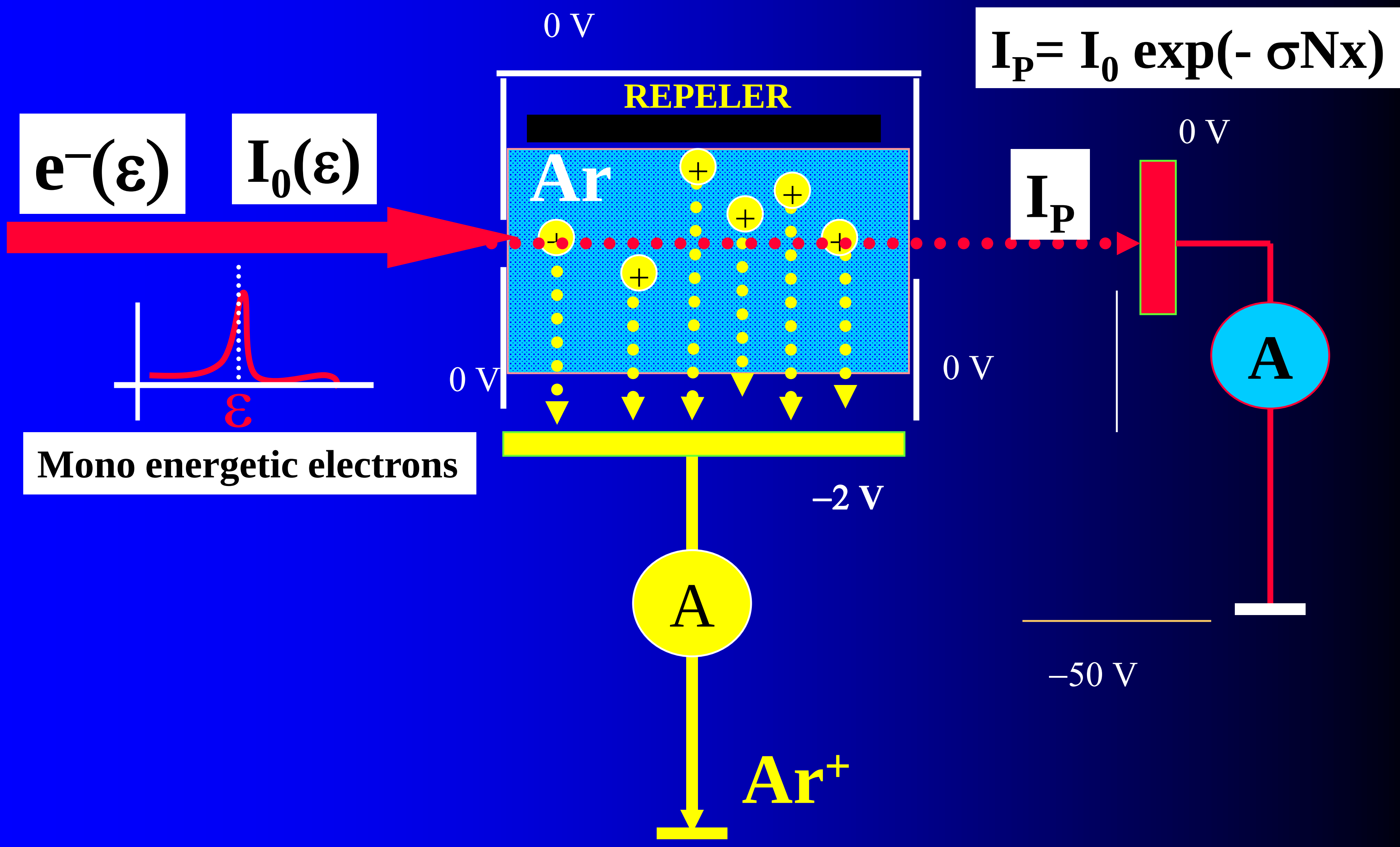

# Electron impact ion source – ion source of mass spectrometer

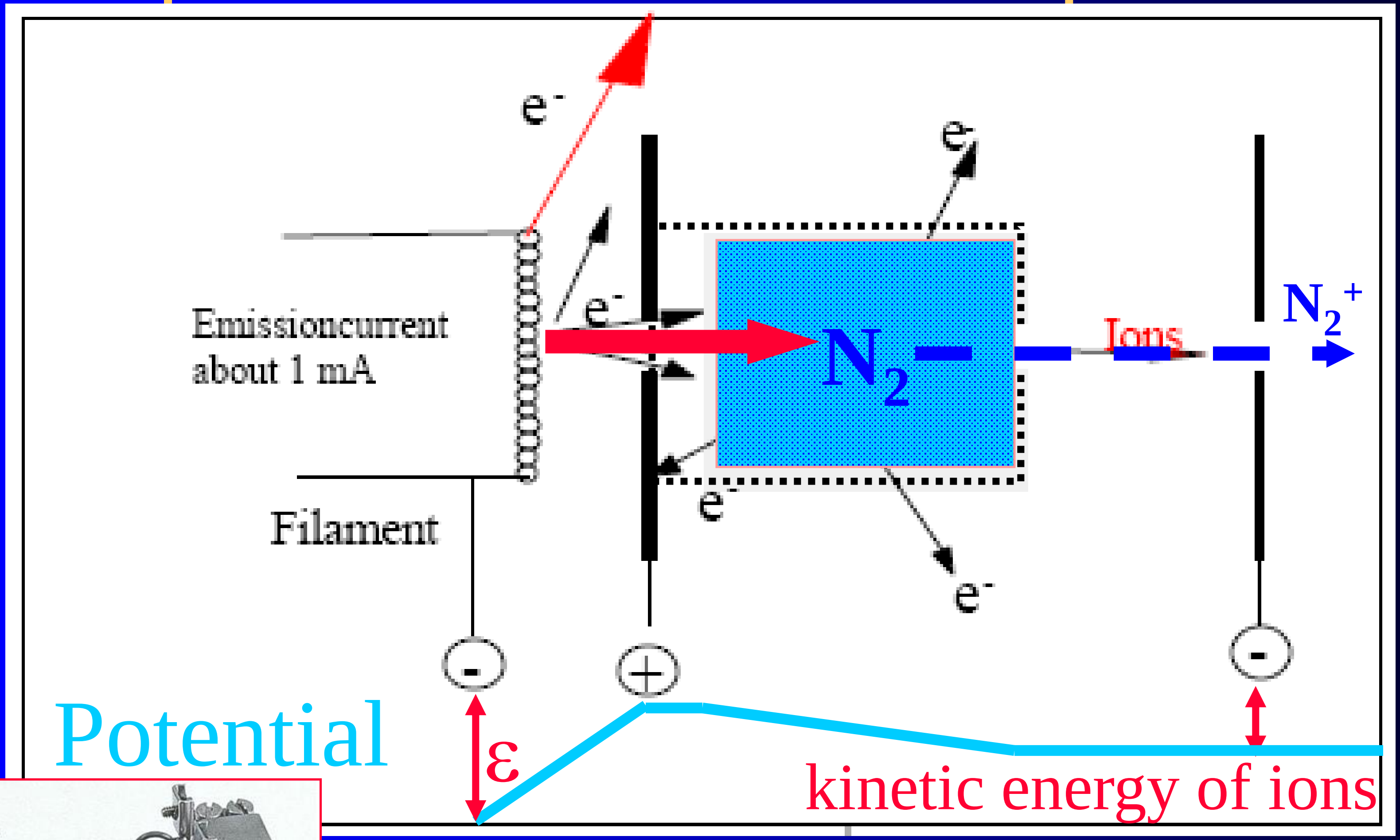


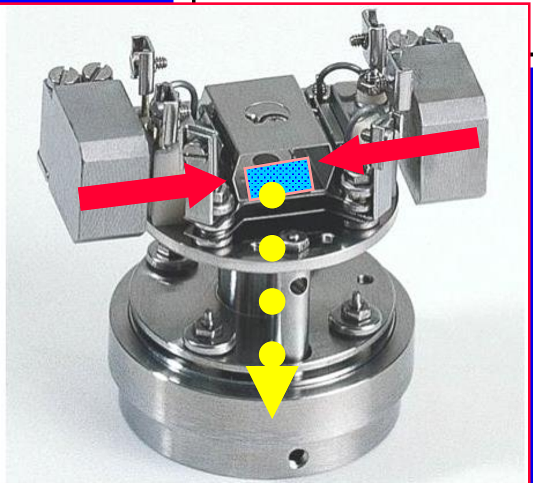

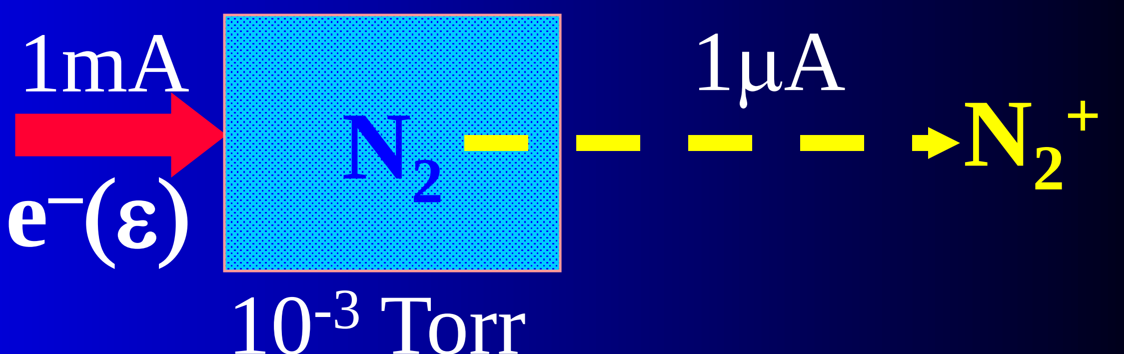

# He +e⁻

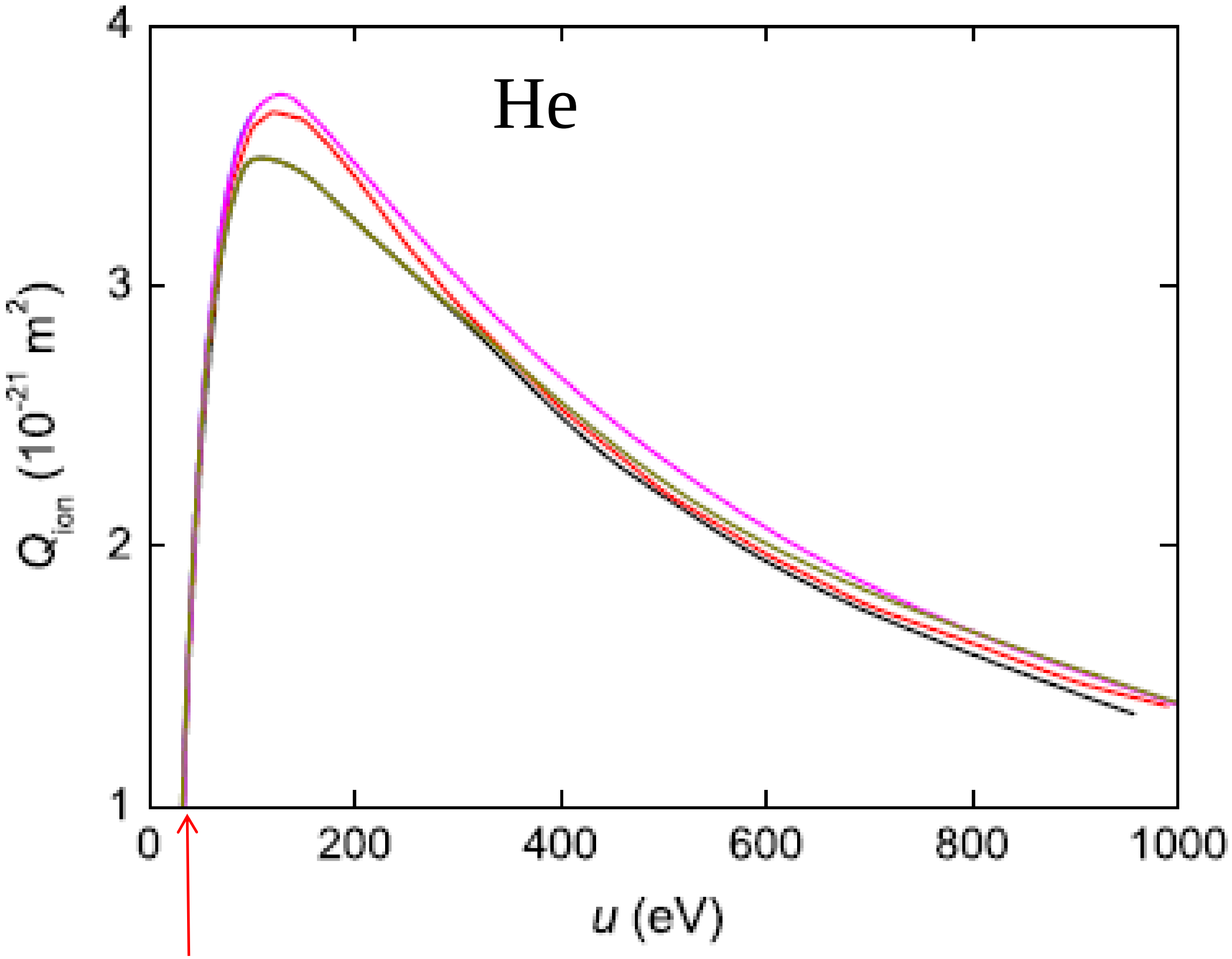


**Figure 4.** Ionization cross sections versus electron energy in helium, from the different databases: BIAGI-v8.9 (——), BIAGI-v7.1 (——), IST-LISBON (——), MORGAN (——), PHELPS (——).

# Standart definition cross section σ (in units …. ~ …cm$^{-2}$)

Experimental results. Rare gases.

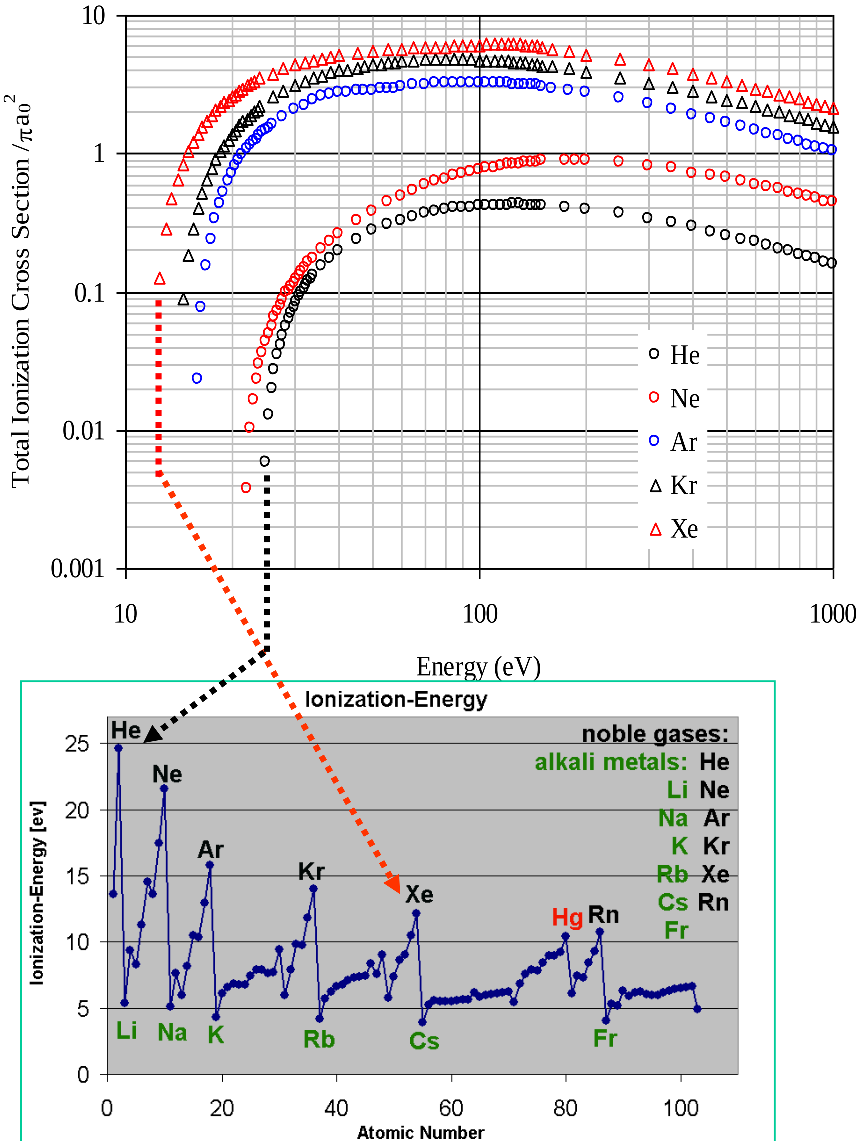


Experimental results. ….. molecules.

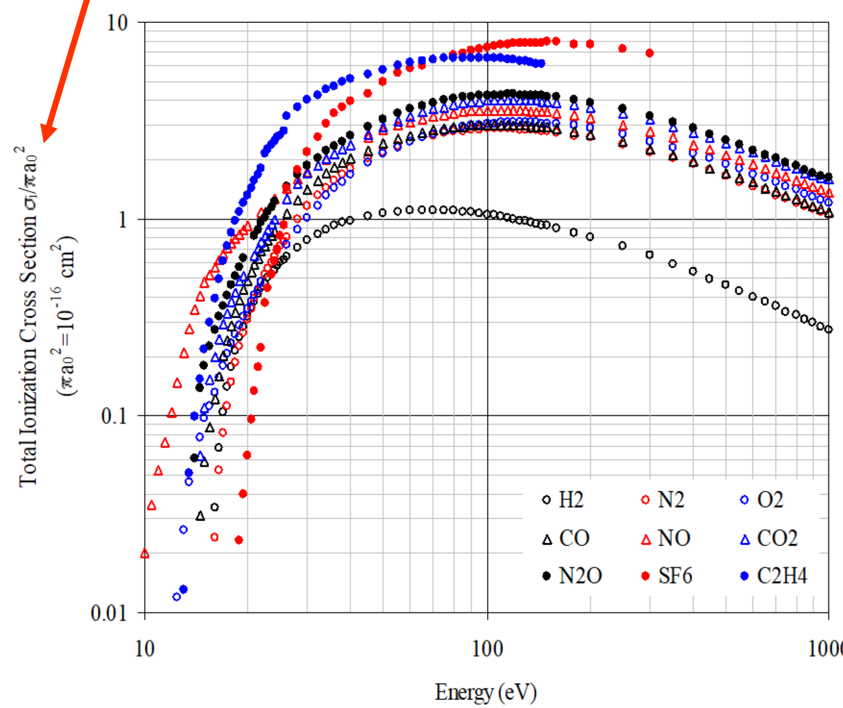


Steinar Stapnes

D. Rapp et al., Journal of Chemical Physics, 43, 5 (1965) 1464

# Ionization by electron impact

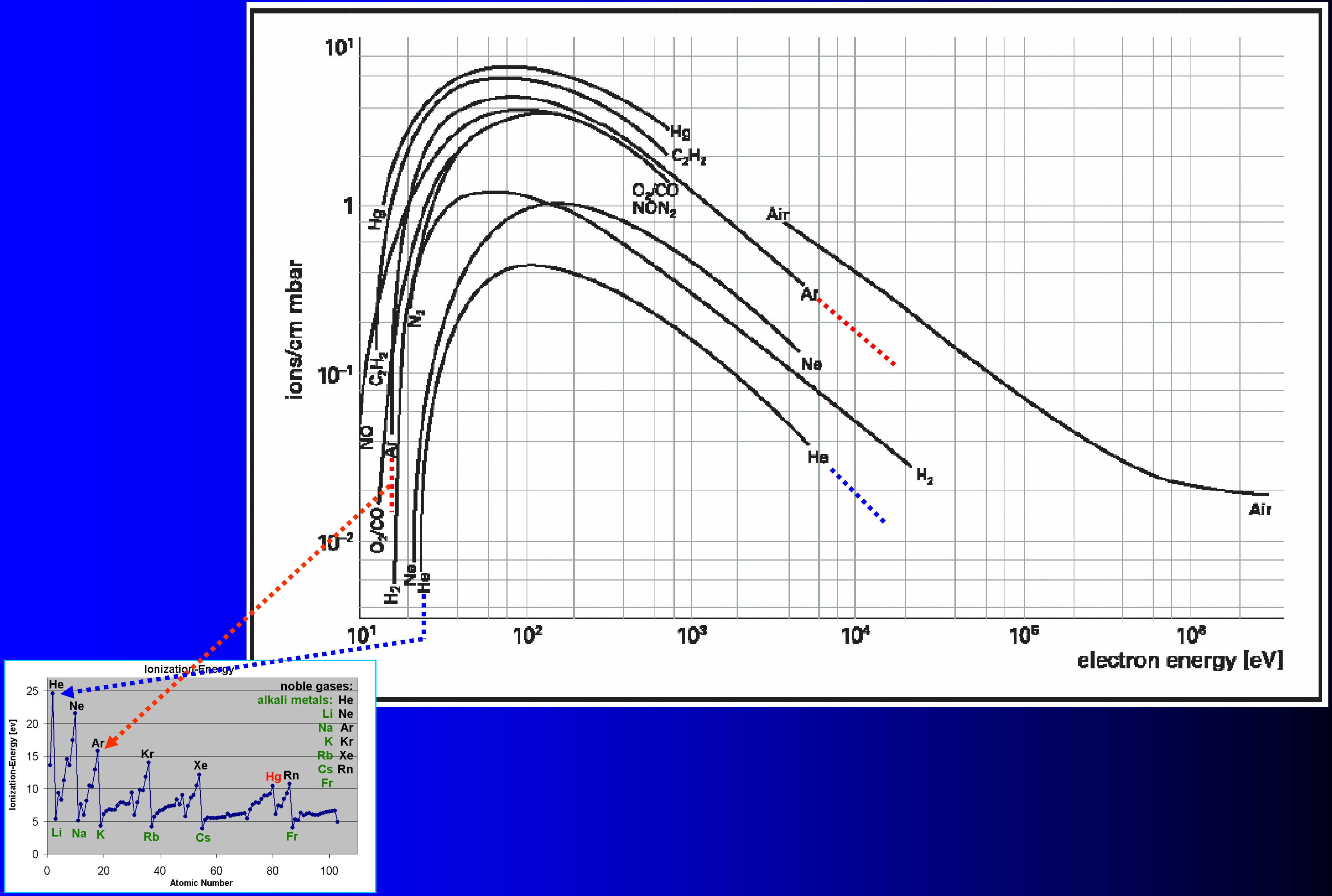

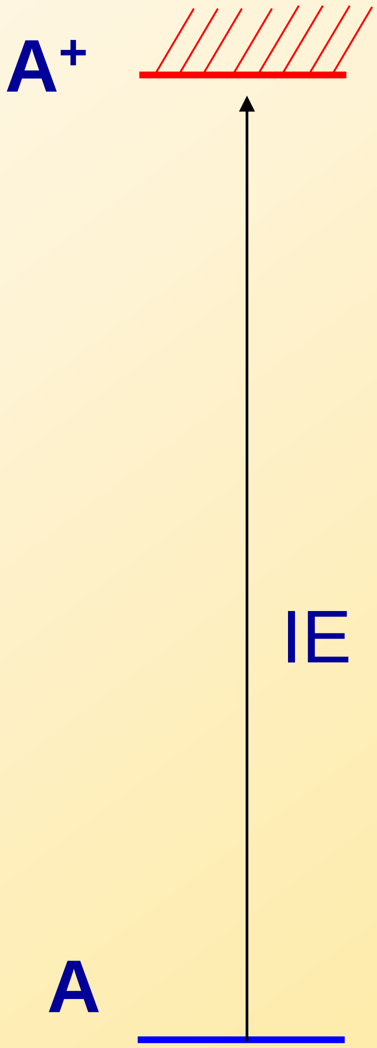


**In case of atoms we have simple situation, the atom in the ground state and the ground state of the ion. The ionization energy is defined as a difference between this two states.**

Adapted from lecture of prof. Š. Matejčik

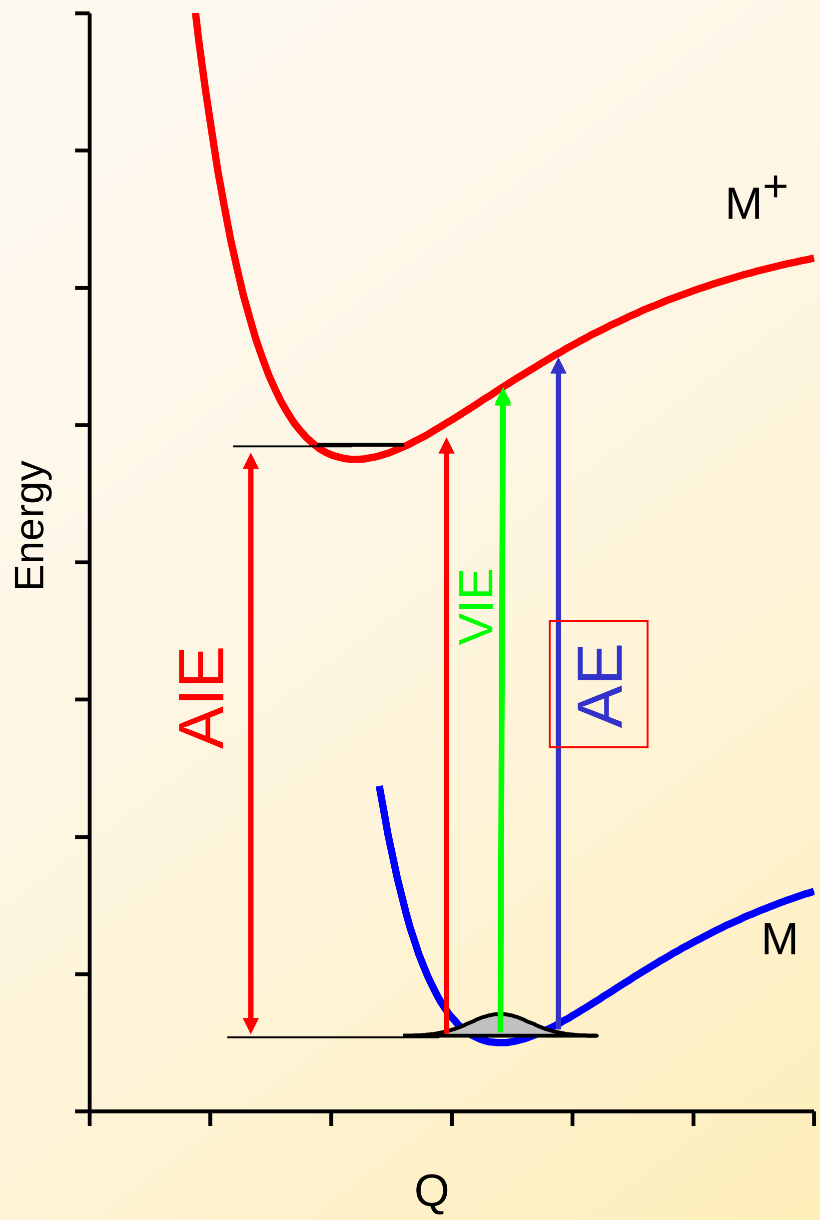


In the molecules is the situation more difficult. We have to work with potential curves or potential energy surfaces and thus the IE depends on the initial geometry of the molecules. For molecule usually two ionization energies are given, vertical IE and adiabatic IE.

**<u>Vertical VIE</u> is defined as the energy necessary to ionise the molecule in the equilibrium geometry**

**<u>Adiabatic AIE</u> is defined as the energy difference between the energies of the ion and molecule in its ground states**

The experiments are sensitive on the lowest energy necessary to ionize molecule and this is called **<u>appearance energy</u>**. This corresponds to the ionization energy at low distances. As the geometry changes in the molecule and the molecular ion are only moderate, often is the AE very close to the AIE.

Adapted from lecture of prof. Š. Matejčik

# Experimental setup:

**E = 0 – 150 eV**
**FWHM ~50-140 meV**
**Ie~20-100nA**

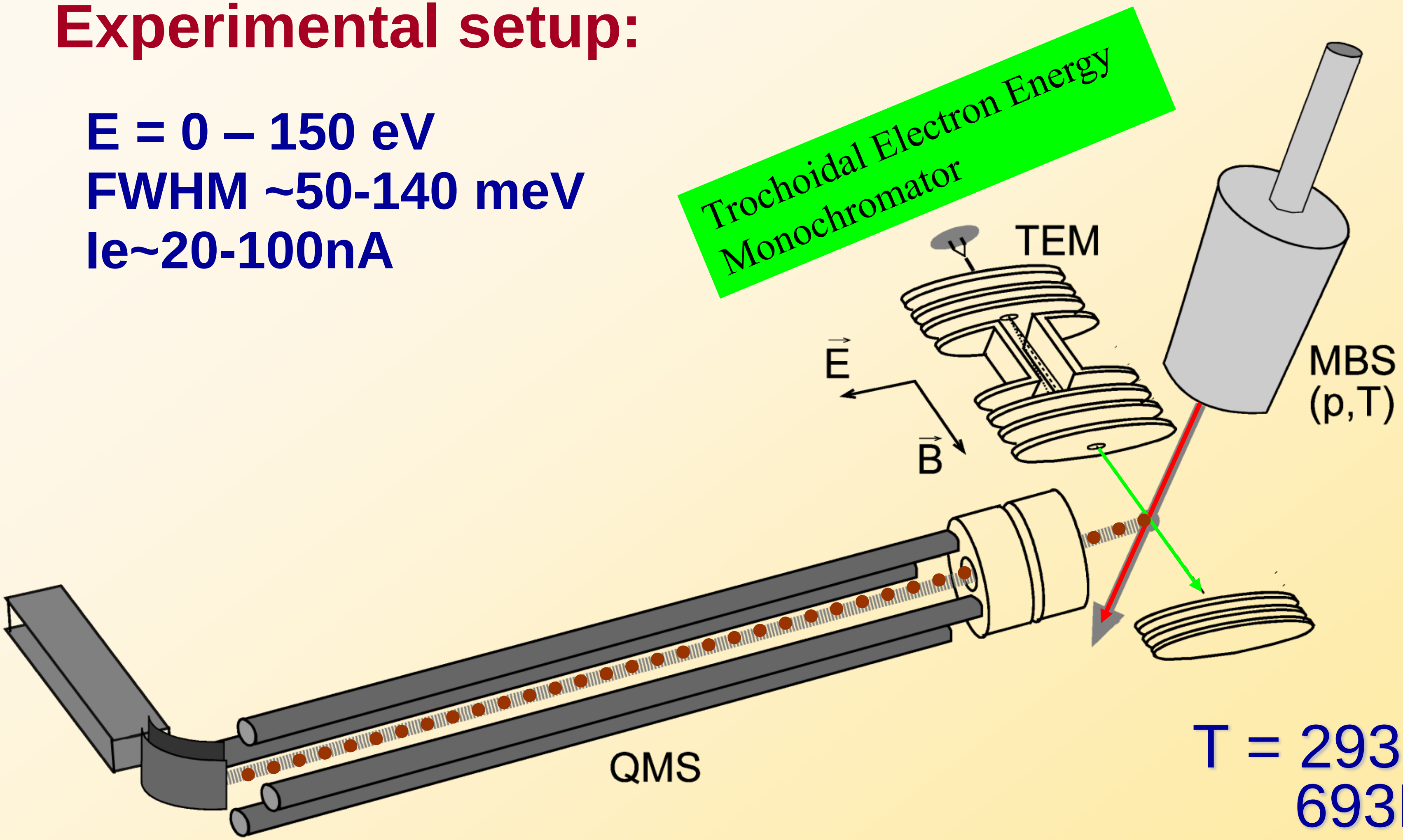


T = 293K
693K

The apparatus consist of TEM, MBS and QMS. The TEM is well known, the FWHM was about 140 meV and the Ie ~100 nA
MBS- effusive type, the molecules in the beam have translational, vibrational and rotational temperature identical to the temperature of the MBS
The mass selected ions are registered as a function of the electron energy

# Electron impact ionization

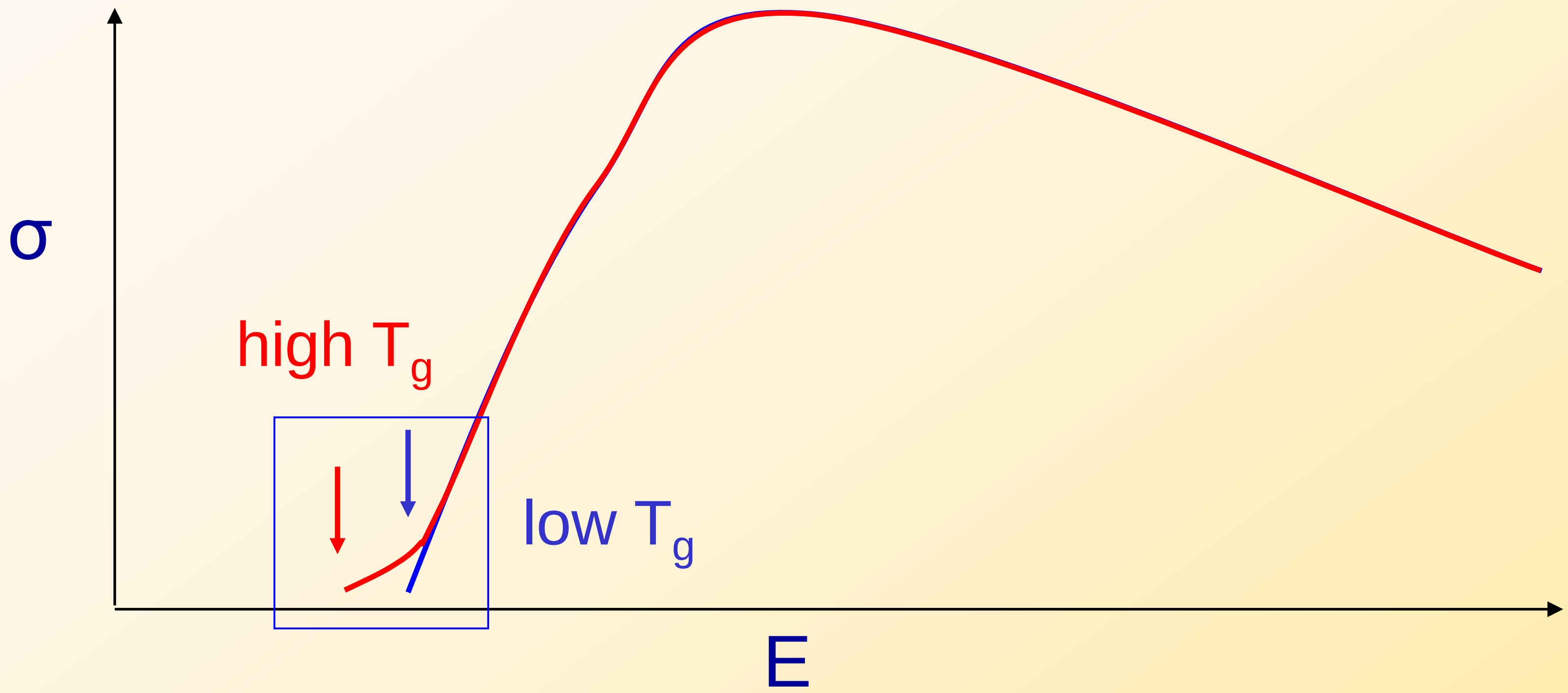


The EII is characterised from point of view of the kinetics by the cross section

The cross section has a monotonic character with maximum at about 100 eV

The EII is endothermic reaction with a threshold, called appearance energy of the ions

In present experimet we have focused on the estimation of the threshold behaviour of the CS, estimation of the AE

At elevated temperatures there are changes in the ion yield in the vicinity of the threshold

Adapted from lecture of prof. Š. Matejčik

**Another definition $\alpha$ in units $cm^{-1}$**

# Mathematical Analysis

When these n electron move through a distance *dx*, they produce another *dn* electrons due to collision. Therefore:

$$dn = \alpha\, n\, dx$$

$$\frac{dn}{n} = \alpha\, dx$$

$$\ln n = \alpha x + A$$

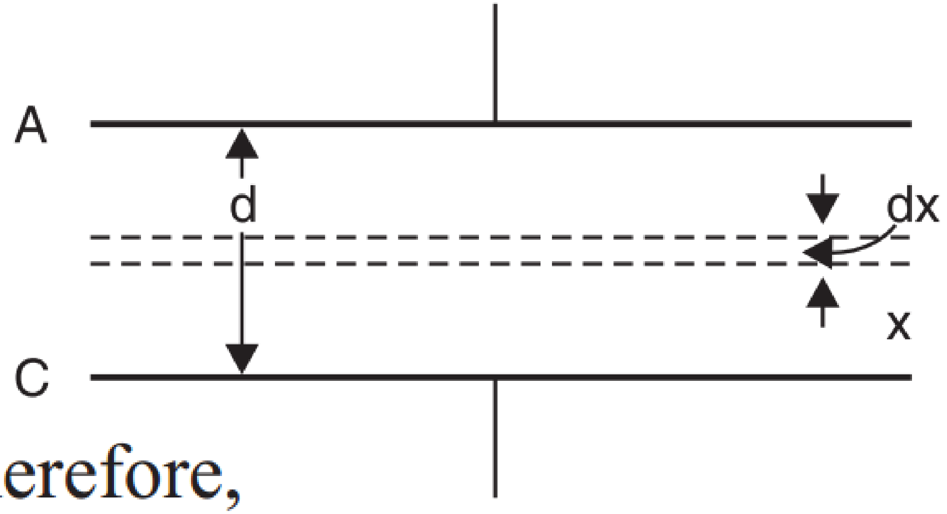


Now at $x = 0$, $n = n_0$. Therefore,

$$\ln n_0 = A$$

$$\ln n = \alpha x + \ln n_0$$

$$\ln \frac{n}{n_0} = \alpha x$$

$$n = n_0 e^{\alpha x}$$

# Another definition $\alpha$ in units $cm^{-1}$

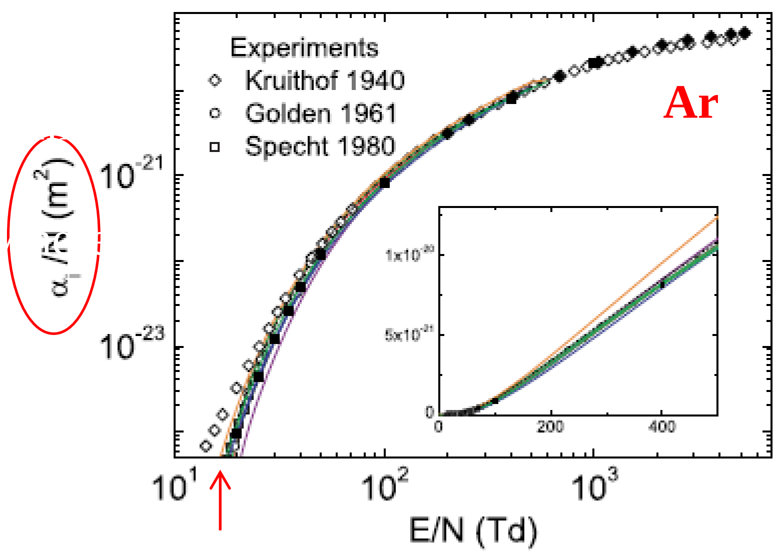


**Figure 8.** Measured and calculated reduced ionization coefficients. The solid lines are results from two-term Boltzmann calculations and the solid symbols (■) are from the Monte Carlo calculations using MAGBOLTZ (Biagi 2011). The colour code is BIAGI-v8.9 (——); BSR (——); HAYASHI (——); IST-LISBON (——); MORGAN (——); PHELPS (——); PUECH (——). The measurements are referenced in the text.

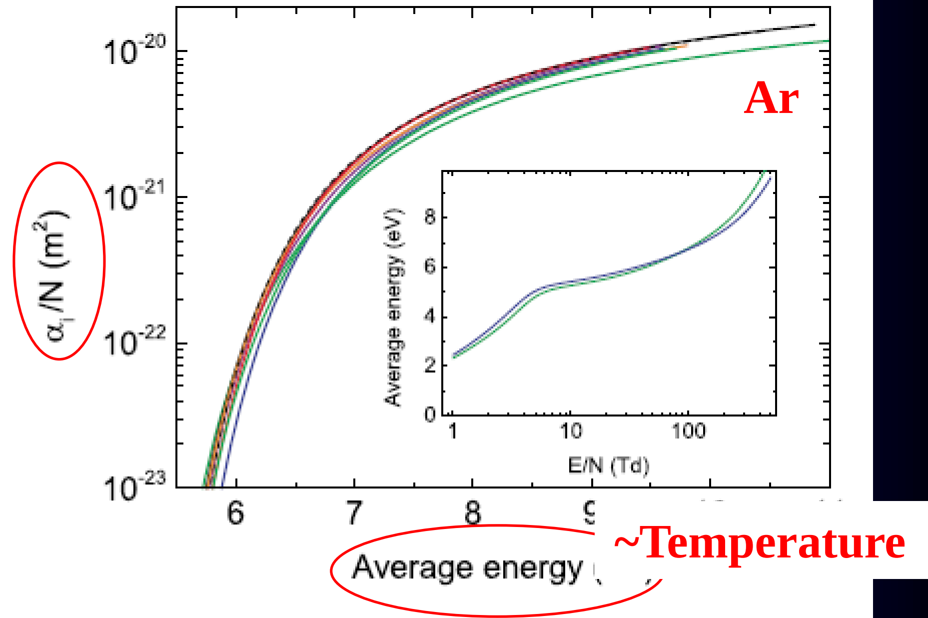


**Figure 9.** Reduced ionization coefficient versus average electron energy, calculated using a two-term Boltzmann solver. The inset shows the average energy versus $E/N$, and the colour code is BIAGI-v8.9 (——); BIAGI-v7.1 (- - - -); BSR (——); HAYASHI (——); IST-LISBON (——); MORGAN (——); PHELPS (——); PUECH (——).

## 2.3. Electron impact ionization

The electron impact ionization is the most fundamental ionization process for the operation of ion sources.

Why?

- The cross section for the impact ionization is by orders of magnitudes higher than the cross section for the photo ionization.
- The cross section depends on the mass of the colliding particle. Since the energy transfer of a heavy particle is lower, a proton needs for an identical ionization probability an ionization energy three orders of magnitudes higher than an electron

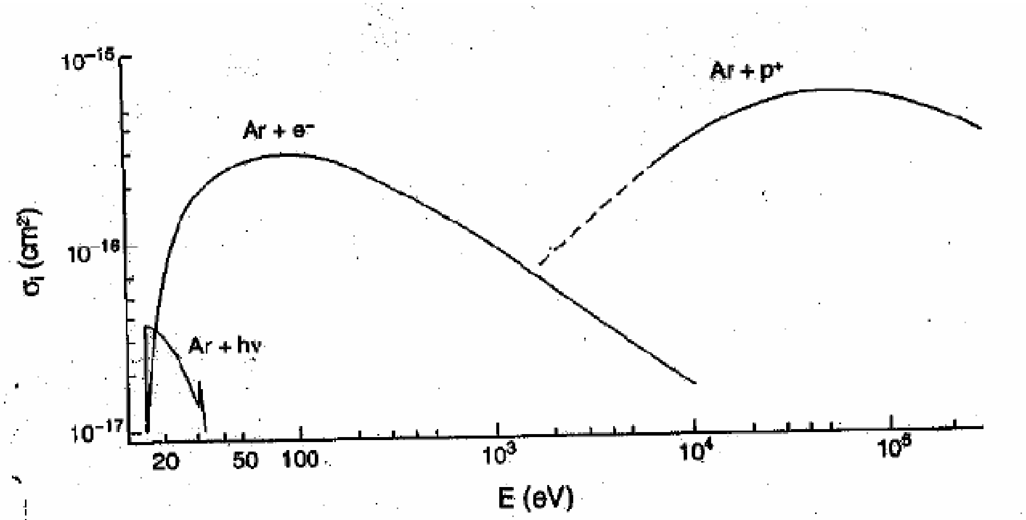


**FIGURE 4**
Ionization cross sections as functions of energy for ionizing collisions with fast electrons, protons, and photons. (From Winter, H., in *Experimental Methods in Heavy Ion Physics*, Springer-Verlag,

# p + $H_2$ Ionization Cross Section

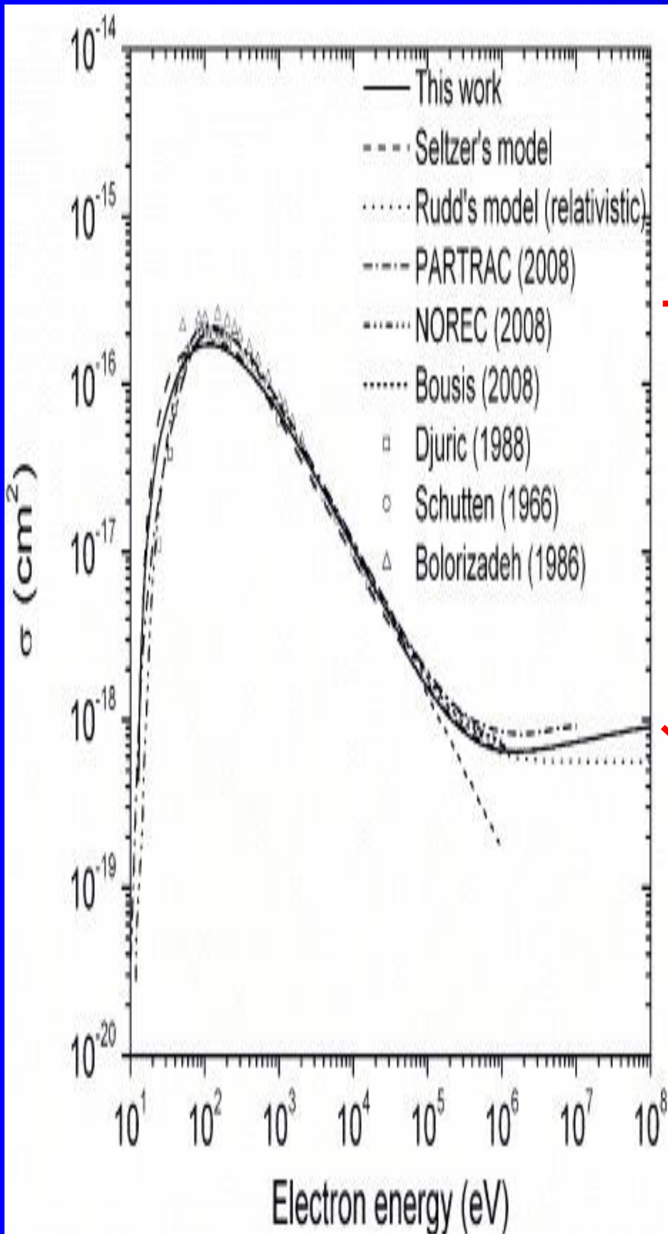


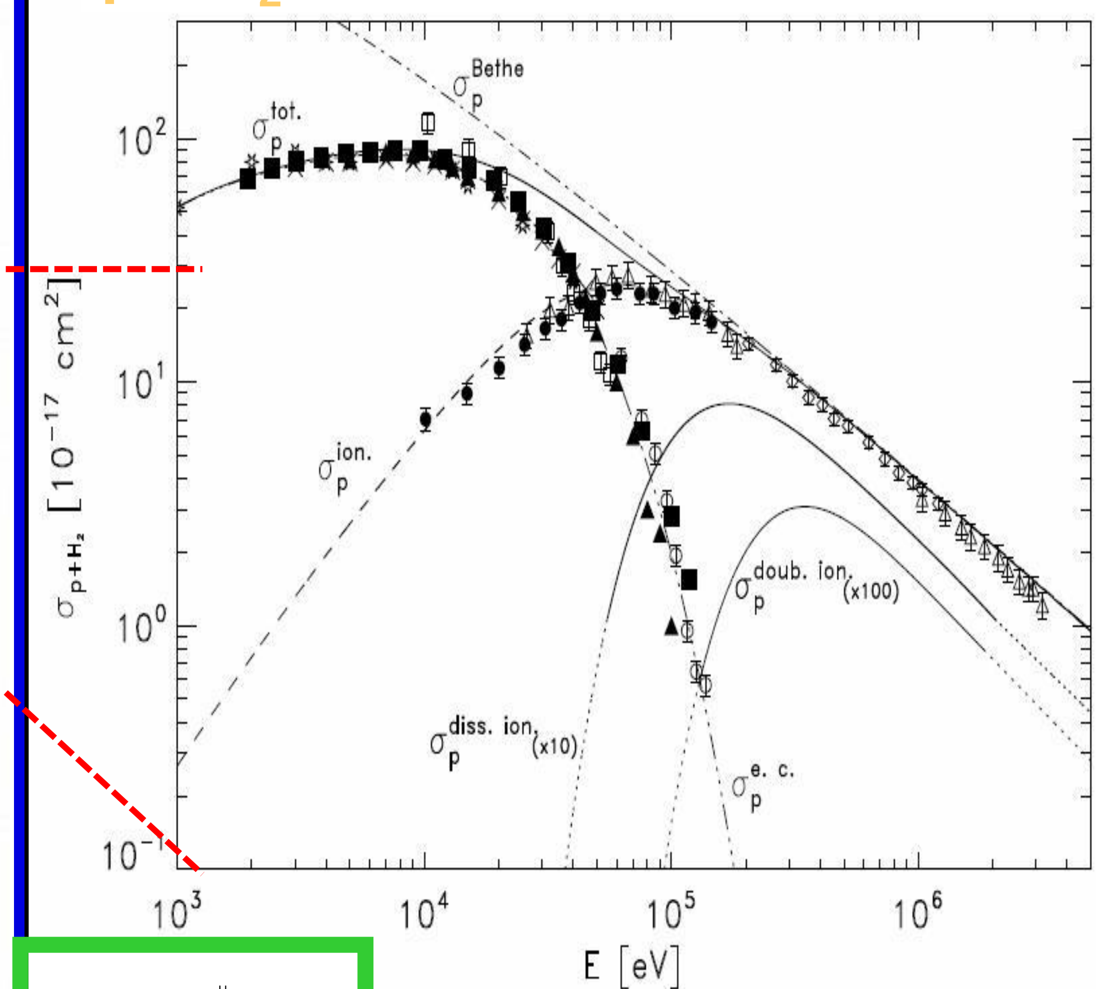


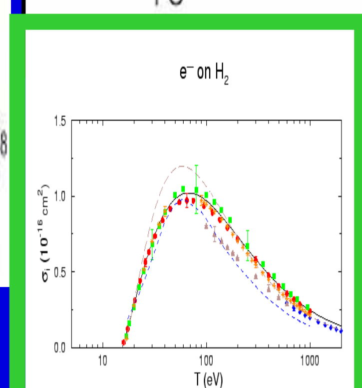


Padovani et al. 2009, A&A, 501, 619

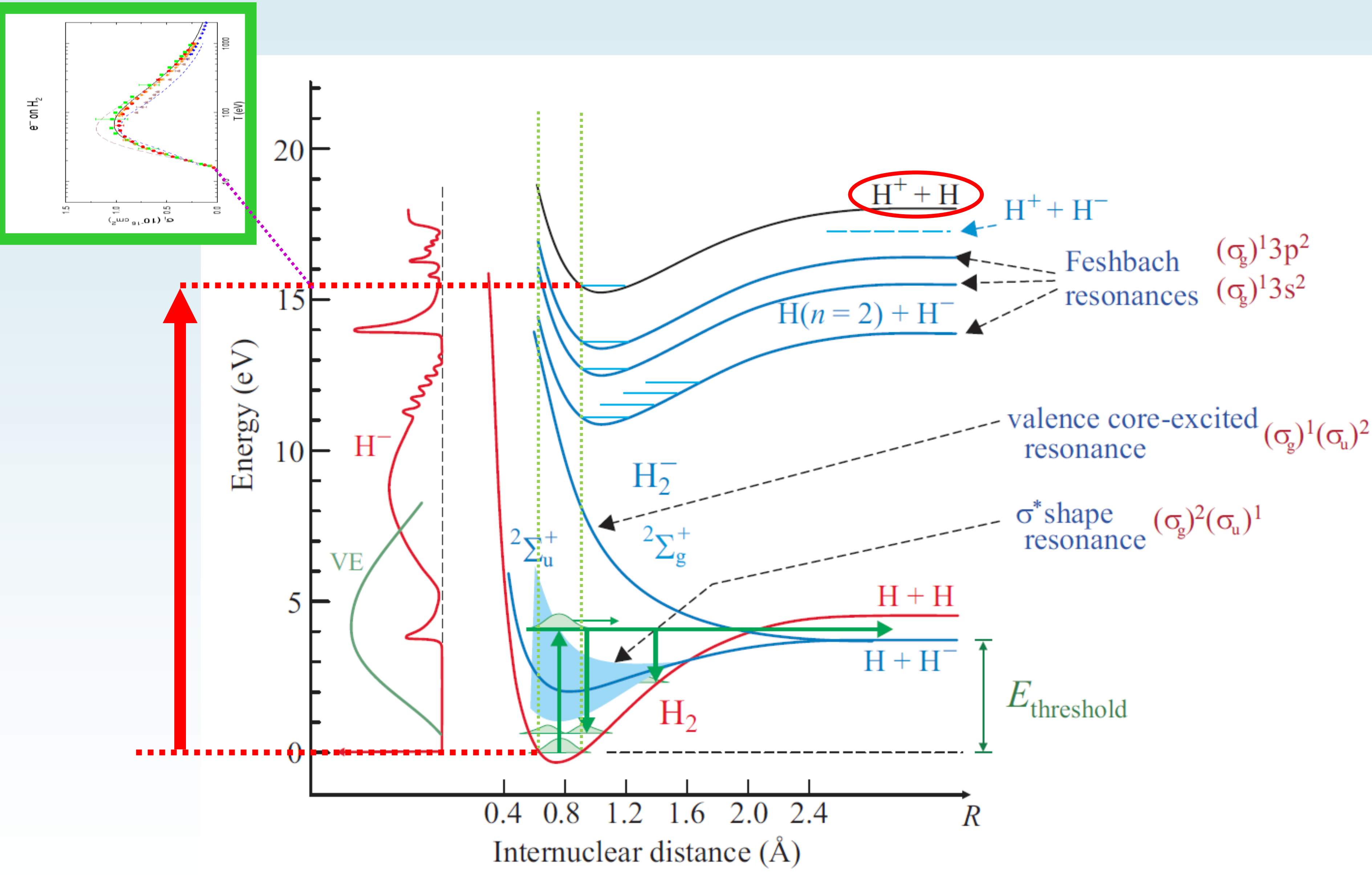

e⁻ on H2
T (eV)
H⁺ + H
H⁺ + H⁻
Feshbach
resonances
(σg)¹3p²
(σg)¹3s²
H(n = 2) + H⁻
valence core-excited
resonance
(σg)¹(σu)²
σ*shape
resonance
(σg)²(σu)¹
H + H
H + H⁻
E threshold
H2
H2⁻
H⁻
VE
²Σu⁺
²Σg⁺
Energy (eV)
Internuclear distance (Å)
R

# Cross sections for vibrational excitation, dissociation, ionization…$H_2$

| $H_2 + e$ | | |
|---|---|---|
| → | $H_2(v) + e$ ……. | Vibrational excitation |
| → | $H + H + e$……. | Dissociation |
| → | $H_2^* + h\nu + e$ … | Photon excitation |
| → | $H_2^+ + e + e$….. | Ionization |
| → | $H^+ + H + e + e$ | Dissociative Ionization |

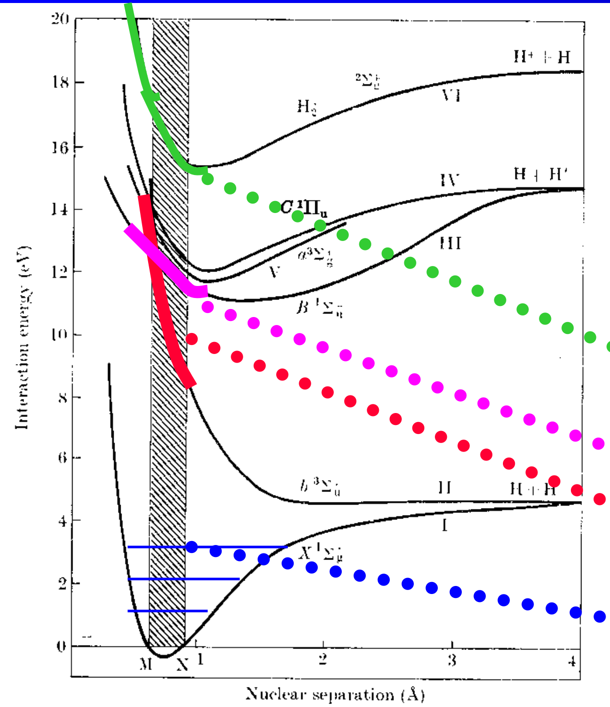


FIG. 13.1. Potential energy curves for electronic states of $H_2$ and $H_2^+$ lying within 20 eV of the ground state.

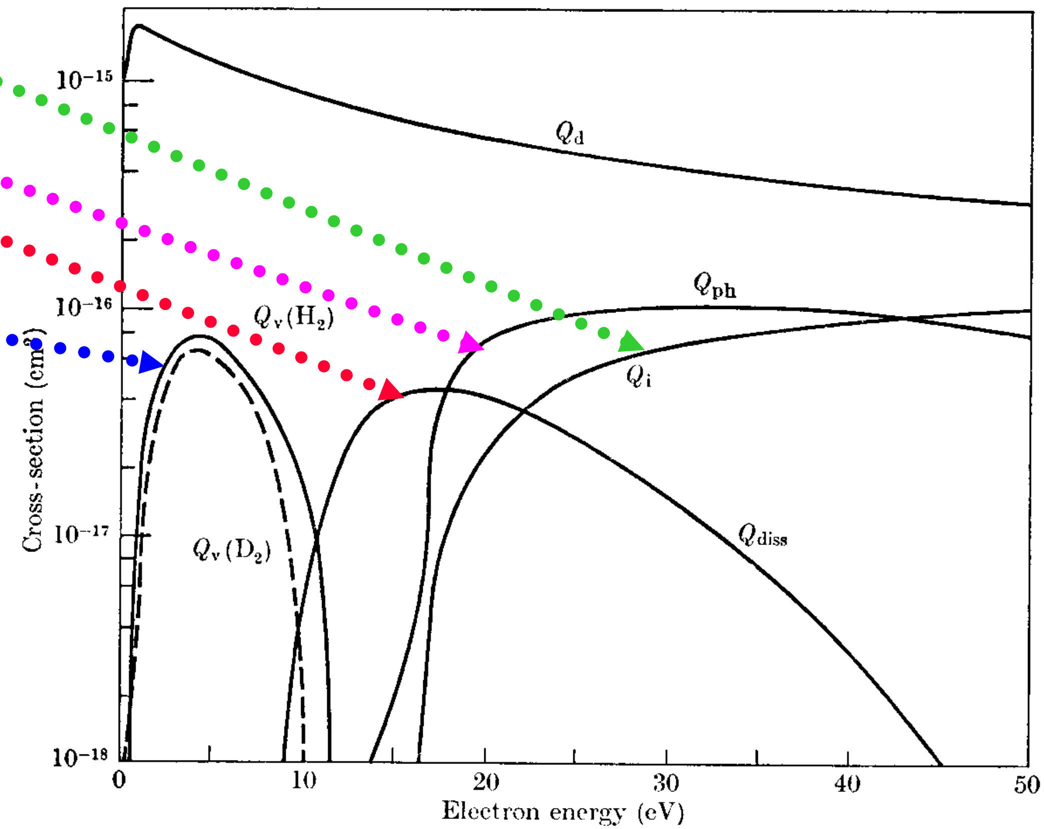


FIG. 13.37. Cross-sections assumed by Engelhardt and Phelps in their analysis of swarm data in $H_2$ and $D_2$ for electrons of characteristic energy greater than 1 eV. $Q_d$ momentum-transfer cross-section, $Q_i$, ionization cross-section, $Q_{diss}$ dissociation cross-section, $Q_{ph}$ photon excitation cross-section, $Q_v$ vibrational excitation cross-section (—— $H_2$, – – – $D_2$).

# Potential Energy Surface Description of the Ionization of $H_2$

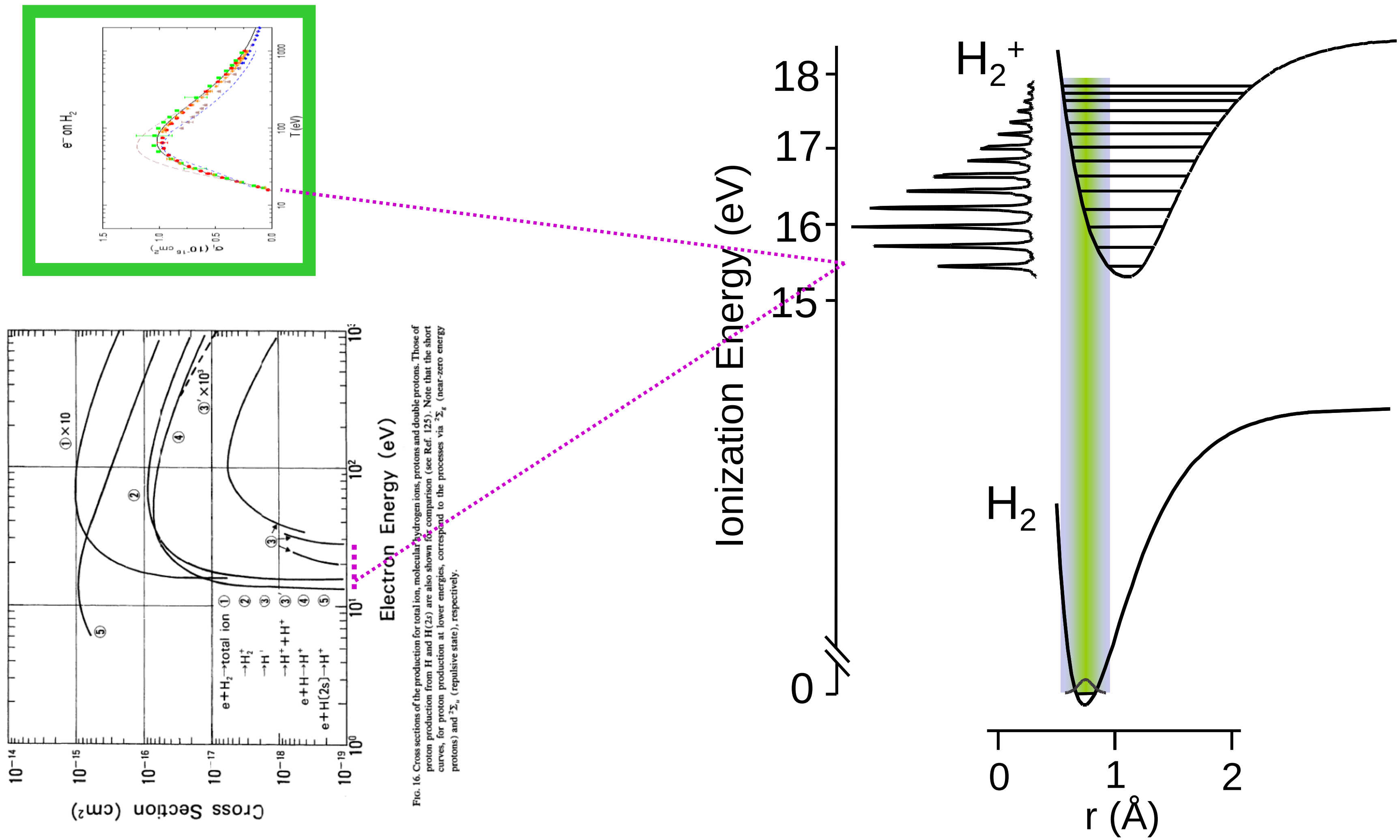

# Details of interaction of electron with $H_2$ (1990)



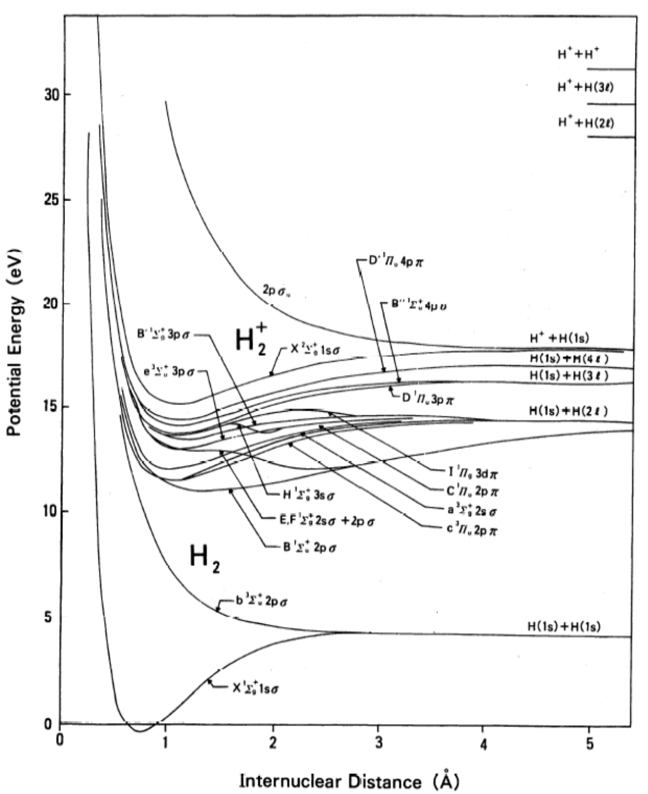


FIG. 1. Some important energy levels of molecular hydrogen and molecular ion (see Ref. 5).

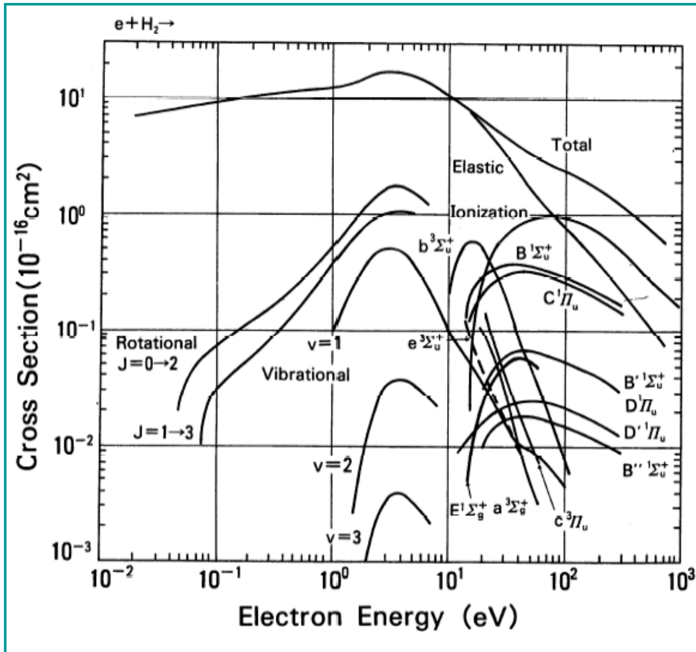


FIG. 2. Comparison of cross sections for various collision processes in neutral $H_2$. Also for comparison, cross sections of ionization of atomic hydrogen are shown. These data are taken at room temperatures.

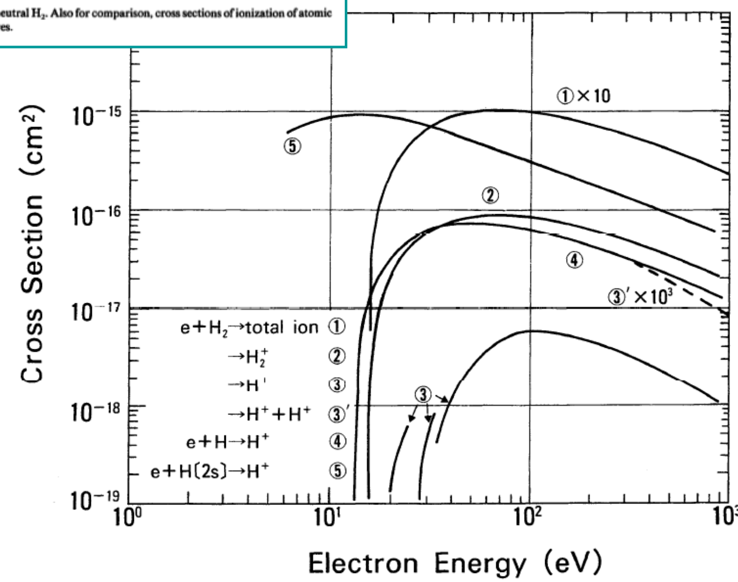


FIG. 16. Cross sections of the production for total ion, molecular hydrogen ions, protons and double protons. Those of proton production from H and H(2s) are also shown for comparison (see Ref. 125). Note that the short curves, for proton production at lower energies, correspond to the processes via $^2\Sigma_g$ (near-zero energy protons) and $^2\Sigma_u$ (repulsive state), respectively.

## Cross Sections and Related Data for Electron Collisions with Hydrogen Molecules and Molecular Ions[a)]


H. Tawara, Y. Itikawa,[b)] H. Nishimura,[c)] and M. Yoshino[d)]

*National Institute for Fusion Science,[a)] Nagoya 464-01, Japan*


(Received July 5, 1989; revised manuscript received November 1, 1989)


Data are compiled and evaluated for collision processes of excitation, dissociation, ionization, attachment, and recombination of hydrogen molecules and molecular ions ($H_2^+$, $H_3^+$) by electron impact as well as for properties of their collision products.


Key words: electron impact; hydrogen molecule; hydrogen molecular ion; scattering; elastic integral; vibrational excitation; rotational excitation; dissociation; ionization; photon emission; cross section.

# Partial cross section for excitation

# NO

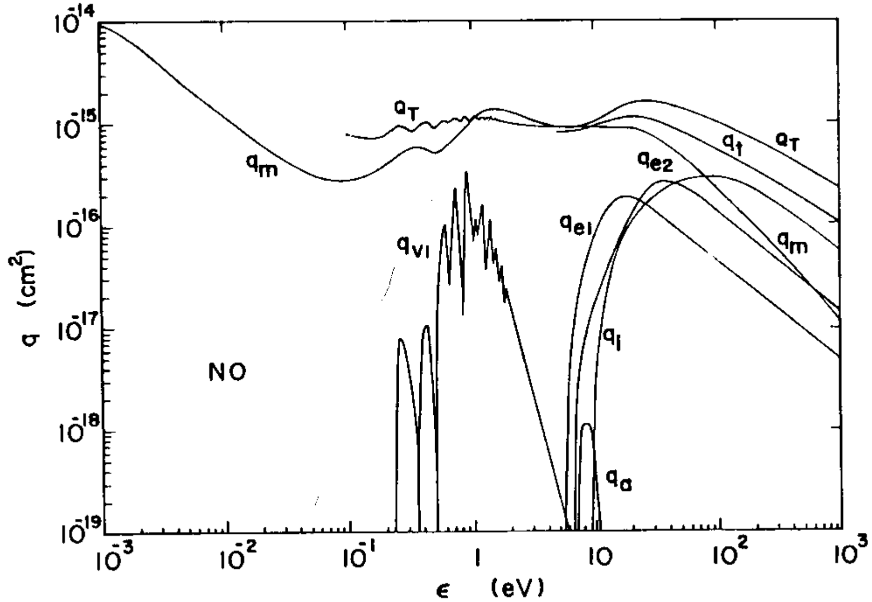


Fig. 4. Cross-section set for NO (1986).

# $NH_3$

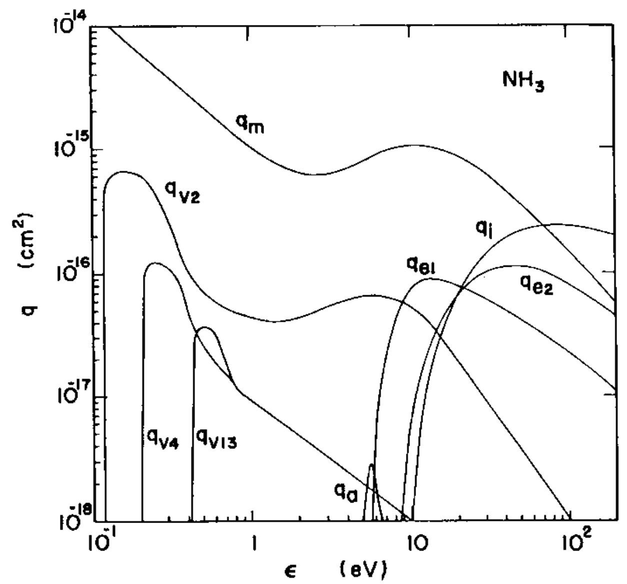


Fig. 6. Electron collision cross-section set for $NH_3$ (1986).

# Ionization cross section He and $N_2$

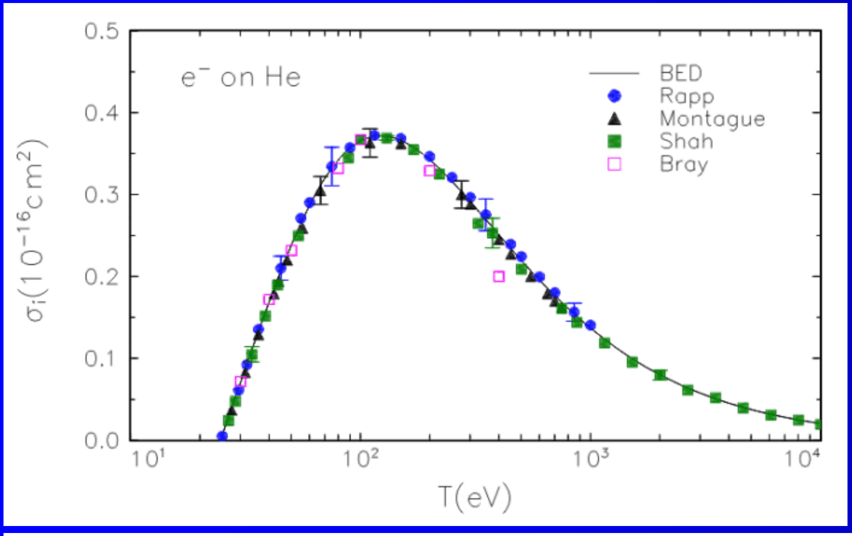


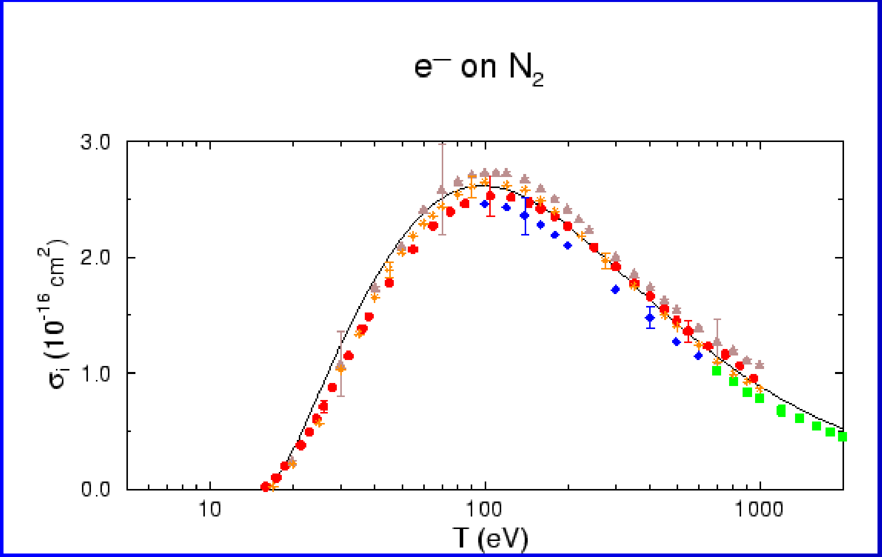


## Electron impact

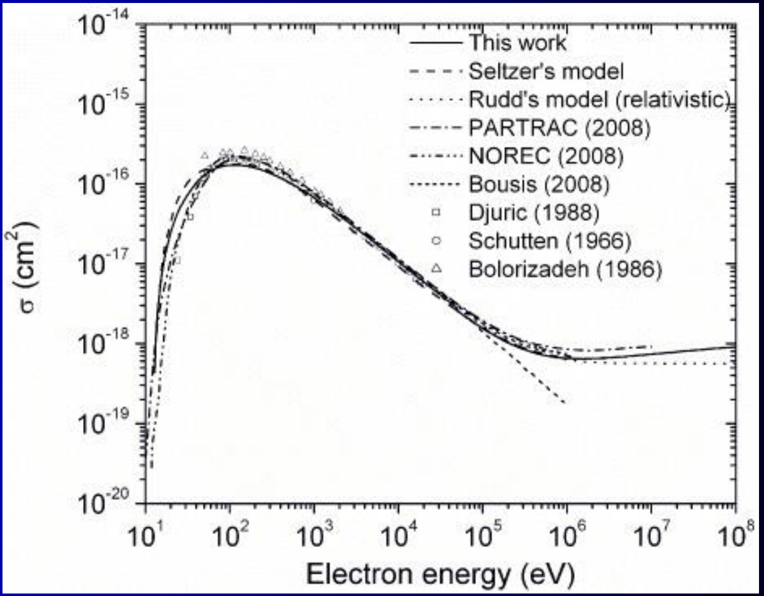


BEB W. Hwang, Y.-K. Kim and M.E. Rudd,
J. Chem. Phys. **104**, 2956 (1996).

New J. Phys. **11** (2009) 063047
doi:10.1088/1367-2630/11/6/063047
**Cross sections for the interactions of 1 eV–100 MeV electrons in liquid water and application to Monte-Carlo simulation of HZE radiation tracks**

Ianik Plante[1,2] and Francis A Cucinotta[1]

# Life is not so simple – Total ionization cross section

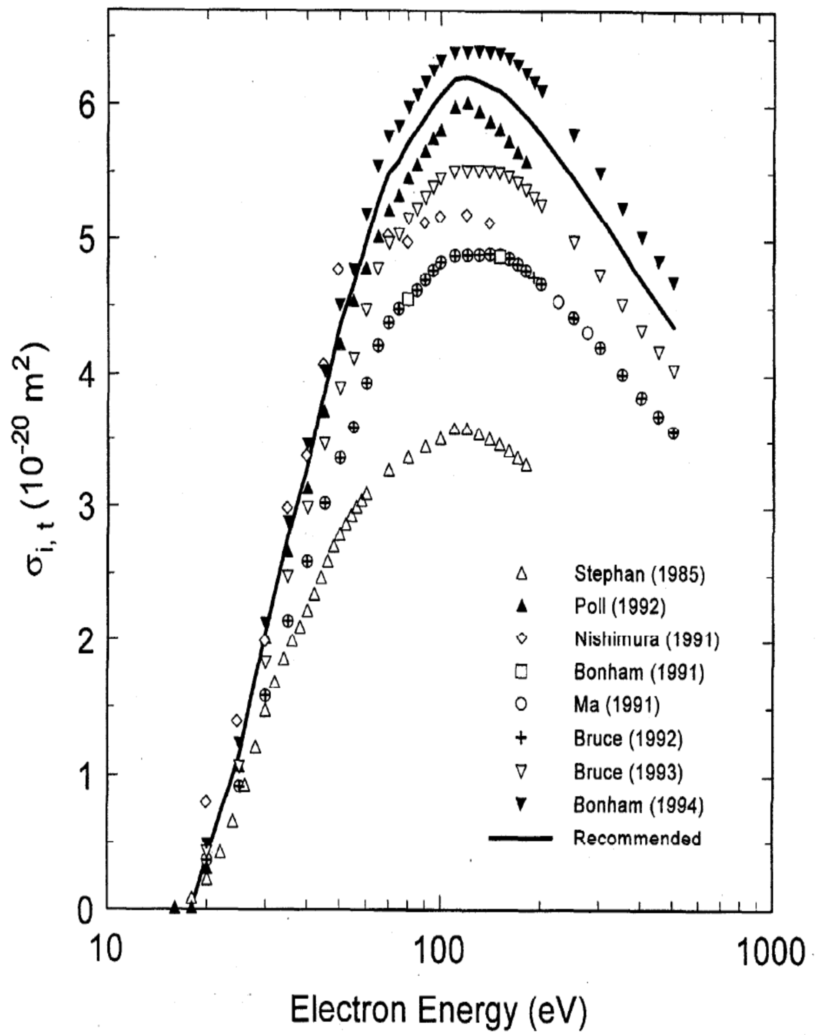


FIG. 17. Total ionization cross section $\sigma_{i,t}(\epsilon)$ as a function of electron energy for $CF_4$. Measured values: △, Ref. 43; ▲, Ref. 103; □, Ref. 69; ○, Ref. 98; +, Ref. 100; ▽, Ref. 104; ▼, data of Ref. 104 multiplied by 1.16 (per Bonham in Ref. 73); ◇, Ref. 106. Recommended: —, average of ▲ and ▼ (see Sec. 4.1 and Table 12).

**Electron Interactions with $CF_4$**


L. G. Christophorou,[a)] J. K. Olthoff, and M. V. V. S. Rao
*National Institute of Standards and Technology, Gaithersburg, Maryland 20899-0001*



**J. Phys. Chem. Ref. Data, Vol. 25, No. 5, 1996**

# Ionization cross section,
# Different channels have different cross sections and dependencies on energy

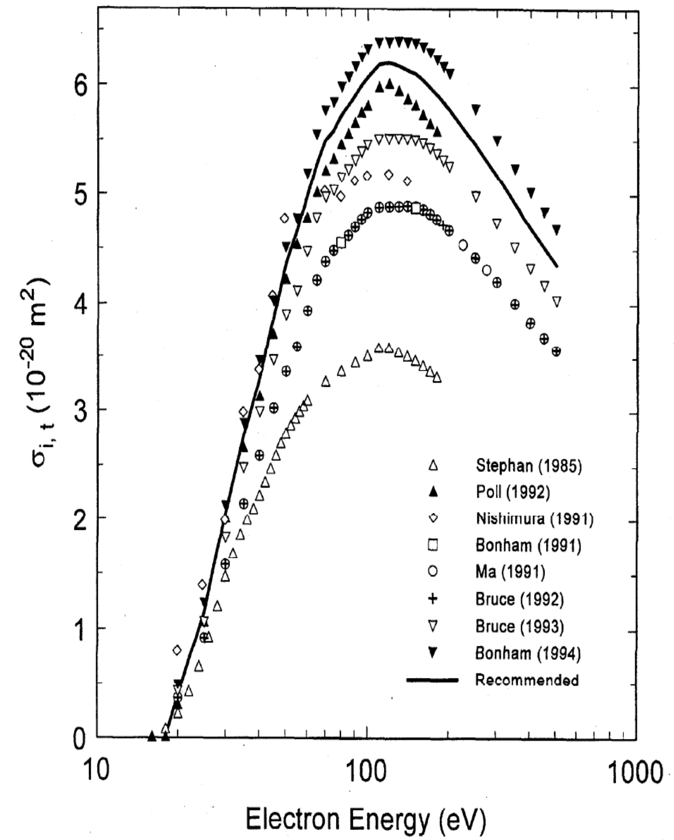


FIG. 17. Total ionization cross section $\sigma_{i,t}(\epsilon)$ as a function of electron energy for $CF_4$. Measured values: △, Ref. 43; ▲, Ref. 103; □, Ref. 69; ○, Ref. 98; +, Ref. 100; ▽, Ref. 104; ▼, data of Ref. 104 multiplied by 1.16 (per Bonham in Ref. 73); ◇, Ref. 106. Recommended: —, average of ▲ and ▼ (see Sec. 4.1 and Table 12).

J. Phys. Chem. Ref. Data, Vol. 25, No. 5, 1996



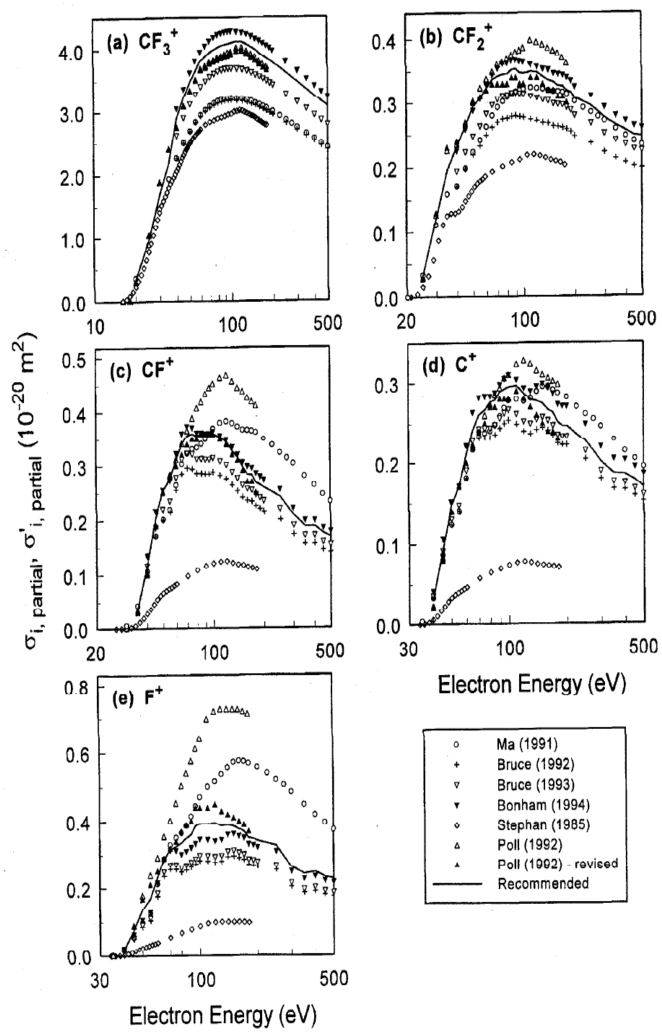


FIG. 19. Partial ionization cross section for the production of (a) $CF_3^+$, (b) $CF_2^+$, (c) $CF^+$, (d) $C^+$, and (e) $F^+$ by electron collision on $CF_4$. $\sigma'_{i,partial}(\epsilon)$: ◇, Ref. 43; △, Ref. 103; ○, Ref. 98. $\sigma_{i,partial}(\epsilon)$: +, Ref. 100; ▽, Ref. 104; ▼, Ref. 73; ▲, revised data of Ref. 103 (see text). —, average of ▼ and ▲ (see Sec. 4.2 and Table 15).

**Electron Interactions with $CF_4$**

L. G. Christophorou,[a] J. K. Olthoff, and M. V. V. S. Rao
*National Institute of Standards and Technology, Gaithersburg, Maryland 20899-0001*

# Thomson's formula

$$\sigma_j = C_j(\varepsilon - E_{ION})$$

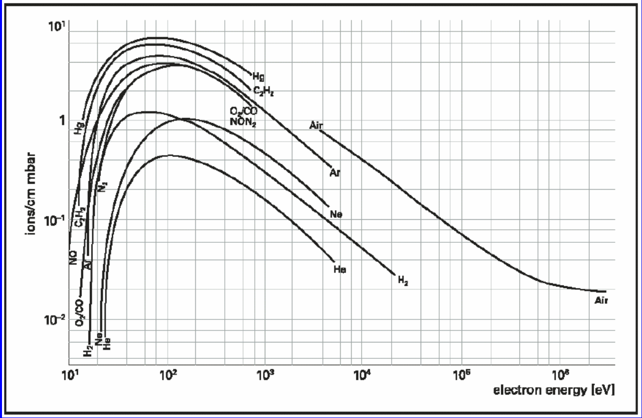


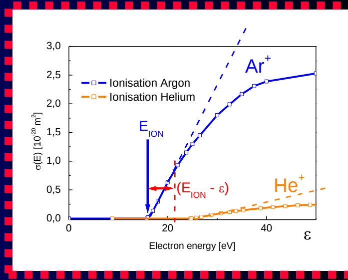


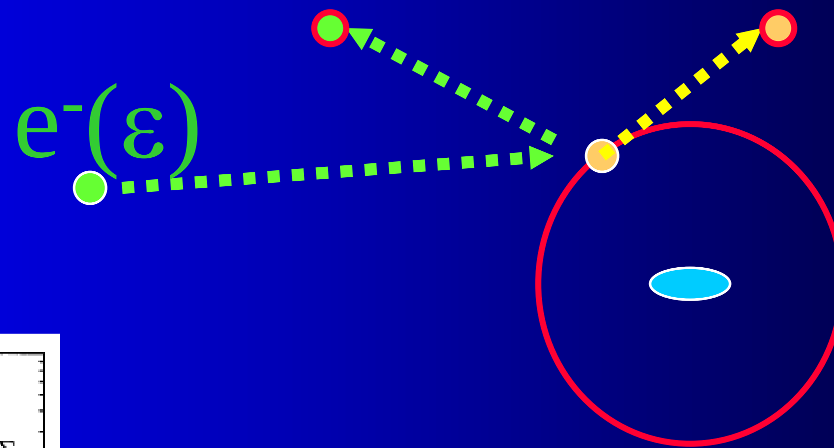


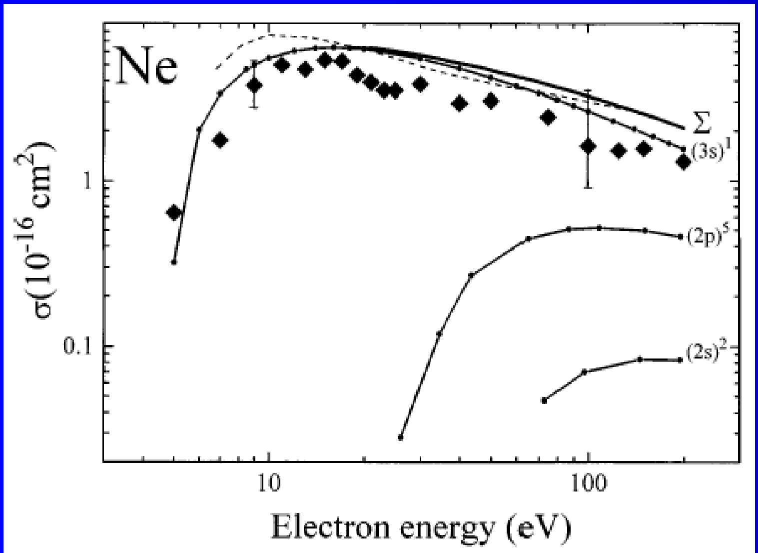


Ionization if $\Delta\varepsilon > I$

Formula of Rutherford for coulomb force

$d\sigma = e^4 d\Theta / 4\varepsilon^2 \sin^4(\phi/2)$….. $\sigma_i = \pi e^4/I \,.\, (\varepsilon - I)/\varepsilon^3$

$$\sigma_i = 4\pi a_0^2 (I_H/\varepsilon)^2 \,.\, (\varepsilon - I)/I$$

➔ $\sigma_i = 4\pi a_0^2 (I_H/\varepsilon)^2 \,.\, (\varepsilon/I - 1) = f_{function}(\varepsilon/I)$

$\sigma_i = \Sigma\, \sigma_{in}$ **sum of the various subshell contributions**

Calculated ionization cross section of the $^3P_0$ state in Ne using the DM formalism. The full curves refer to the contributions from the various subshells and have been labeled appropriately. The sum of the various subshell contributions has been labeled by the symbol*6*. Also shown is the Born calculation of Ton-That and Flannery (broken curve, see text for details). The experimental data points (diamonds) are those of Johnston *et al* . Two typical error bars (combined systematic and statistical uncertainty) are shown for the experimental data.

# Near the threshold ➔ linear approximation

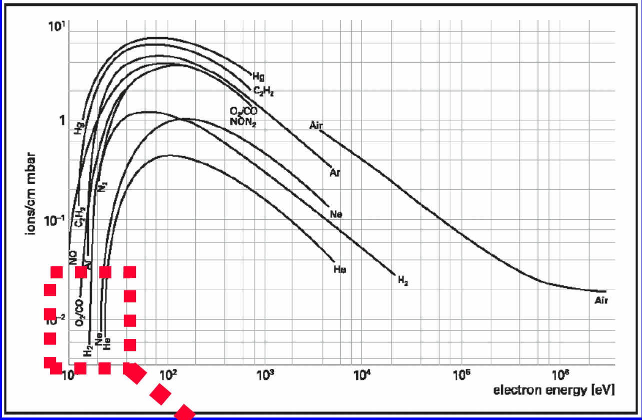


$$\sigma_i = 4\pi a_0^2 (I_H/\varepsilon)^2 \,.\, (\varepsilon - I)/I$$

➔ $\sigma_i = 4\pi a_0^2 (I_H/\varepsilon)^2 \,.\, (\varepsilon/I - 1) = f_{function}(\varepsilon/I)$

$$\sigma_j = C_j(\varepsilon - E_{ION})$$

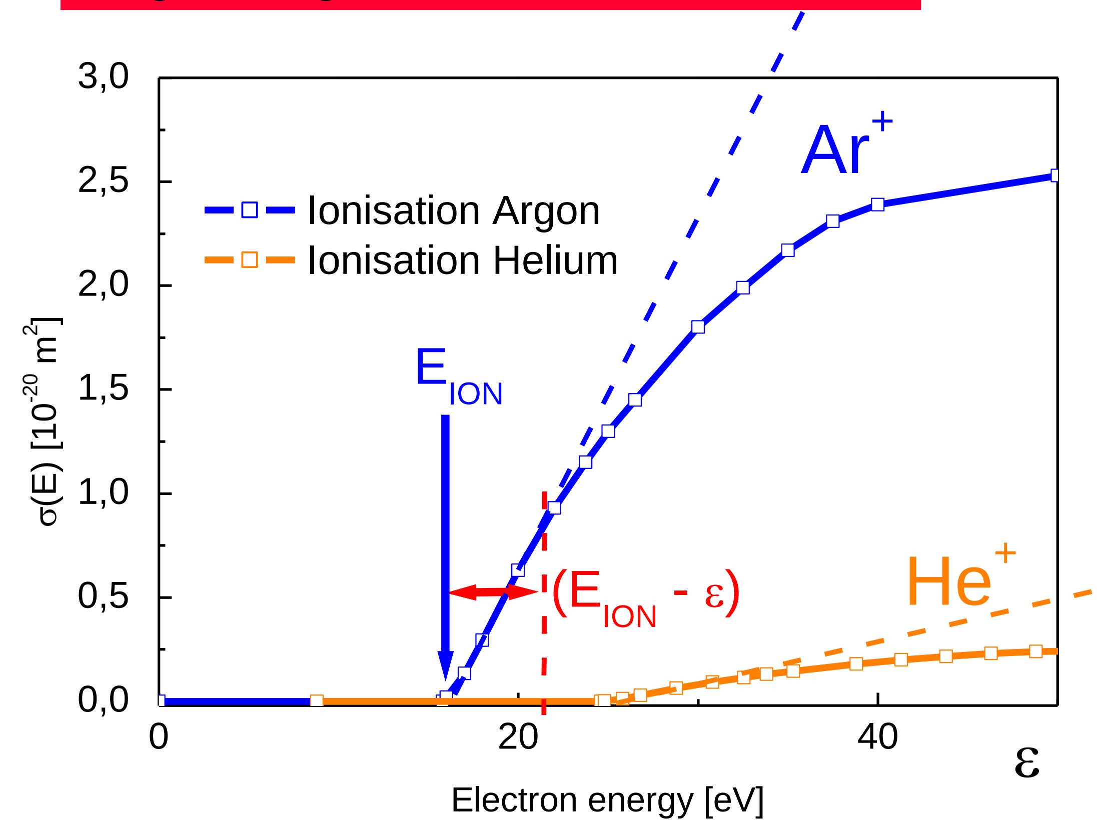

# Ionization cross section recent studies Ar - higher approximation

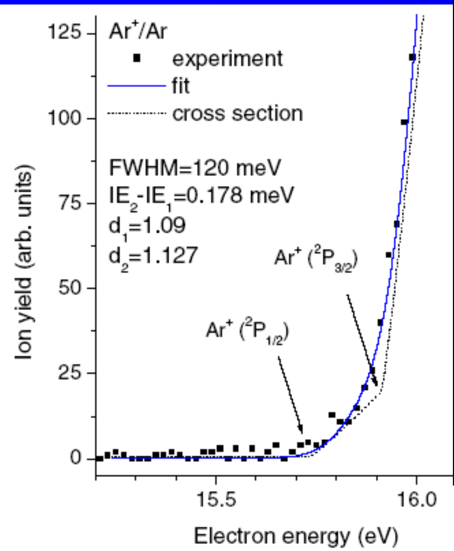


**Figure 2.** The ion yield curve $Ar^+/Ar$ as measured in the present experiment. The full curve is the result of the fitting procedure, involving a convolution of the cross section (dotted curve; the arrows indicating the thresholds for the two spin states) and an electron energy distribution function with a width of 120 meV FWHM (for details see text).

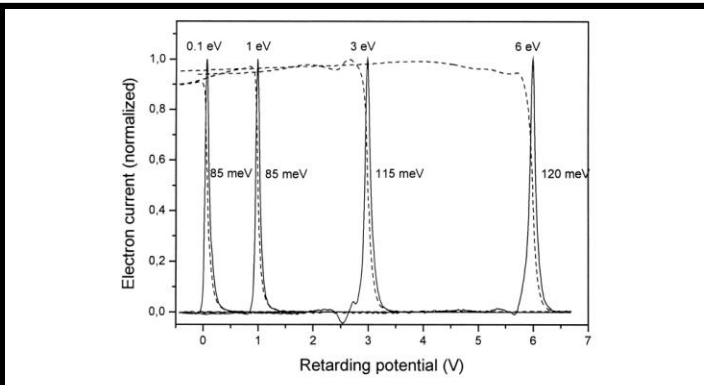


Fig. 11. Electron current versus retarding field for different electron energies (from 0.1 to 6 eV). Note that the alignment of the magnetic field is very crucial as, otherwise, the transmitted electron current varies significantly with energy. The alignment in the present case is still not perfect, as the coils used to generate the magnetic field have not Helmholtz geometry. Hence, the electron current shows some small variations with energy. In addition, the energy resolution of the monochromator, as determined by calculating the FWHM of the differentiated electron current, seems to deteriorate slightly at higher electron energies, that is, in this experimental run from ~85 meV FWHM at 0.1 eV to ~120 meV FWHM at 6 eV.

**IE – ionization energy**

**EII – electron Impact Ionization**

**IE of Ar is 15.759+-0.001eV**

**IE$_1$ of $Ar^+(^2P_{1/2})$**

**IE$_2$ of $Ar^+(^2P_{3/2})$**

**IE$_2$ - IE$_1$ = 0.178eV**

The measured $Ar^+$ ion yield is fitted with a function $I(U, \mathbf{p}, s)$:

$$I(U, \mathbf{p}, s) = \int \sigma_w(E, \mathbf{p}) \cdot f(E,U)\, dE + s \qquad (6)$$

where $s$ is the background signal below the ionization threshold and the cross section $\sigma_w$ for EII at the ionization threshold of Ar is assumed to have the form:

$$\sigma w(E, \mathbf{p}) = \begin{cases} 0 & \text{for } E < \mathrm{IE}_1(\mathrm{Ar}) \\ A_1(E - \mathrm{IE1})^{d1} & \text{for } E > \mathrm{IE}_1 \text{ and } E < \mathrm{IE}_2 \\ A_1(E - \mathrm{IE1})^{d1} + A_2(E - \mathrm{IE2})^{d2} & \text{for } E > \mathrm{IE}_2 \end{cases}$$

# Ionization cross sections $H_2$ – details near the threshold

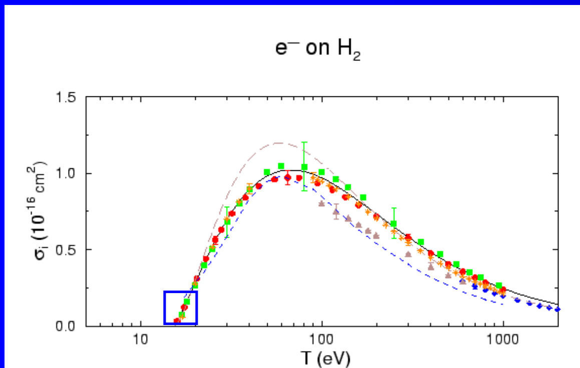


**TABLE 13.6**

*Comparison of observed and calculated energy separation of various vibrational levels of $H_2^+$*

| | Energy separations (eV) | | | | | |
|---|---|---|---|---|---|---|
| Vibnl. levels | 0–1 | 1–2 | 2–3 | 3–4 | 4–5 | 5–6 |
| Calculated | 0·269 | 0·254 | 0·238 | 0·223 | 0·208 | 0·192 |
| Observed | 0·272 | 0·263 | 0·233 | 0·237 | 0·21 | 0·20 |

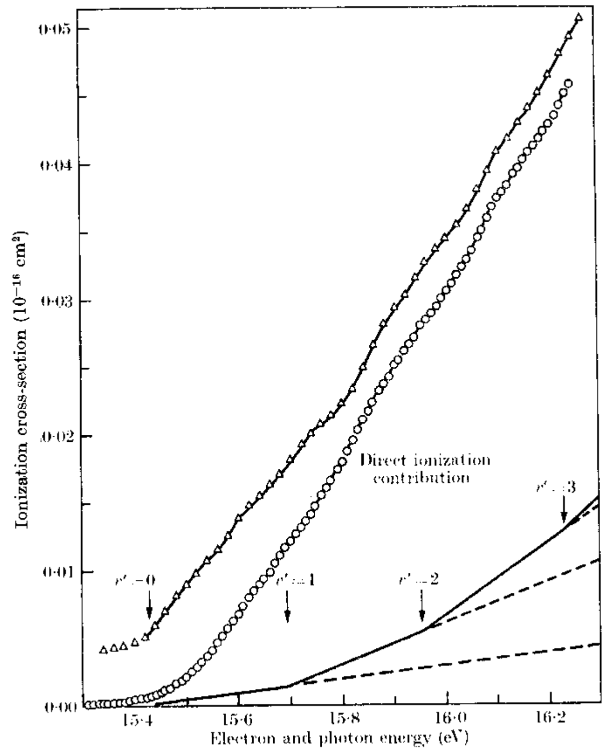


FIG. 13.21. Variation of the ionization cross-section of $H_2$ near the threshold as observed by McGowan, Fineman, Clarke, and Hanson, ○ experimental points. The integrated photo-ionization cross-section observed by Dibeler, Reese, and Krauss is shown for comparison, Δ experimental points. The estimated contribution from direct ionization is also shown.

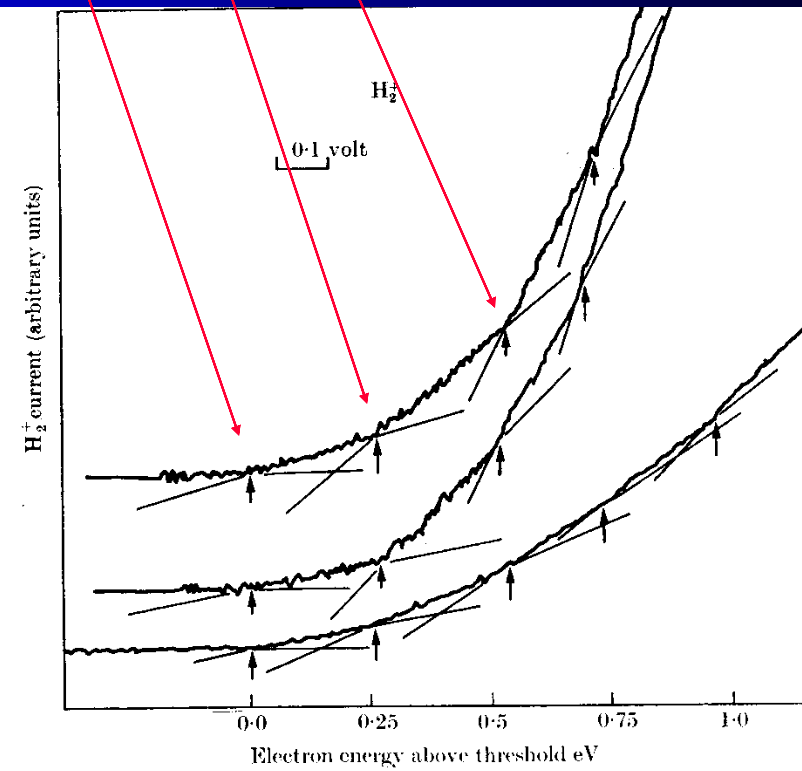


FIG. 13.19. Variation of the ionization cross-section of $H_2$ near the threshold as observed by Marmet and Kerwin.

# Ion source



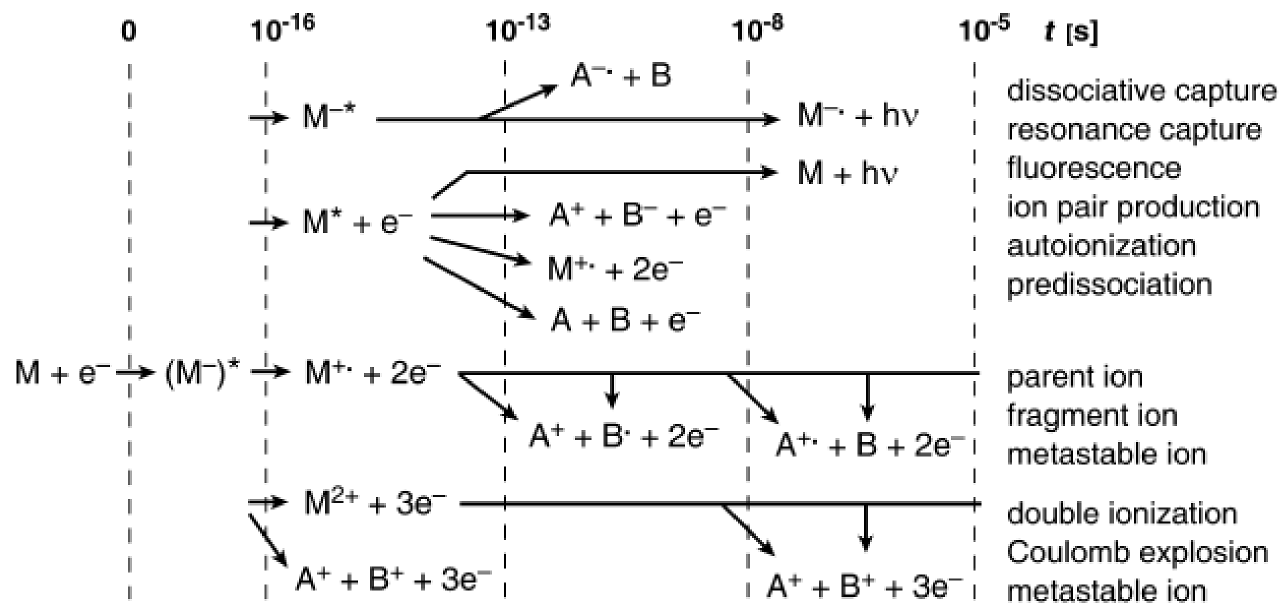


**Fig. 2.10.** Schematic time chart of possible electron ionization processes. Adapted from Ref. [39] with permission. © Wiley & Sons, 1986.

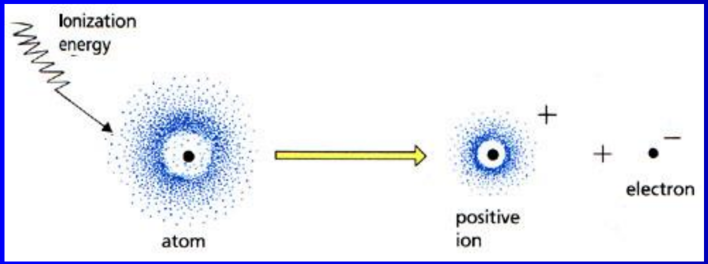


Potential Energy diagram for diatomic molecule.

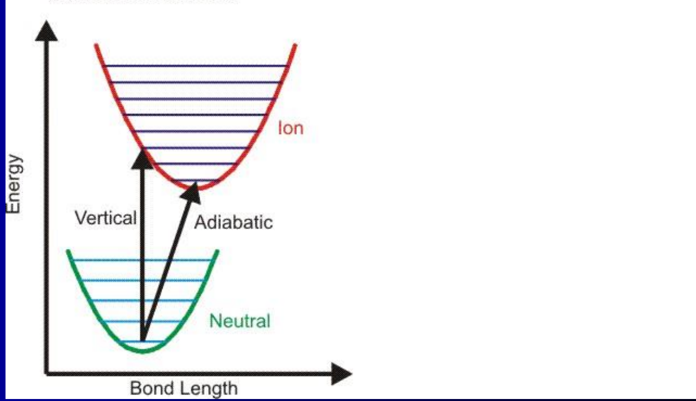

# Ionization cross section $N_2$

BEB
W. Hwang, Y.-K. Kim and M.E. Rudd, J. Chem. Phys. **104**, 2956 (1996).

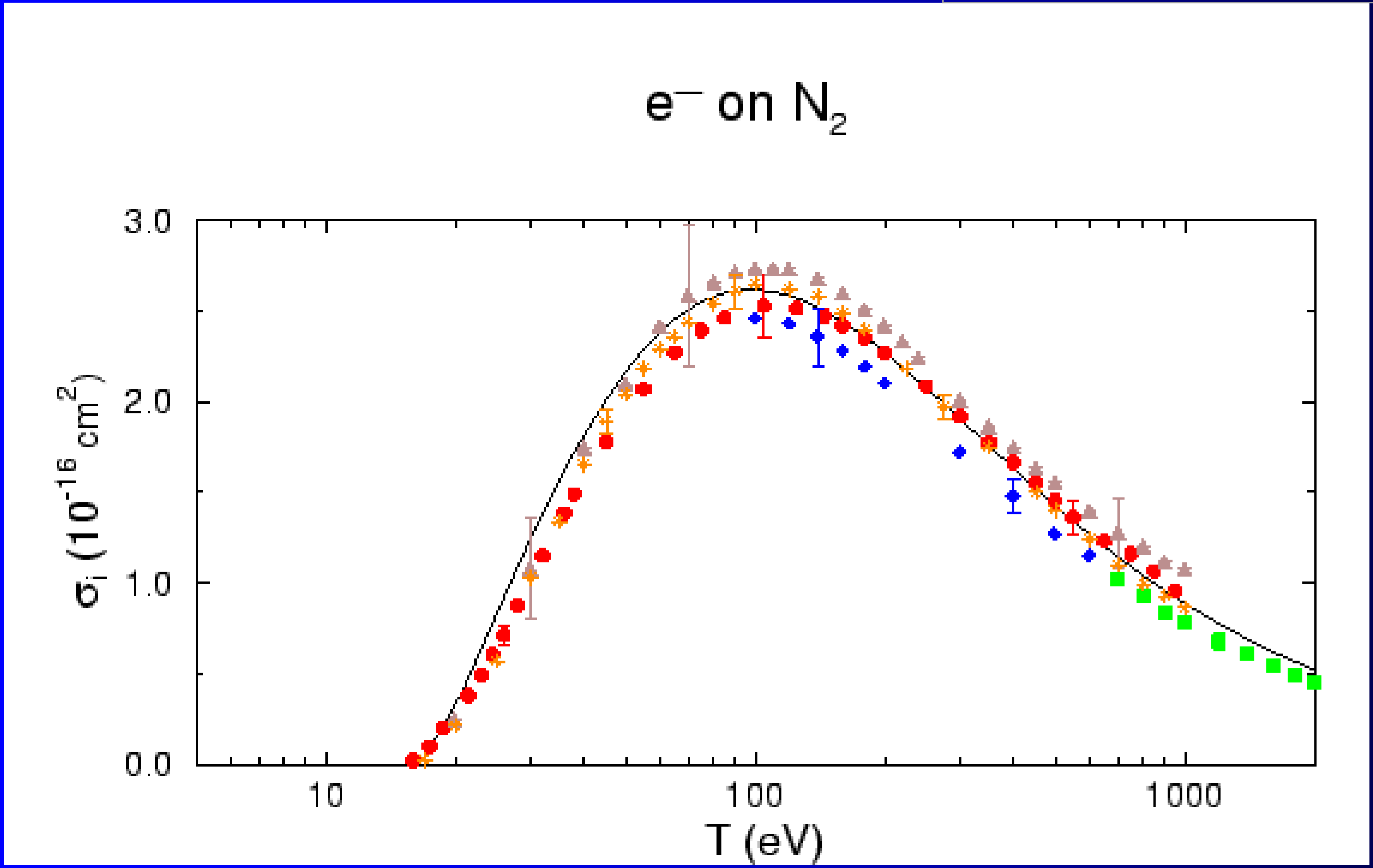

# Ionization cross section -acetylene $C_2H_2$
# Product channels

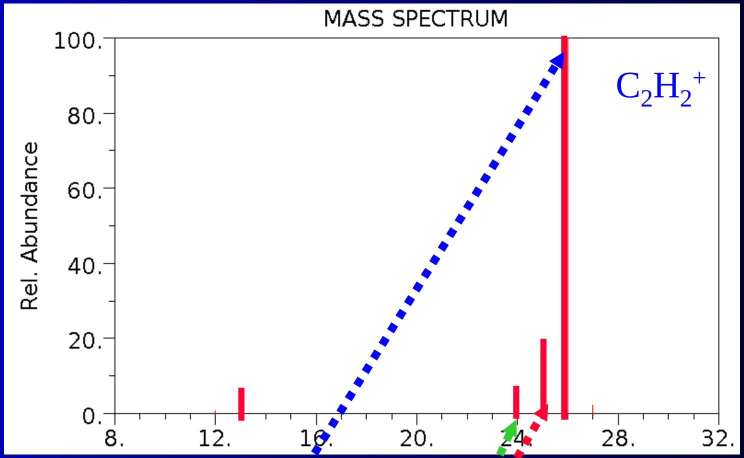


**Pragmatic approach**

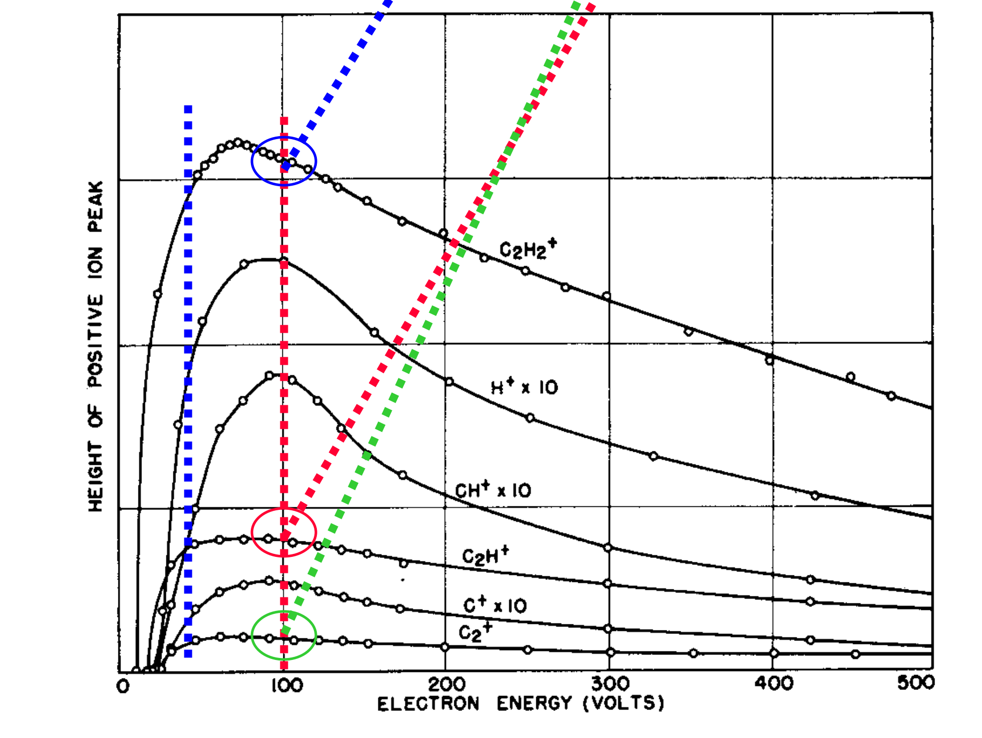


FIG. 6. Ionization efficiency curves for several ions from acetylene (493).

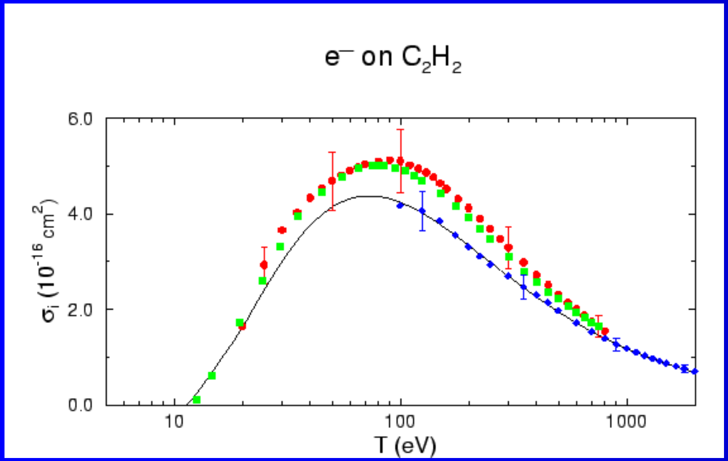

# Ionization cross section data from http://webbook.nist.gov

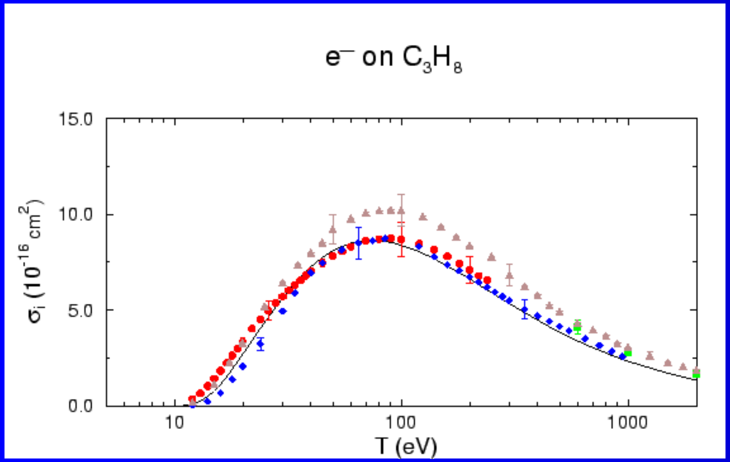


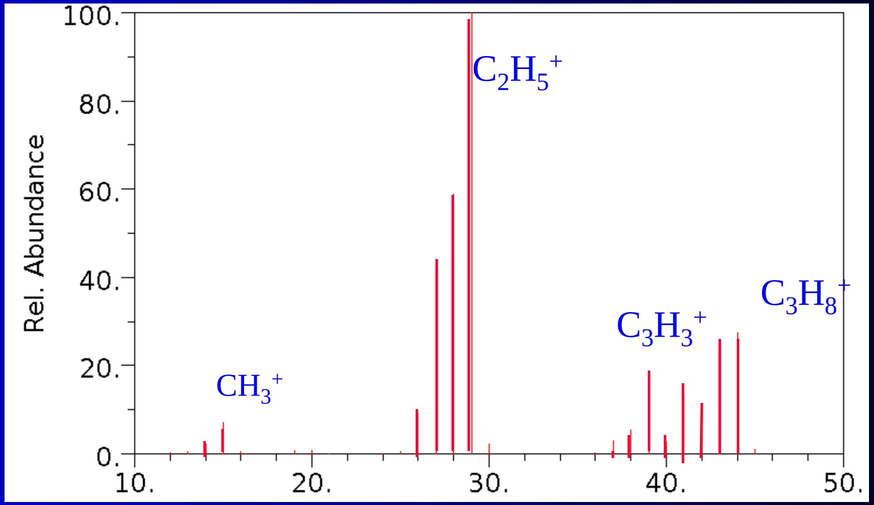


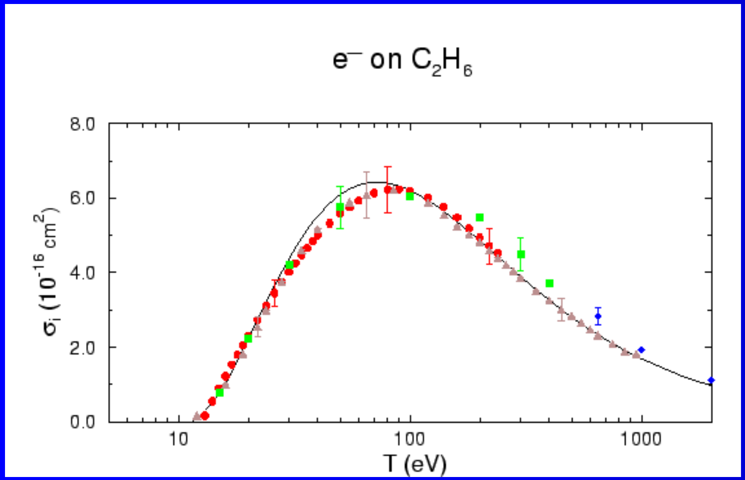


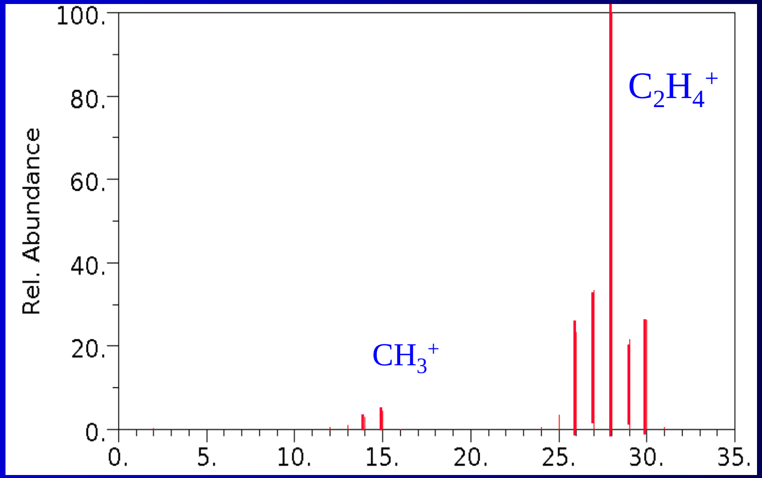


How to recognize spectra ???

# Ionization - EII of $CH_4$

Determination of ionization energies (IEs)

for EII of $CH_4$ for the following reactions:

$$e + CH_4 \rightarrow CH^+_4 + 2e \quad (1)$$

$$\rightarrow CH^+_3 + H + 2e \quad (2a)$$

$$\rightarrow CH^+_3 + H^- + e \quad (2b)$$

$$\rightarrow CH^+_2 + H_2 + 2e \quad (3)$$

$$\rightarrow CH^+ + H + H_2 + 2e \quad (4a)$$

$$\rightarrow CH^+ + H^- + H_2 + e \quad (4b)$$

$$\rightarrow C^+ + 2H_2 + 2e. \quad (5)$$

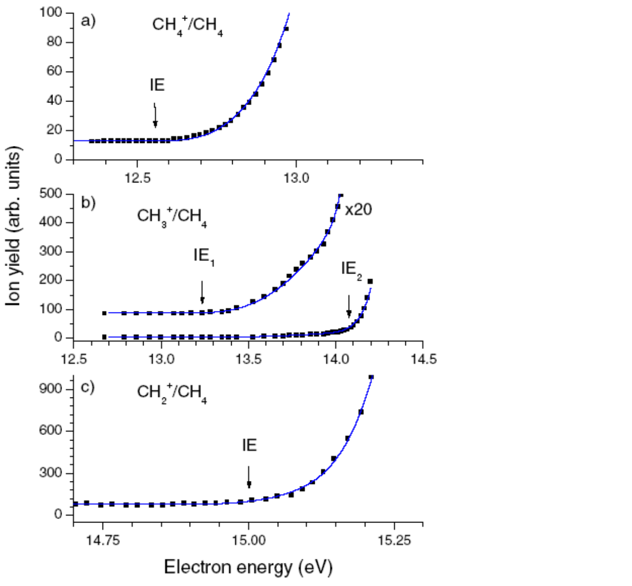


**Figure A.1.** Ion yield curve for $CH_4^+$, $CH_3^+$ and $CH_2^+/CH_4$ obtained through digitalization of the data from [3]. Full curves present fits through these data. Arrows indicate the estimated IEs derived by the fitting procedure.

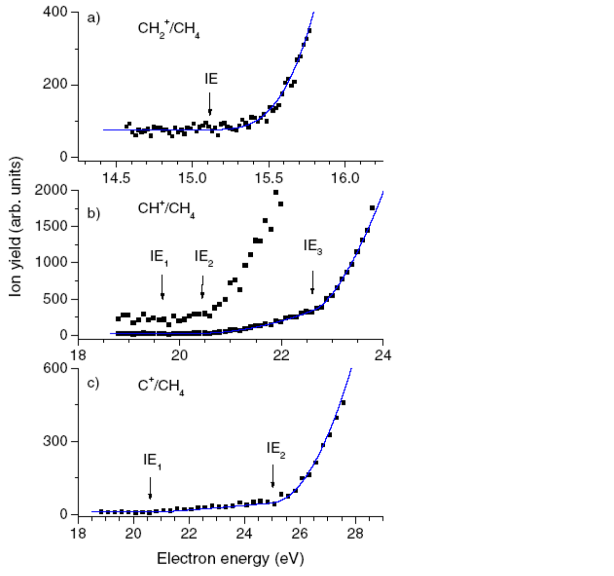


**Figure 5.** Ion yield curve for $CH_2^+$, $CH^+$ and $C^+/CH_4$ as measured at 293 K. Full curves present fits through the experimental data. Arrows indicate the IEs derived by the fitting procedure. Note that for the case of $CH^+$ only $IE_2$ and $IE_3$ have been derived from the present data; $IE_1$ has been calculated from the known EA of H (see text).

$\sigma w(E, \mathbf{p}) =$ 0 for $E < IE_1(Ar)$

$A_1(E - IE1)^{d1}$ for $E > IE_1$ and $E < IE_2$

$A_1(E - IE1)^{d1} + A_2(E - IE2)^{d2}$ for $E > IE_2$

# Ionization of He

Single-ionisation: He + e → $He^{+}$ + 2e

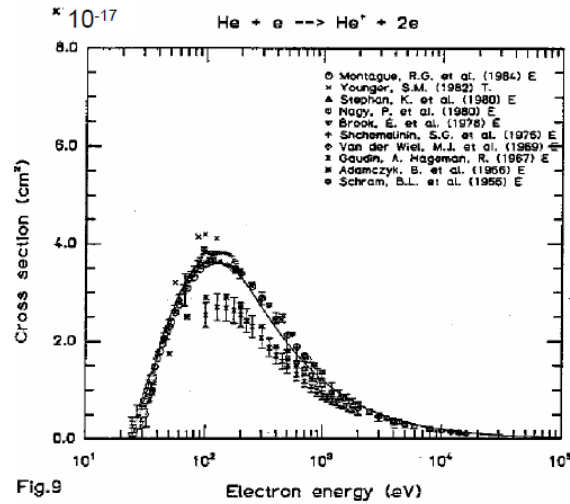


Multi-ionisation: He + e → $He^{2+}$ + 3e

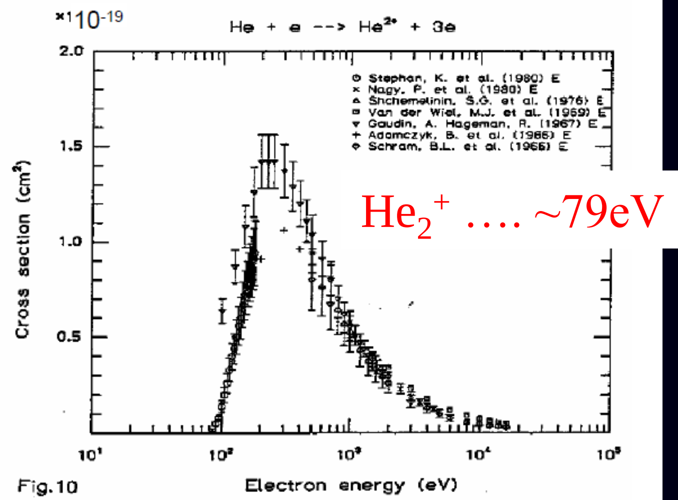


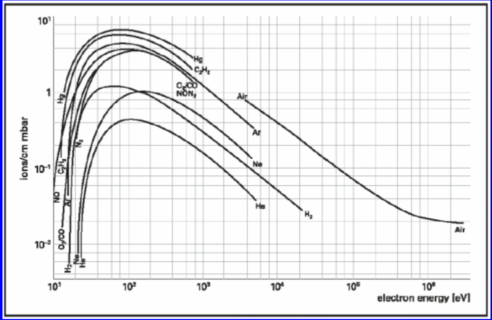


Ionization of the excited state

He (2s) + e → $He^{+}$ + 2e

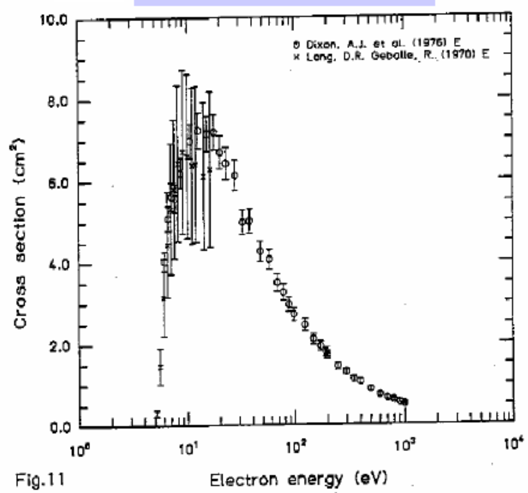


Ionization of singly charged He

$He^{+}$ + e → $He^{2+}$ + 2e

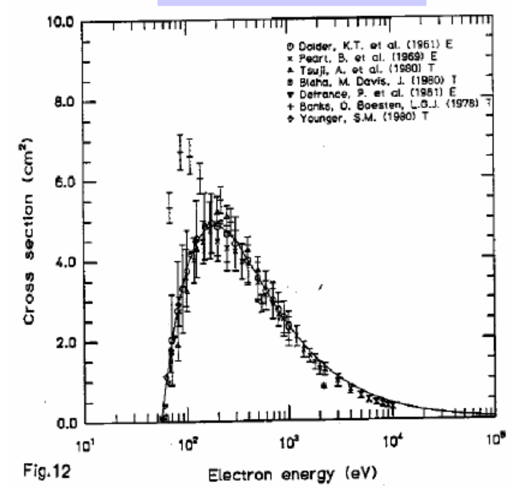

# Multiple ionization

## Multiple ionization of helium and krypton by electron impact close to threshold: appearance energies and Wannier exponents

J. Phys. B: At. Mol. Opt. Phys. **35** (2002) 4685–4694

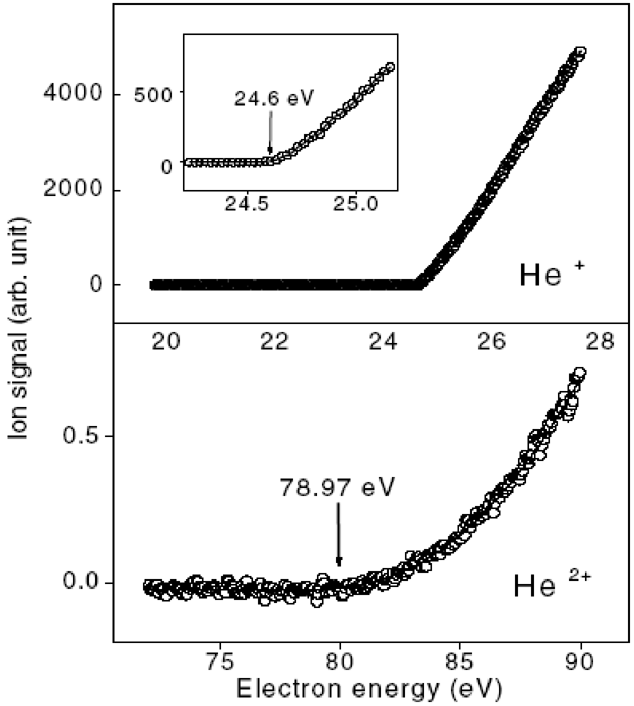


**Figure 1.** Ion signal as a function of electron energy for the formation of $He^+$ ions (top) and $He^{2+}$ ions (bottom) in the near-threshold region. The measured data are shown as open circles, the fits are shown as solid curves. The AEs, which are indicated, are the AEs for the individual data sets shown and may differ from the AE values listed in table 1 which were obtained from a comprehensive analysis of many individual data sets.

**Table 1.** AE values in eV for the formation of $He^+$ and $He^{2+}$ ions in comparison with other measured or calculated AE values.

| | Spectroscopic value [1] | Redhead [45] | This work |
|---|---|---|---|
| $He^+$ | 24.59 | — | $24.6 \pm 0.15$ |
| $He^{2+}$ | 79.00 | 77.58 | $79.05 \pm 0.3$ |

He2+ …. ~79eV

# Multiple ionization

## Multiple ionization of helium and krypton by electron impact close to threshold: appearance energies and Wannier exponents

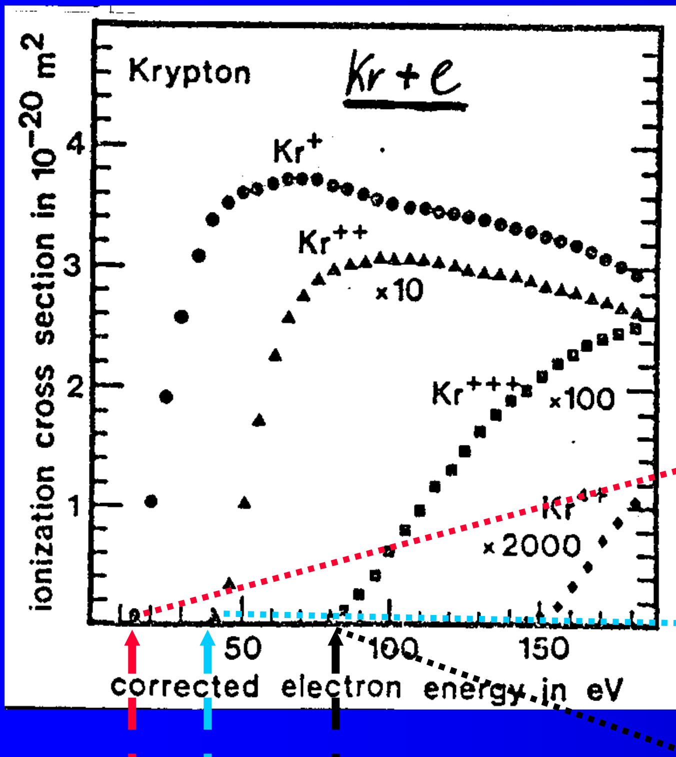


J. Phys. B: At. Mol. Opt. Phys. **35** (2002) 4685–4694

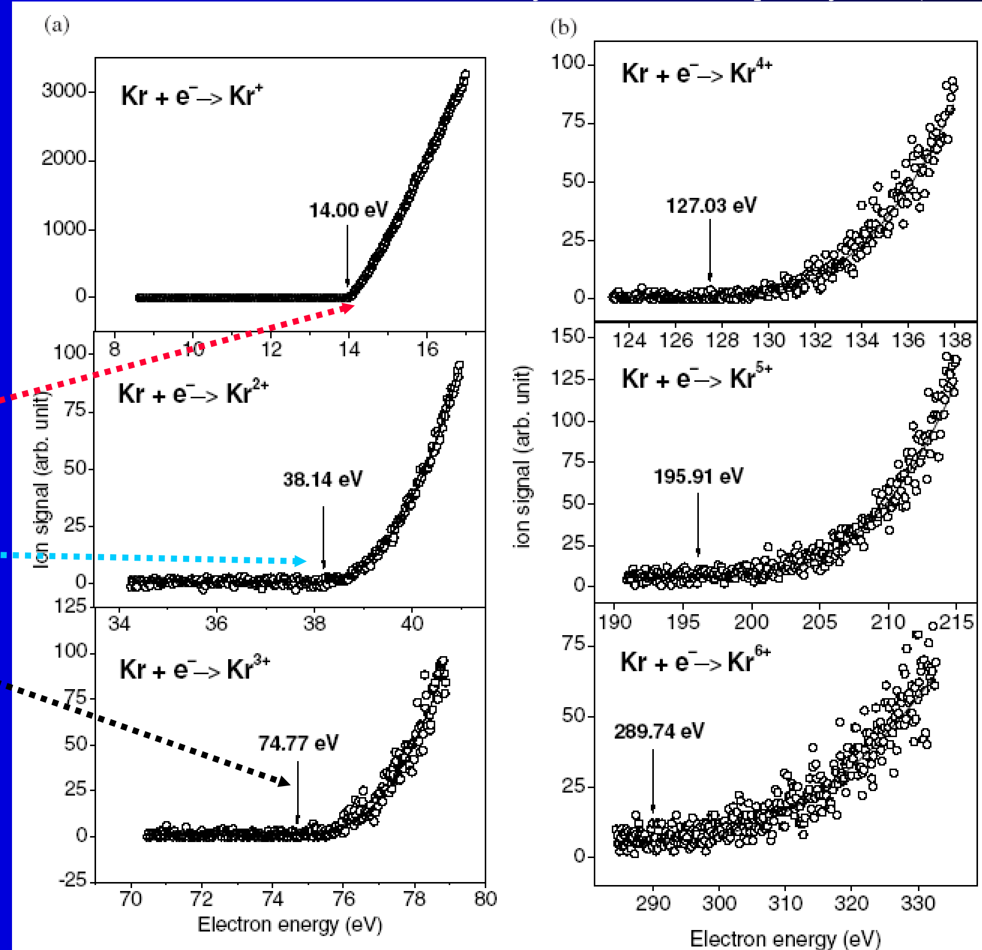


**Figure 2.** Ion signal as a function of electron energy for the formation of $Kr^{n+}$ ions ($n = 1$–6) in the near-threshold region. The measured data are shown as open circles, the fits are shown as solid curves. The AEs, which are indicated, are the AEs for the individual data sets shown and may differ from the AE values listed in table 2 which were obtained from a comprehensive analysis of many individual data sets.

# Multiple ionization

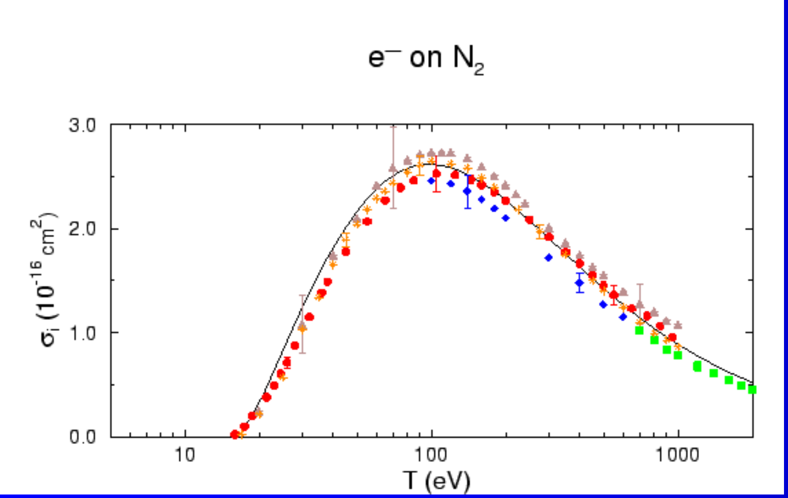


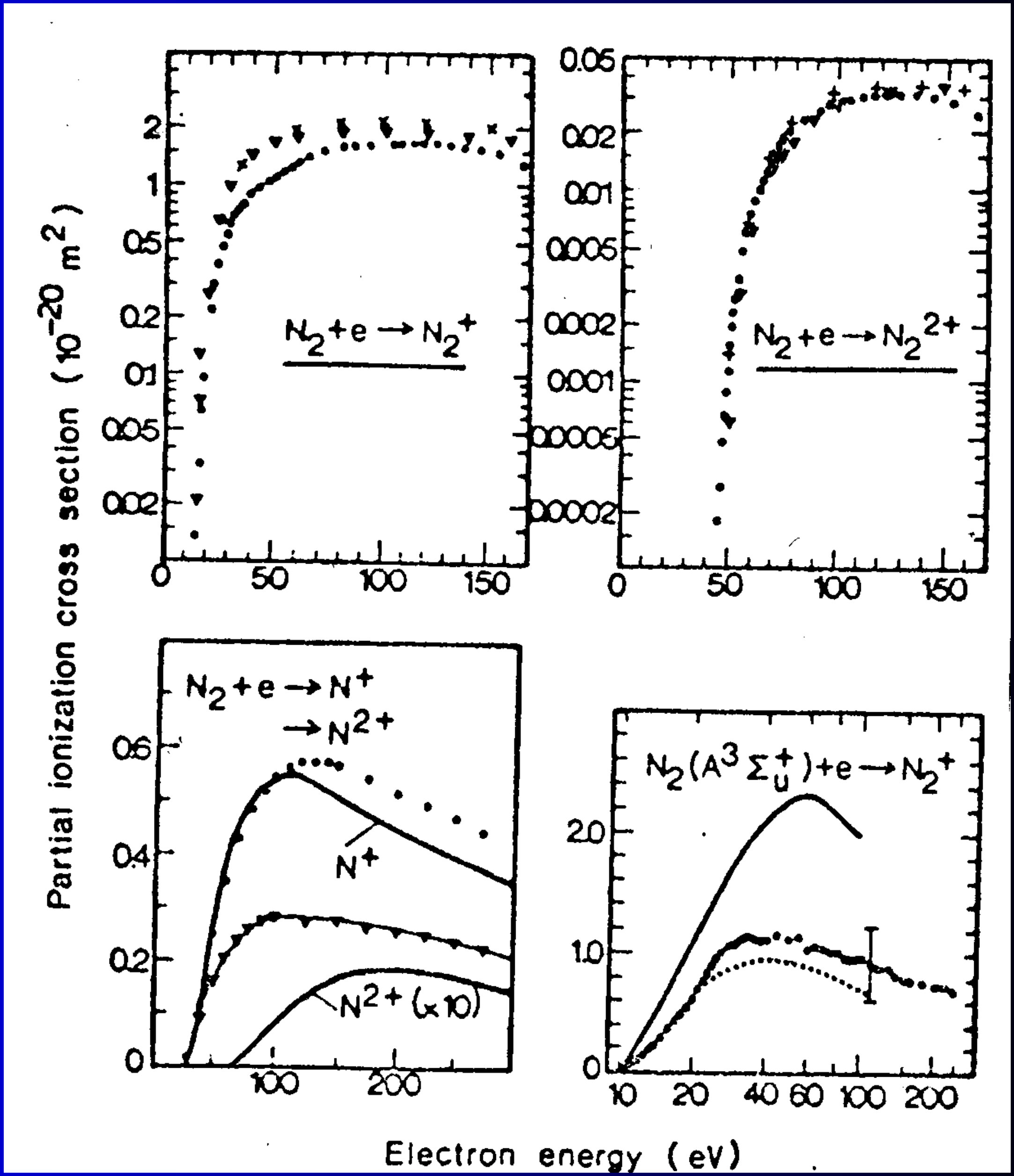

# Ionization of clusters

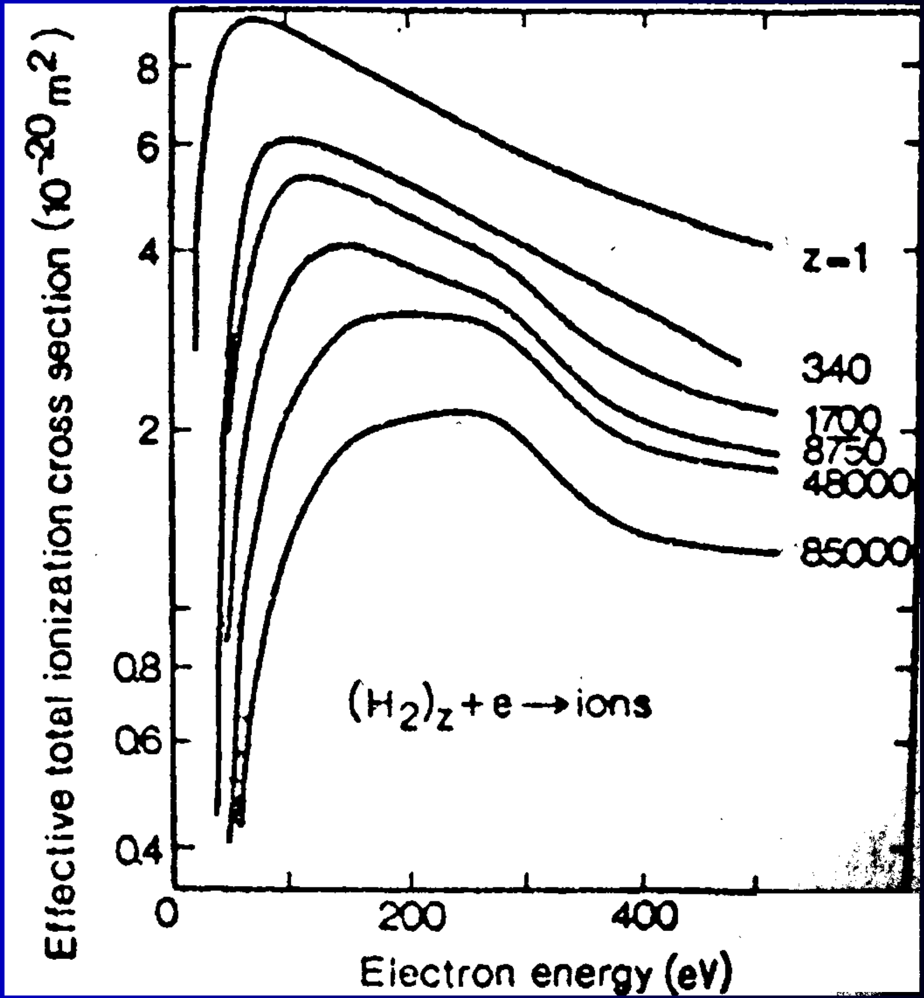


$(H_2)_Z + e \rightarrow$ ions

$\sigma_{average\ total} = Z.\ \sigma_{effective}$

# Ionization of C60 Fulleren

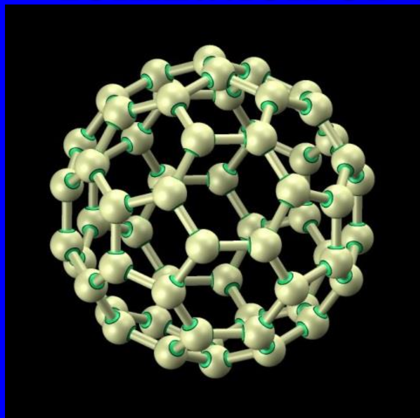

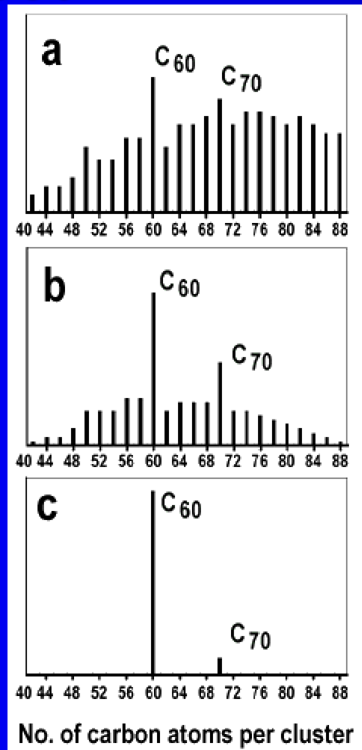


$$e^- + C_{60} \longrightarrow C_{60}^{+} + 2e^-$$

$$e^- + C_{60}^{+} \longrightarrow C_{60}^{2+} + 2e^-$$

$$e^- + C_{60}^{2+} \longrightarrow C_{60}^{3+} + 2e^-$$

$$e^- + C_{60}^{3+} \longrightarrow C_{60}^{4+} + 2e^-$$

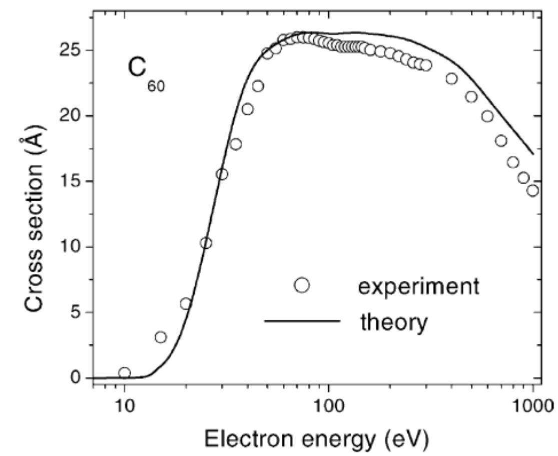


Fig. 6. Cross-section for the formation of $C_{60}^{+}$ ions following electron-impact single ionization of $C_{60}$. The experimental data (○) are from Ref. [18], the solid line represents the present calculation.

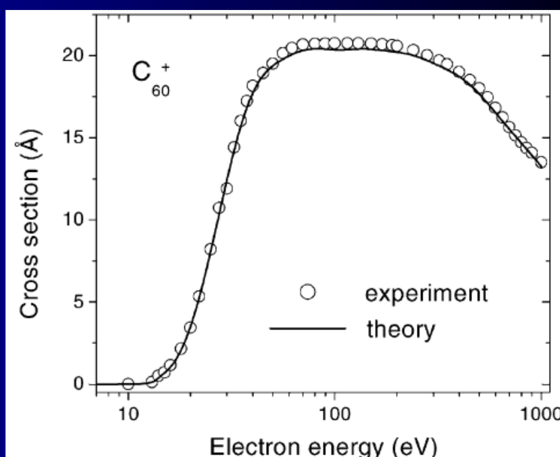


Fig. 3. Cross-section for the formation of $C_{60}^{2+}$ ions following electron-impact single ionization of $C_{60}^{+}$. The experimental data (○) are from Ref. [23], the solid line represents the present calculation.

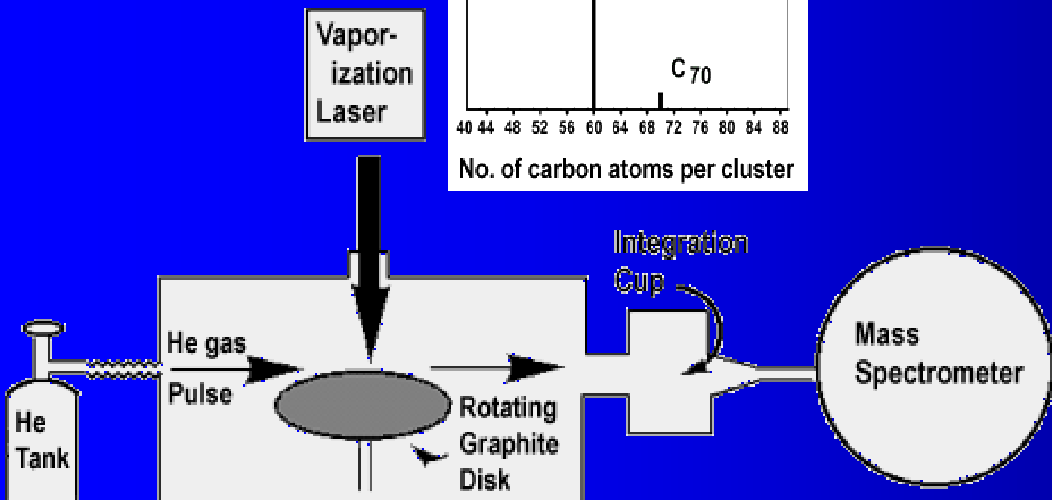


Distribution of carbon clusters produced under various experimental conditions.

a) Low helium density over graphite target at time of laser vaporization.

b) High helium density over graphite target at time of laser vaporization.

c) Same as b), but with addition of "integration cup" to increase time between vaporization and cluster analysis.

PHYSICAL REVIEW LETTERS 23 OCTOBER 2000

# Electron-Impact Induced Fragmentation of Fullerene Ions

The measurements were performed employing the electron-ion crossed-beam setup. A commercially available powder of fullerenes was evaporated with an electrically heated oven. The neutral vapor was introduced into a 10 GHz Electron Cyclotron Resonance Ion Source (ECRIS). The extracted ion beam was collimated to 2x2 $mm^2$ after mass to charge analysis and crossed with an intense electron beam. The energy of the electrons can be varied between 10 and 1000 eV. After the electron-ion interaction the fragment ions $C_{58}{}^{q+}$ were separated from the incident ion beam of $C_{60}{}^{q+}$ by a $90^0$ magnet and detected by a single-particle detector. The flight time between the interaction of the $C_{60}{}^{q+}$ ions and the analysis of the product ions is in the order of 10 μs. The current of the parent ion beam was measured simultaneously in a Faraday cup.

## Binding energy value of about 11 eV

$$e^- + C_{60}{}^{+} \rightarrow C_{58}{}^{+} + C_2 + e^-$$

$$e^- + C_{60}{}^{2+} \rightarrow C_{58}{}^{2+} + C_2 + e^-$$

$$e^- + C_{60}{}^{3+} \rightarrow C_{58}{}^{3+} + C_2 + e^-$$

## IONIZATION

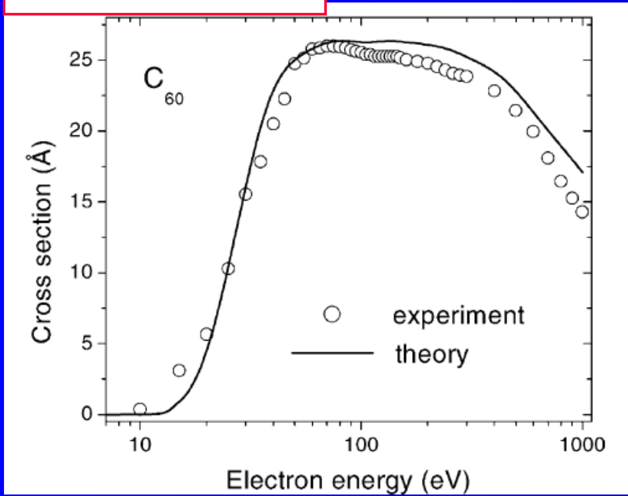


## FRAGMENTATION

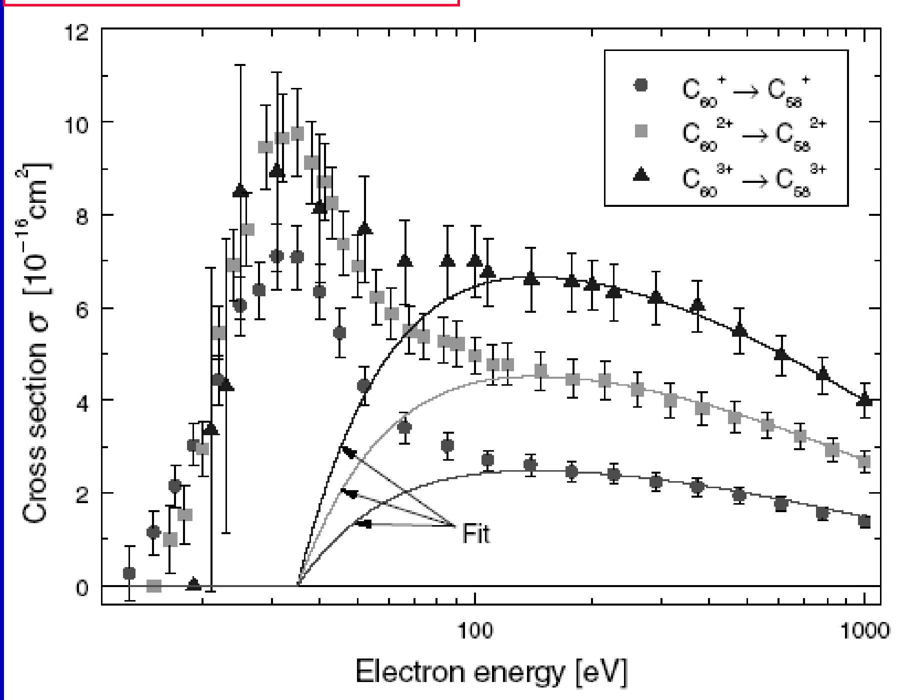


**Absolute cross sections s for the electron-impact induced $C_2$ fragmentation of $C_{60}{}^{q+}$ ions.**

# Electron-Impact Induced Ionization of Fullerene Ions

IONIZATION

A semi-empirical concept for the calculation of electron-impac
ionization cross-sections of neutral and ionized fullerenes

International Journal of Mass Spectrometry 223–224 (2003) 1–8

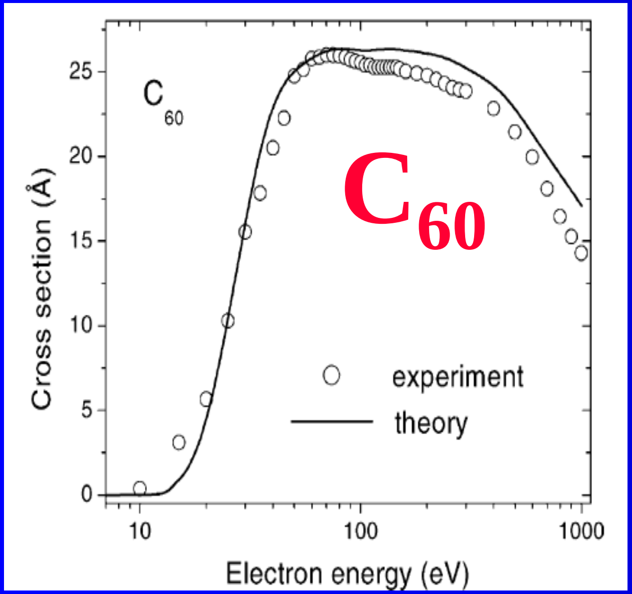


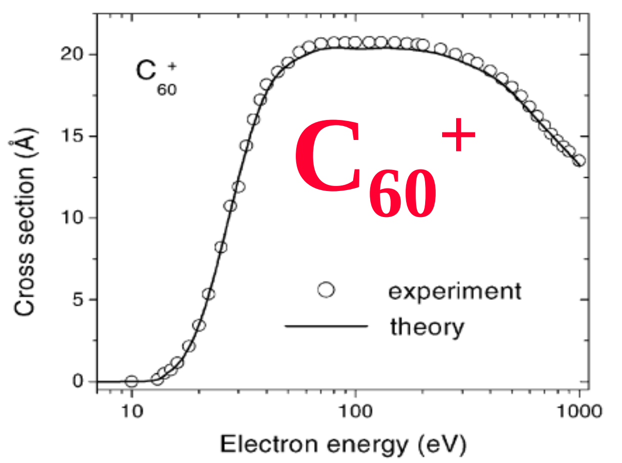


Fig. 3. Cross-section for the formation of $C_{60}^{2+}$ ions following electron-impact single ionization of $C_{60}^{+}$. The experimental data (○) are from Ref. [23], the solid line represents the present calculation.

$C_{60}^{3+}$

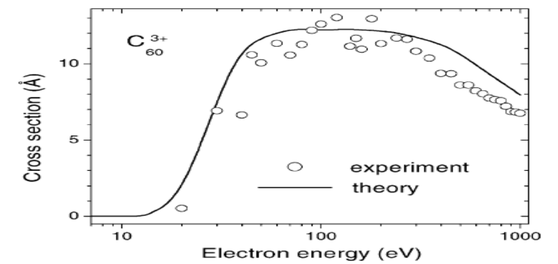


Fig. 4. Cross-section for the formation of $C_{60}^{4+}$ ions following electron-impact single ionization of $C_{60}^{3+}$. The experimental data (○) are from Ref. [23], the solid line represents the present calculation.

# Cross sections for vibrational excitation, dissociation, ionization… $H_2$

| | | | |
|---|---|---|---|
| $H_2 + e$ | → | $H_2(v) + e$ ……. | Vibrational excitation |
| | → | $H + H + e$……. | Dissociation |
| | → | $H_2^* + h\nu + e$ … | Photon excitation |
| | → | $H_2^+ + e + e$….. | Ionization |
| | → | $H^+ + H + e + e$ | Dissociative Ionization |

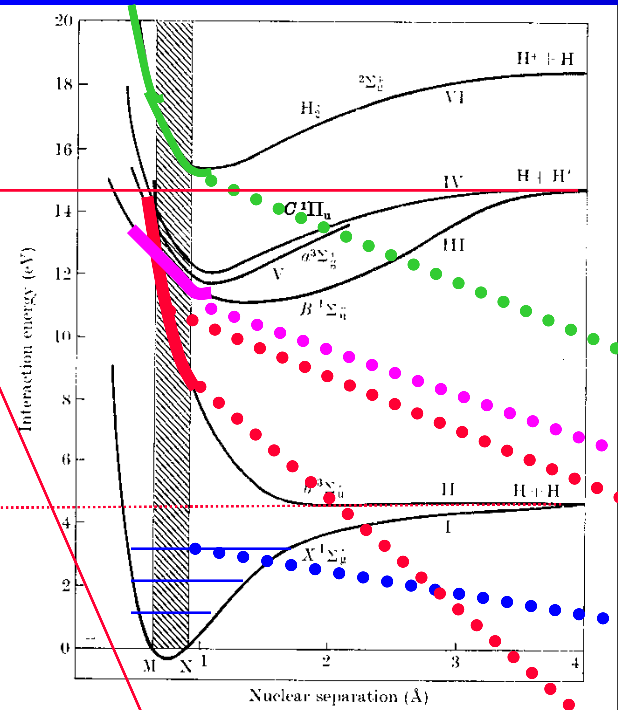


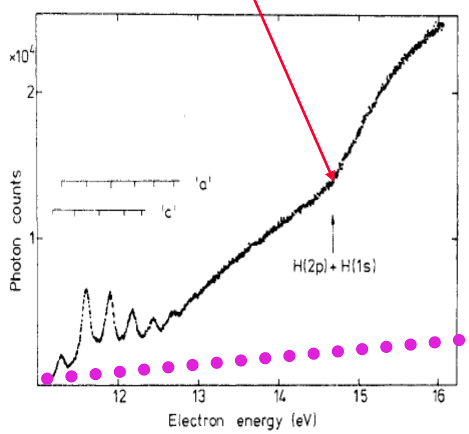


**Figure 3.** Optical excitation function for VUV photons measured with channeltron and $MgF_2$ window (1120–1300 Å); pressure $4 \times 10^{-7}$ bar; collection time 7 h; 4·9 meV/channel. Energy positions of known resonances are indicated. The dissociation energy for H(2p) + H(1s) is marked by an arrow.

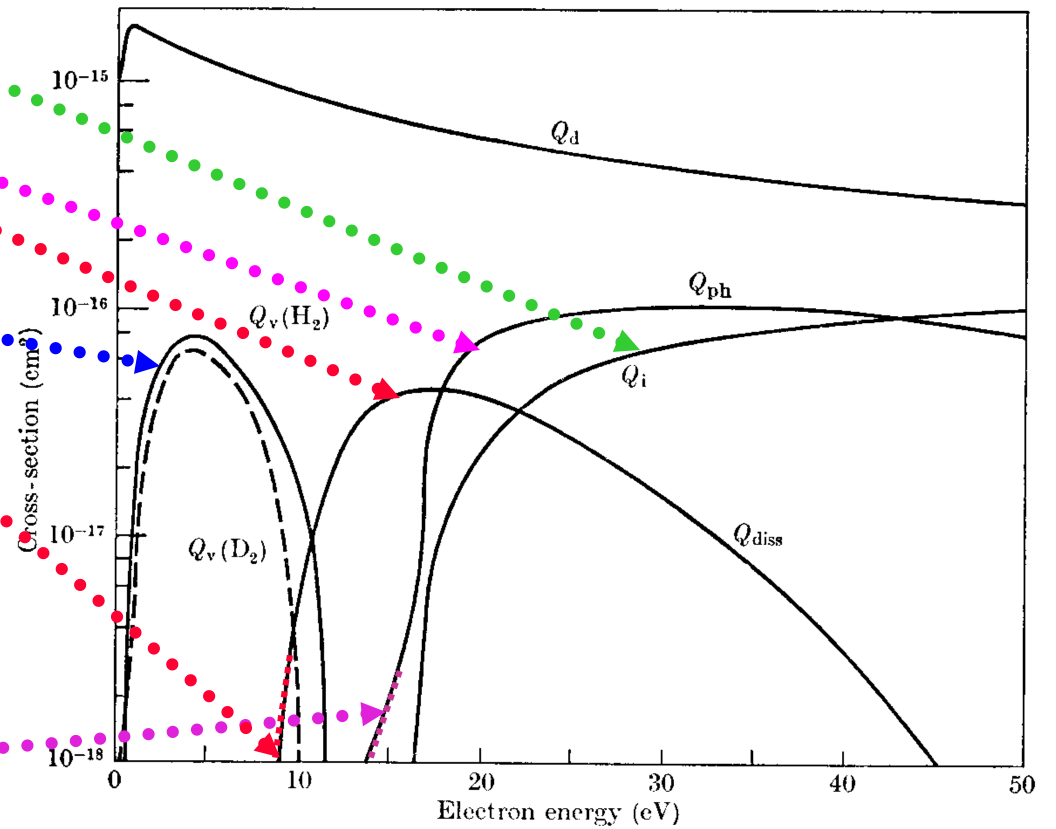


FIG. 13.37. Cross-sections assumed by Engelhardt and Phelps in their analysis of swarm data in $H_2$ and $D_2$ for electrons of characteristic energy greater than 1 eV. $Q_d$ momentum-transfer cross-section, $Q_i$, ionization cross-section, $Q_{diss}$ dissociation cross-section, $Q_{ph}$ photon excitation cross-section, $Q_v$ vibrational excitation cross-section (—— $H_2$, – – – $D_2$).

# Cross sections for ionization…$H_2$

$H_2$ + e → $H_2(v)$ + e ……. **Vibrational excitation**

→ H + H +e……. **Dissociation**

→ $H_2^*$ + hν + e … **Photon excitation**

→ $H_2^+$ +e + e….. **Ionization**

→ $H^+$ + H + e + e

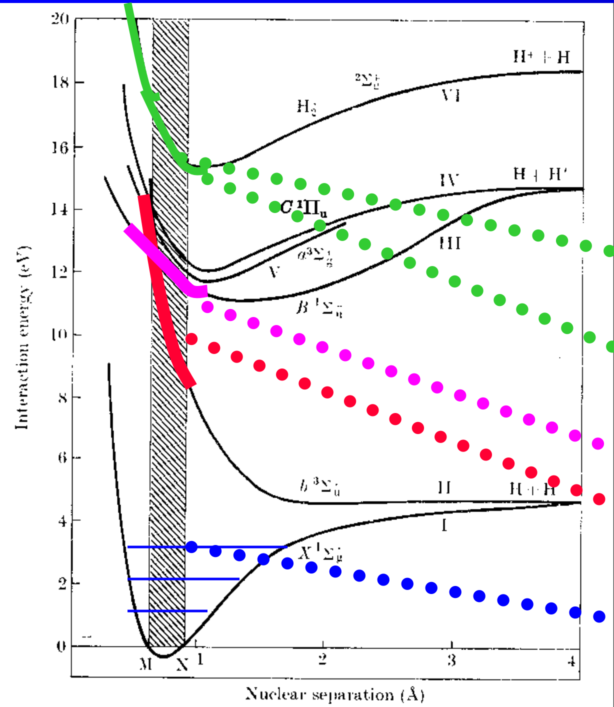


Fig. 13.1. Potential energy curves for electronic states of $H_2$ and

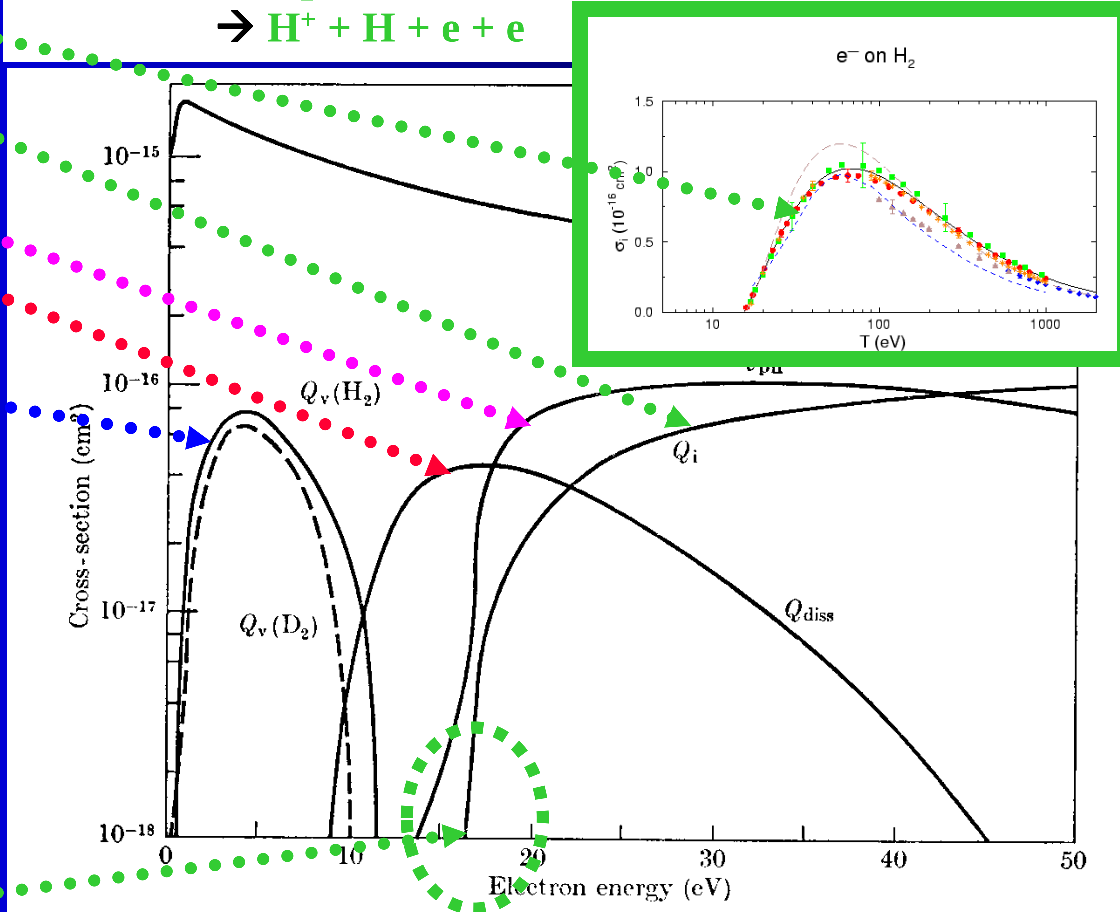


Fig. 13.37. Cross-sections assumed by Engelhardt and Phelps in their analysis of swarm data in $H_2$ and $D_2$ for electrons of characteristic energy greater than 1 eV. $Q_d$ momentum-transfer cross-section, $Q_i$, ionization cross-section, $Q_{diss}$ dissociation cross-section, $Q_{ph}$ photon excitation cross-section, $Q_v$ vibrational excitation cross-section (—— $H_2$, – – – $D_2$).

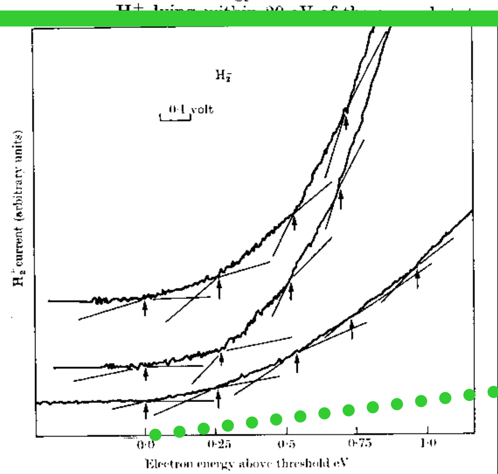


Fig. 13.19. Variation of the ionization cross-section of $H_2$ near the threshold as observed by Marmet and Kerwin.

# High efficiency
# Grid ion source

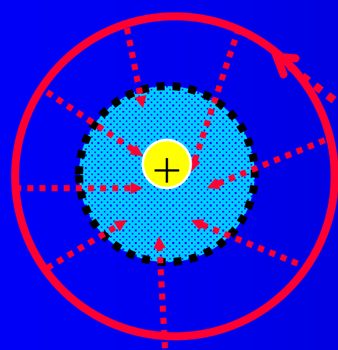

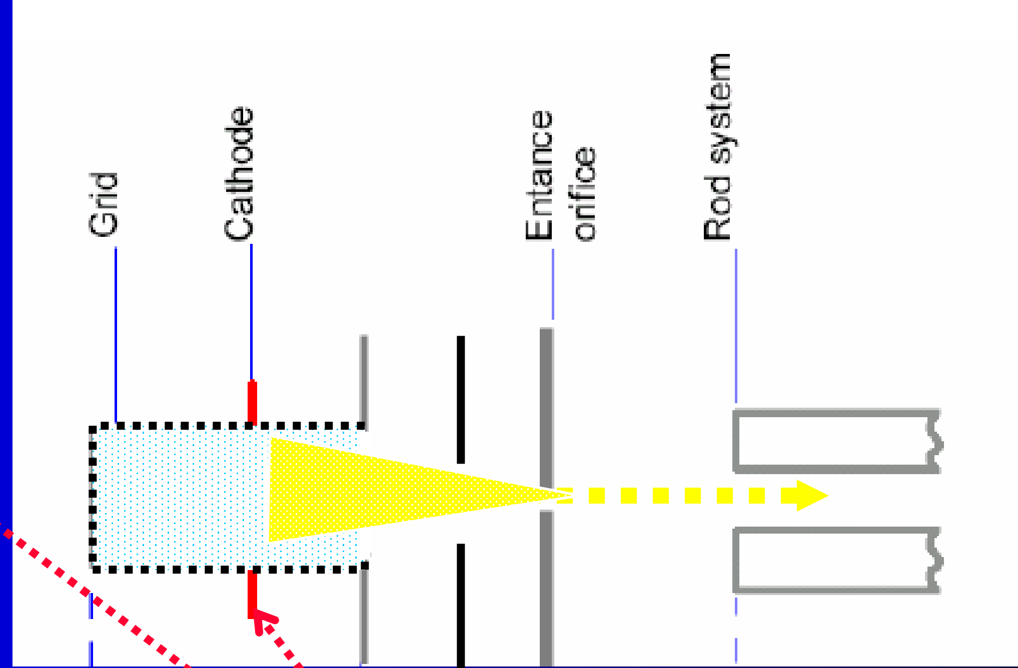


**Ion optics** **Mass filter**

**Filament**

Grid ion source

- Open design
- Two filaments (W)
- Low degassing rate
  - mimimum amount of material
  - Pt-Ir wires for formation chamber
  - Molybdenum filament holders
- Easy to degas via electron bombardment
- Filaments on positive potential

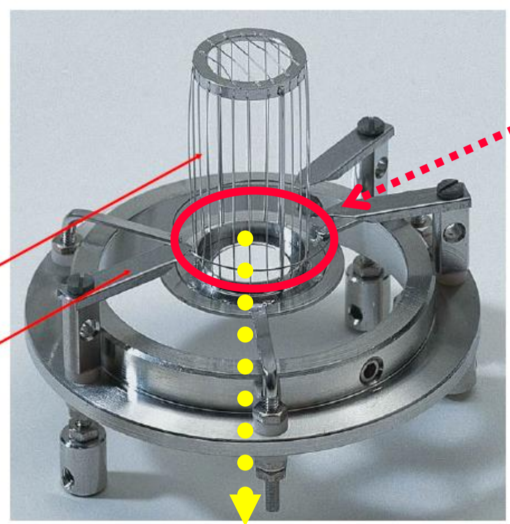

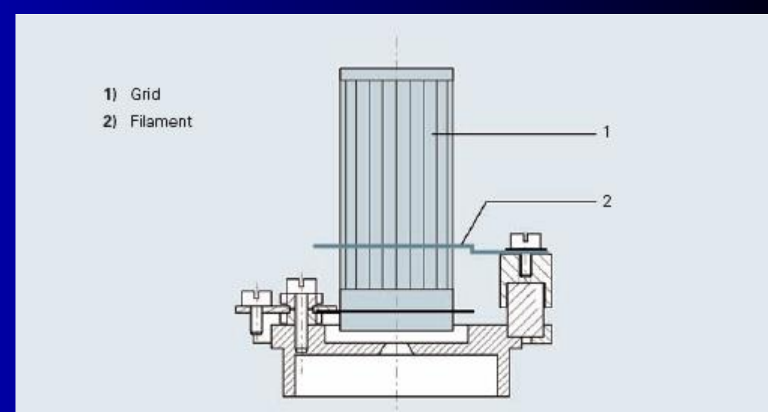

# Flight paths of electrons

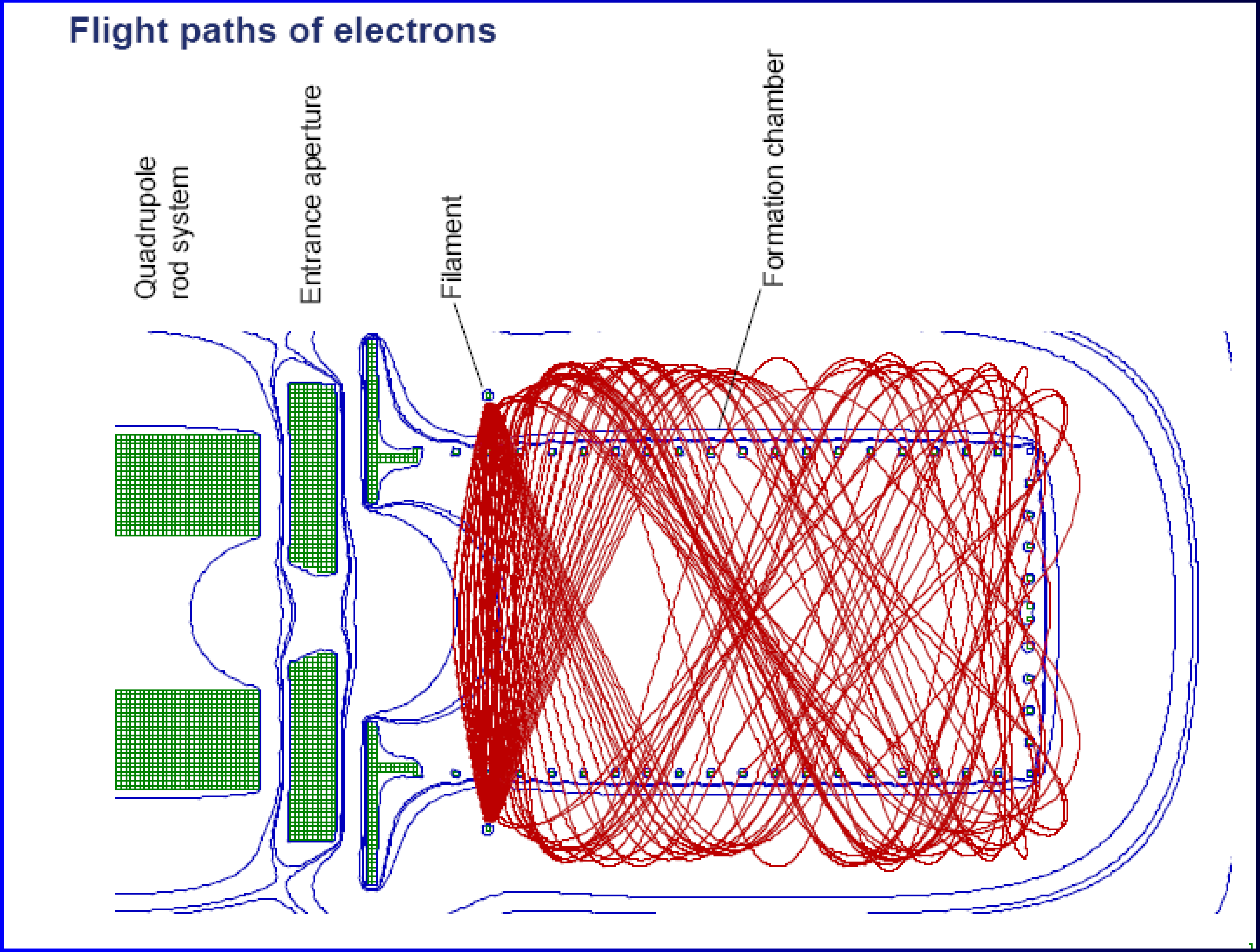

# Flight paths of positive ions

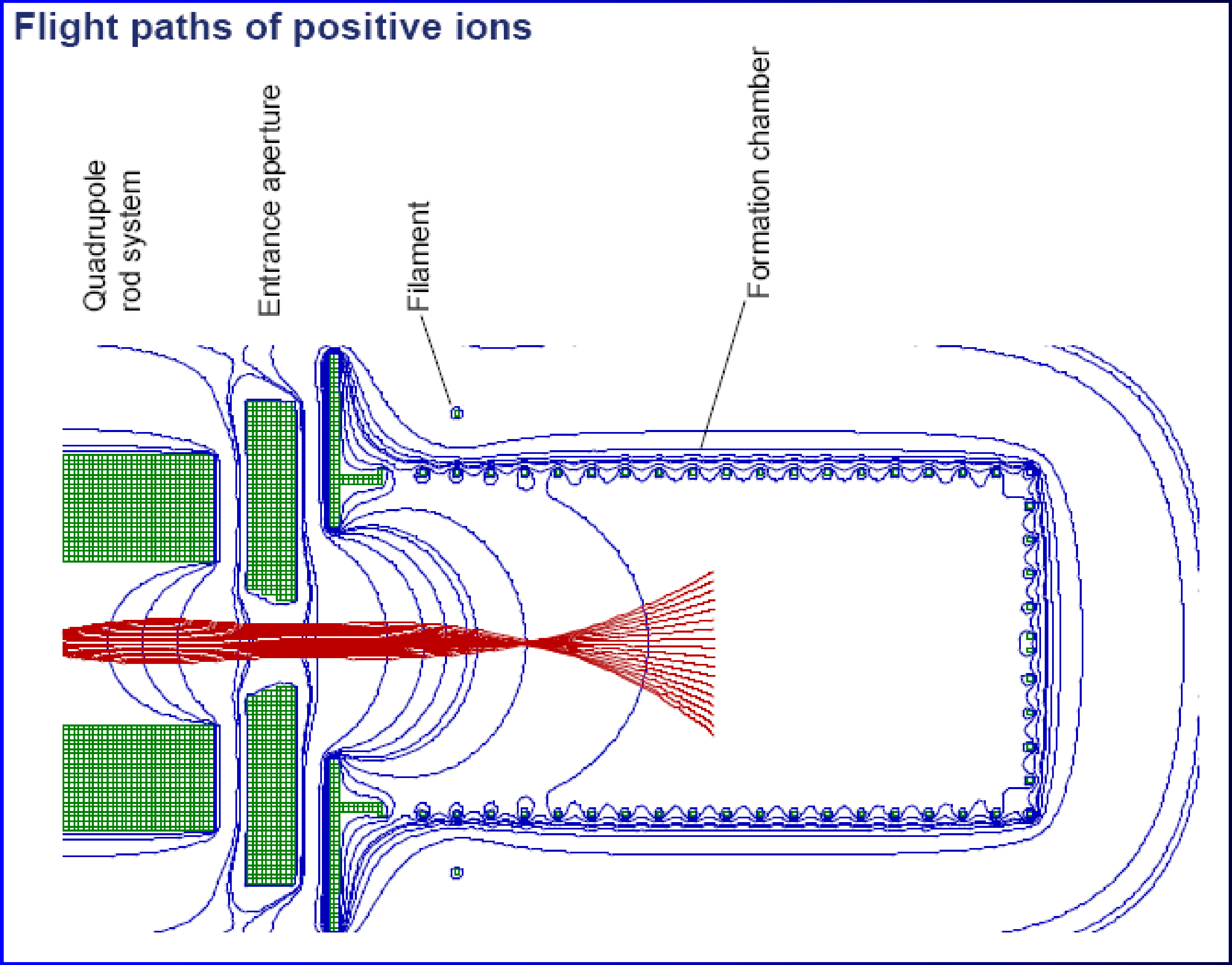

# Cross Beam ion Source, calculations

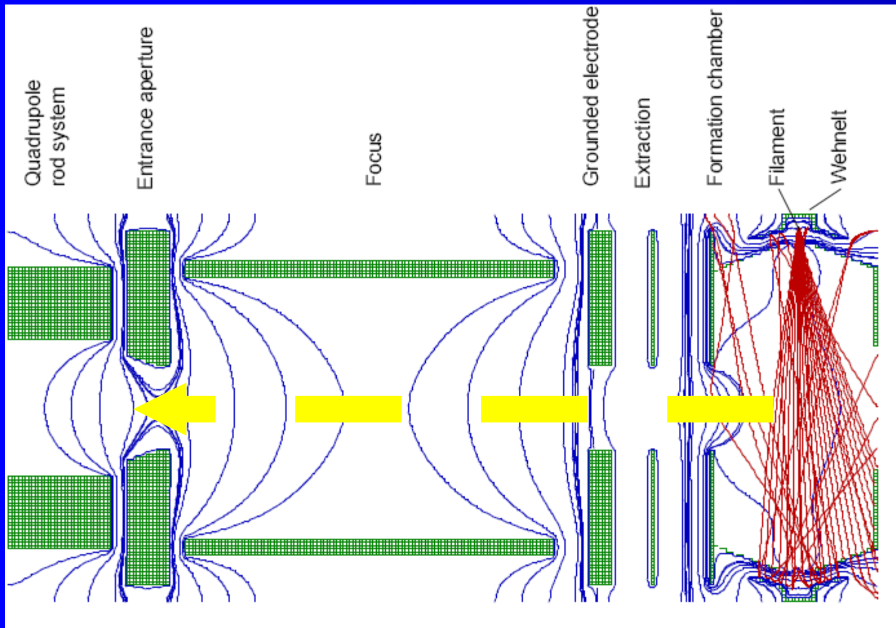


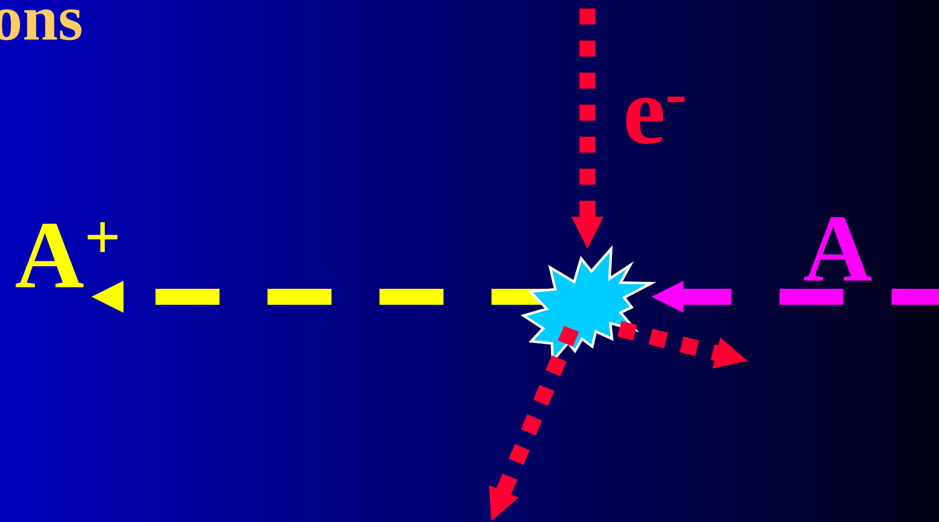


## Crossbeam ion source

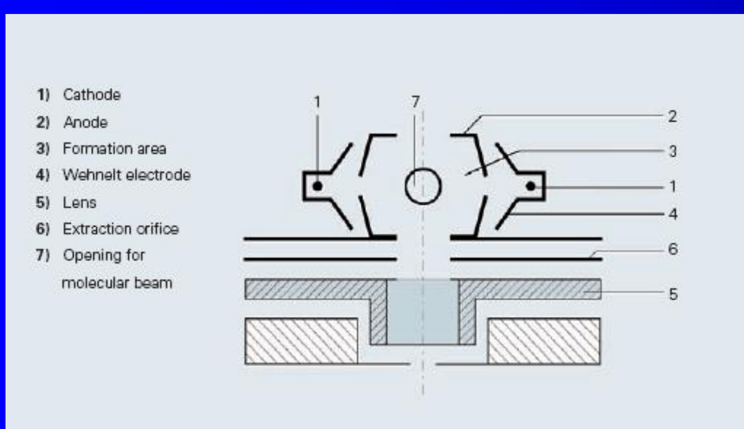


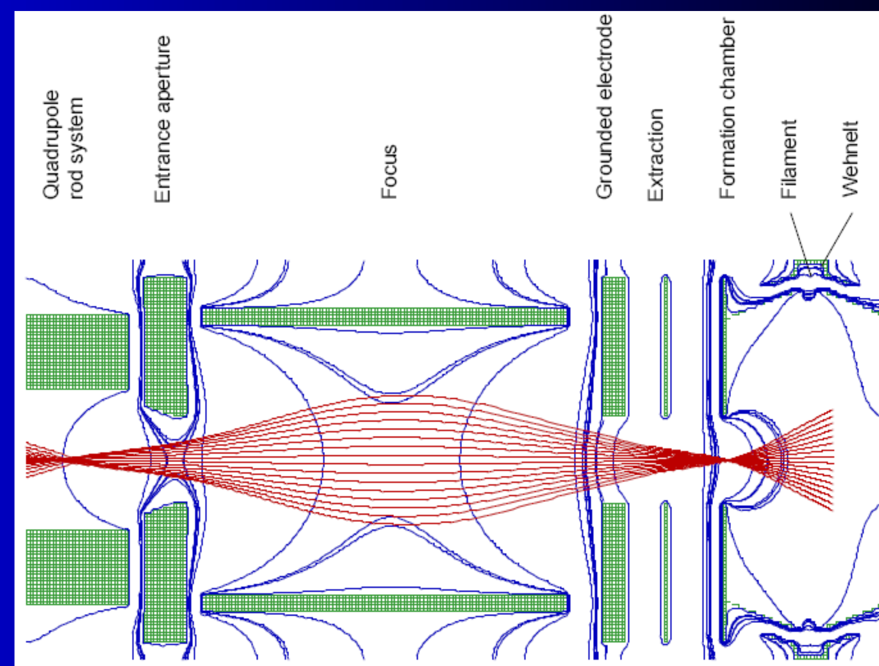

# Cross Beam ion Source

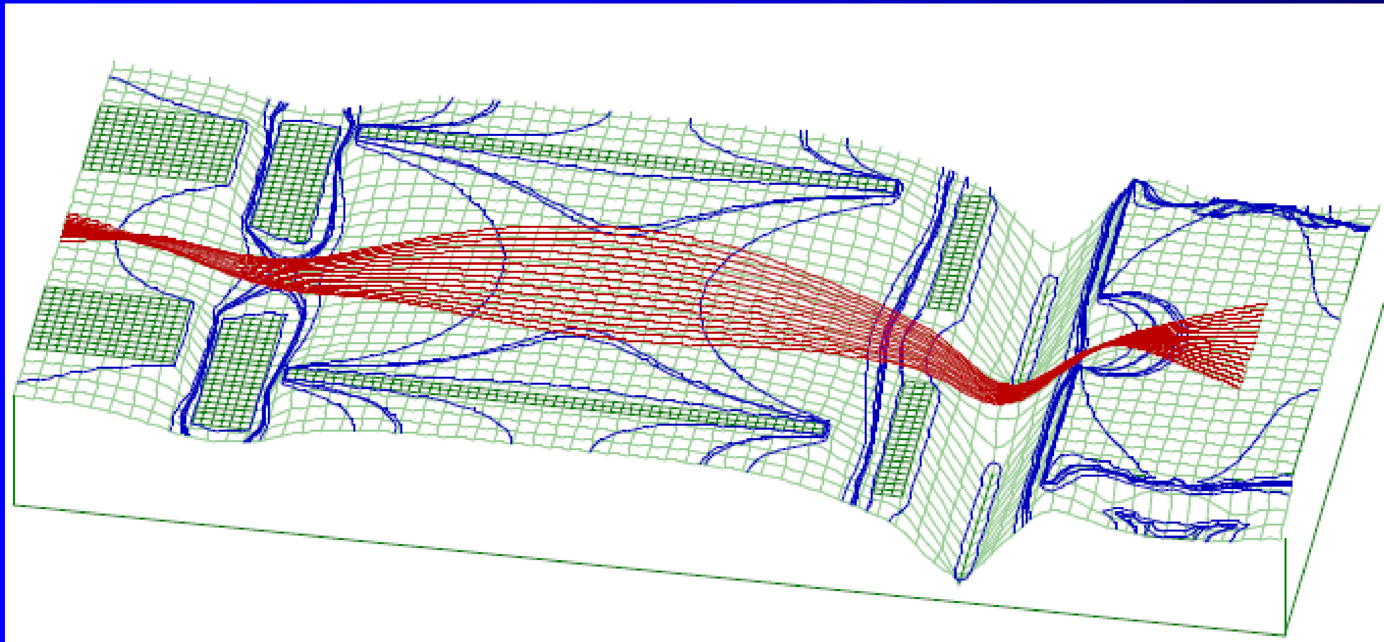

Cross Beam ion source
with magnets

- Two filaments
- Easy to degas
- Good ion focussing
- Bakeable to 300°C

# Mass spectrometer

16 mm rod system for highest resolution, stability and transmission (e.g. $He/D_2$ separation)

8 mm rod system for High-End RGA and analytical applications

6 mm rod system for common RGA

90° off axis arrangement

efficient suppression of

- photons
- fast neutral particles
- stray ions

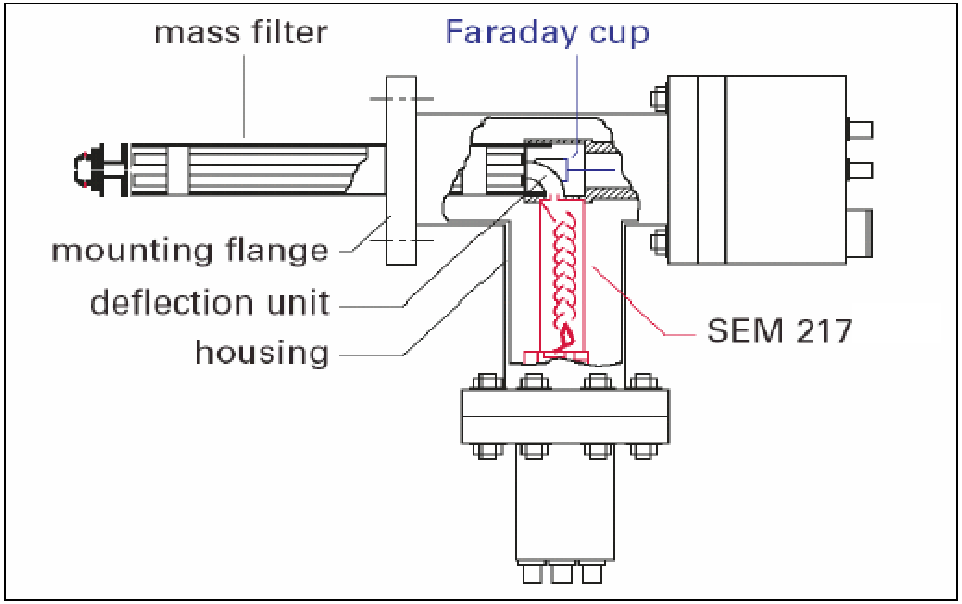

# Ion detector – Discrete dynode SEM

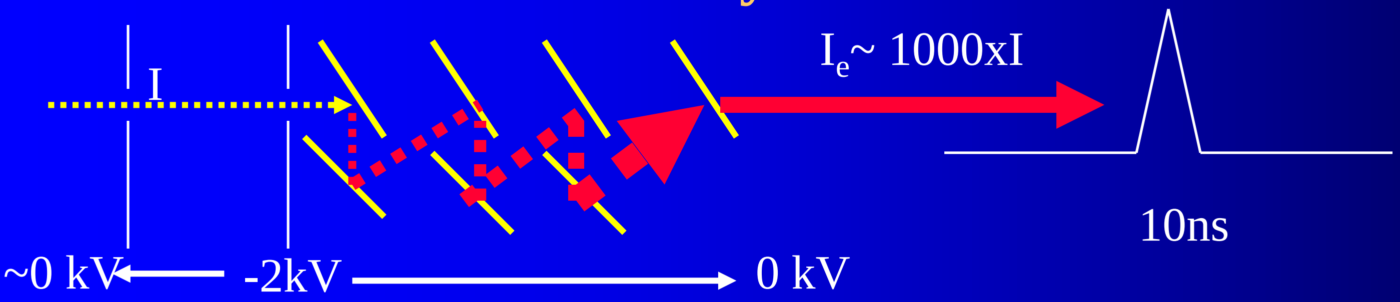


- Ion Detection
  - Discrete Dynode SEM
  - Bakeable to 400°C
  - for analog amplification and for pulse counting
  - Low noise (< 0.1 cps)

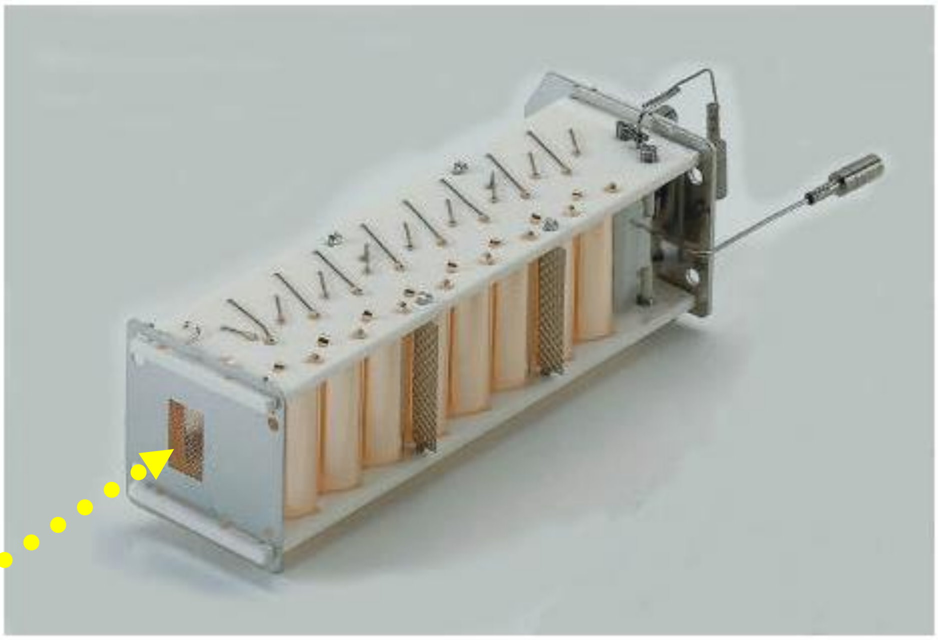

IONS

# QMA

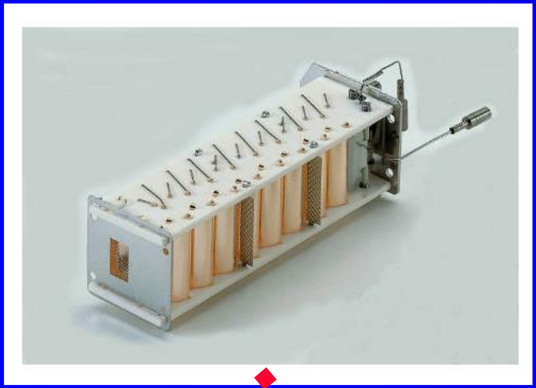

90° off axis arrangement

efficient suppression of

- photons
- fast neutral particles
- stray ions

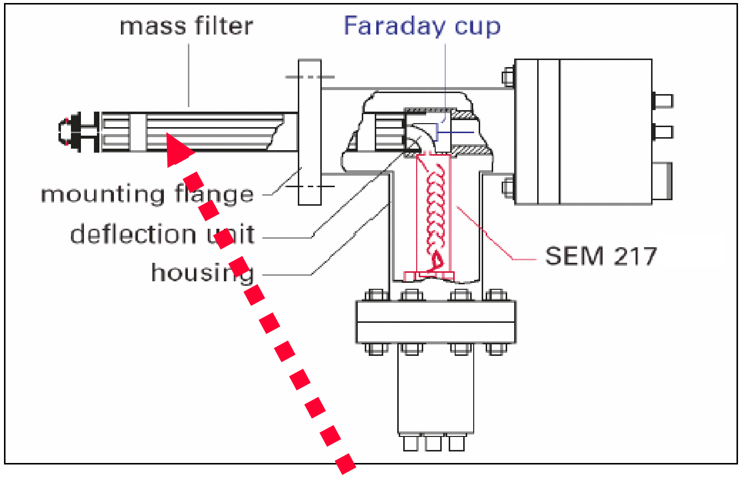


QMA 410 with Cross Beam ion source and 90° off axis SEM

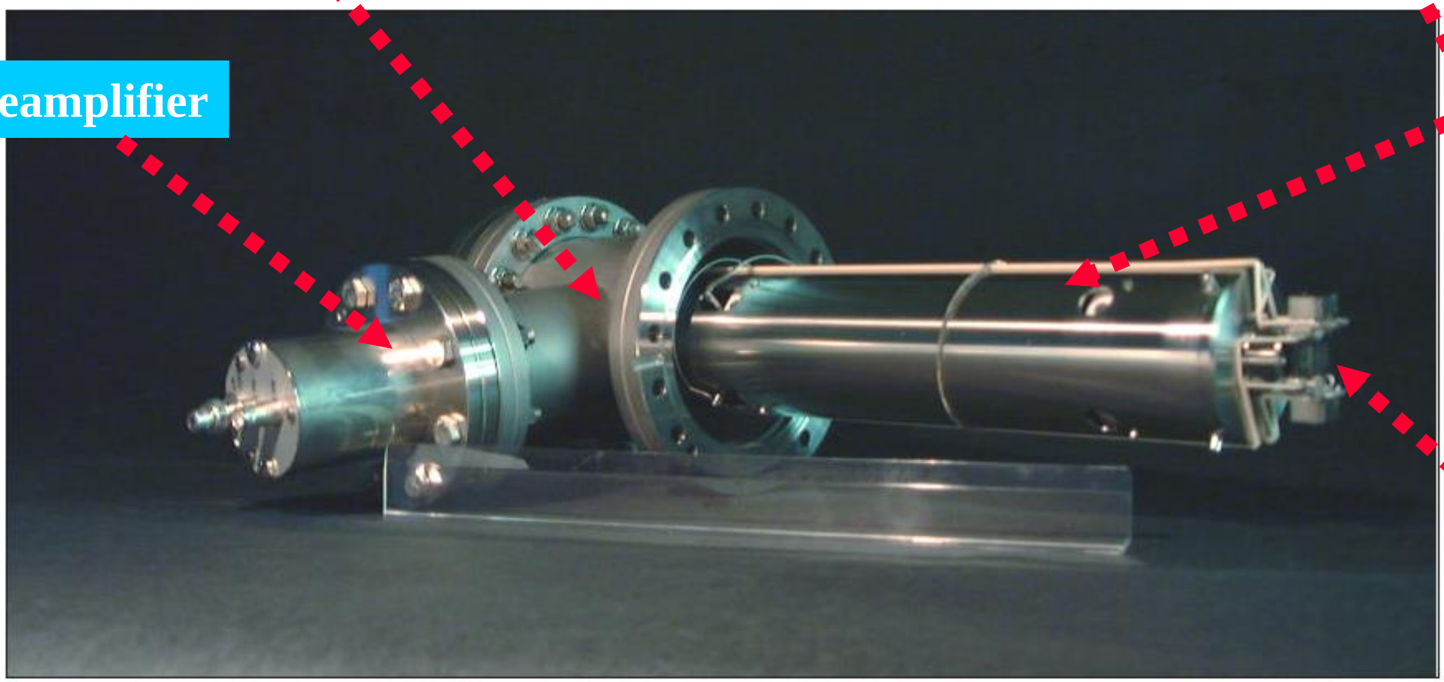

**Preamplifier**

**Cross Beam SOURCE**

# Mass spectrum

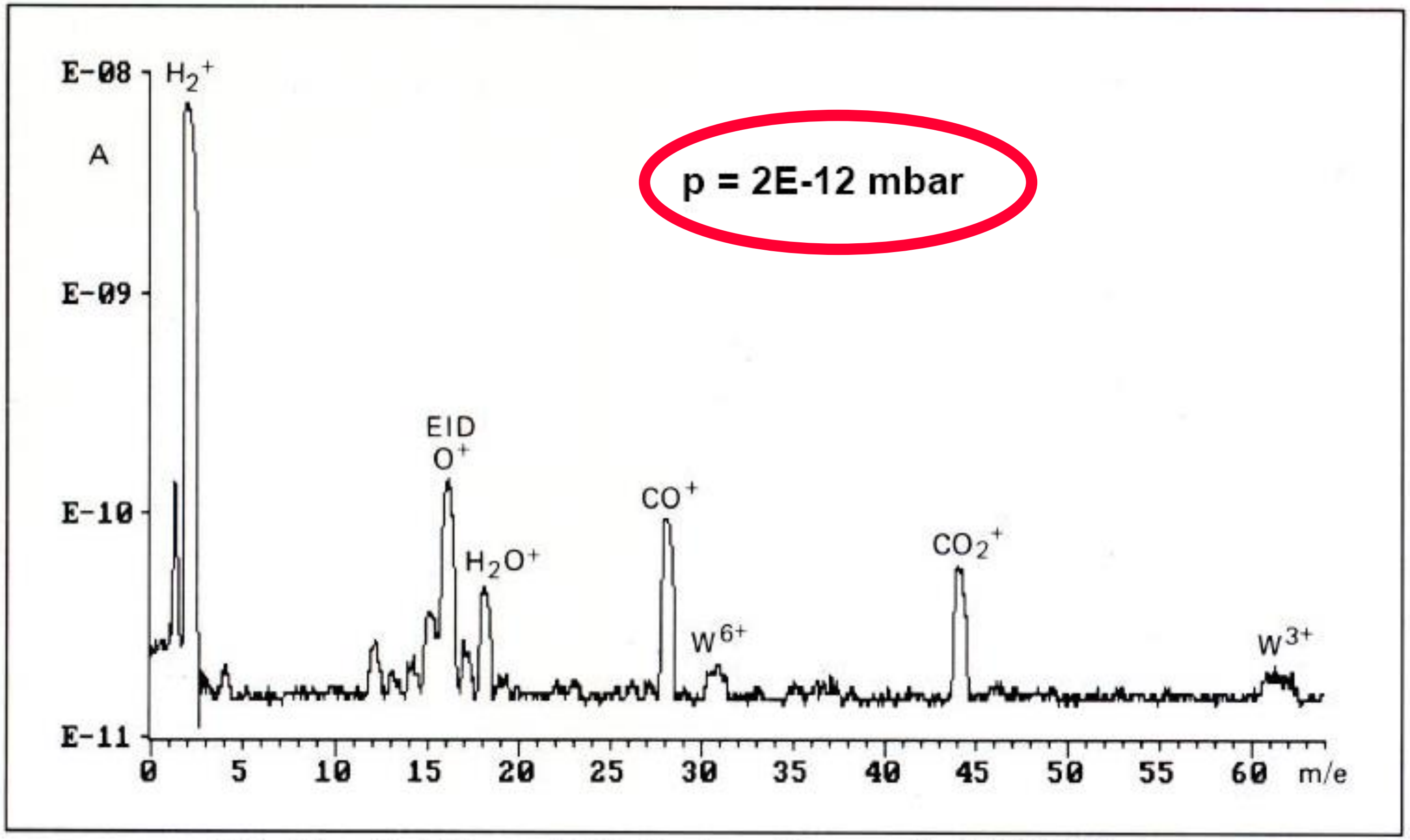


W.K. Huber, N. Müller, and G.Rettinghaus, Vacuum, 41, 2103 (1990)

Typical UHV spectrum

*E*/k←→T
1eV ~ 11 400 K
1K ~ 9x10⁻⁵eV

## Electron impact rot. vibr. exciattion/deexcitation $H_3^+$

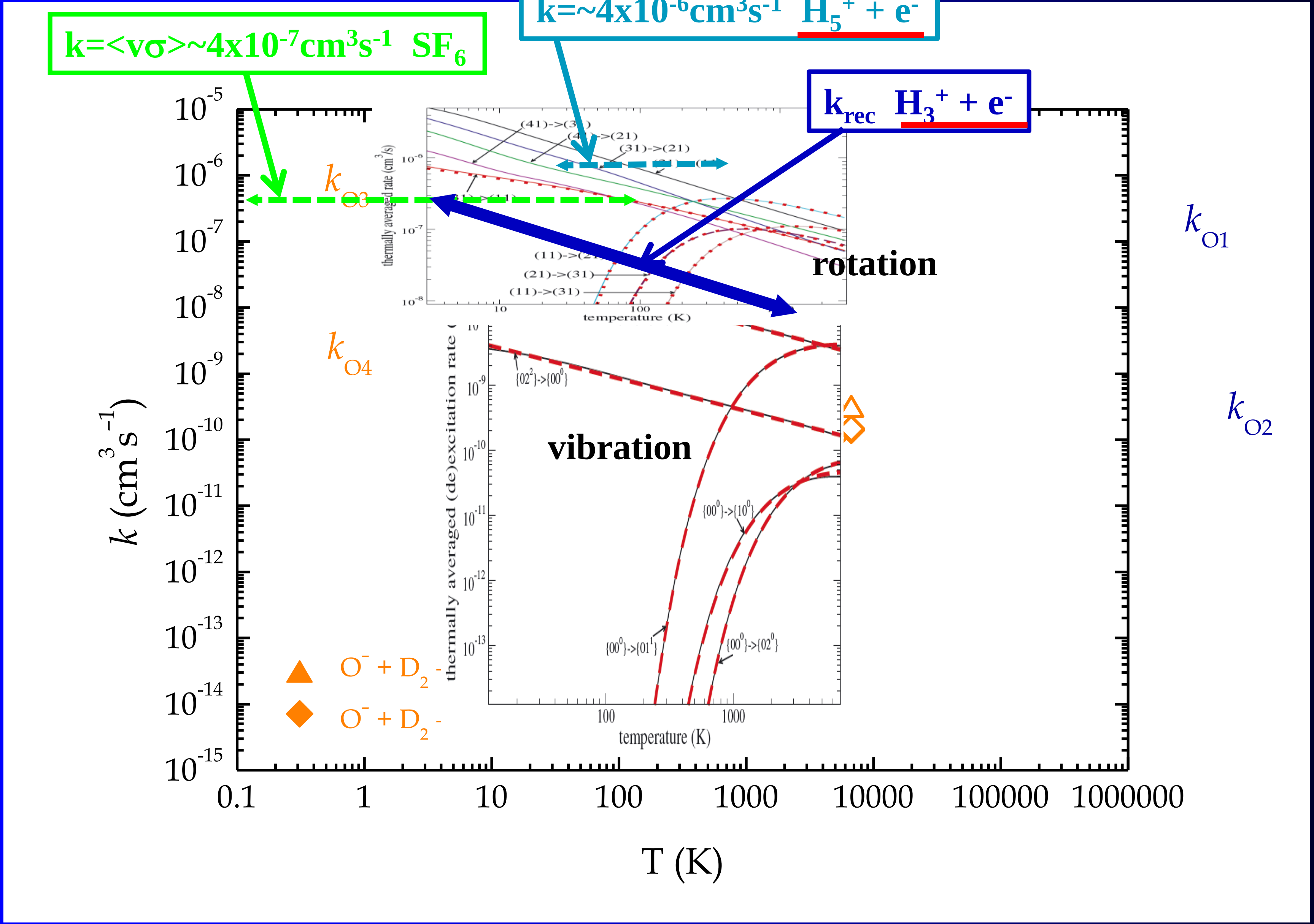

*E*/k←→T
1eV ~ 11 400 K
1K ~ $9 \times 10^{-5}$eV

# Electron impact rotational excitation of $ArH^+$

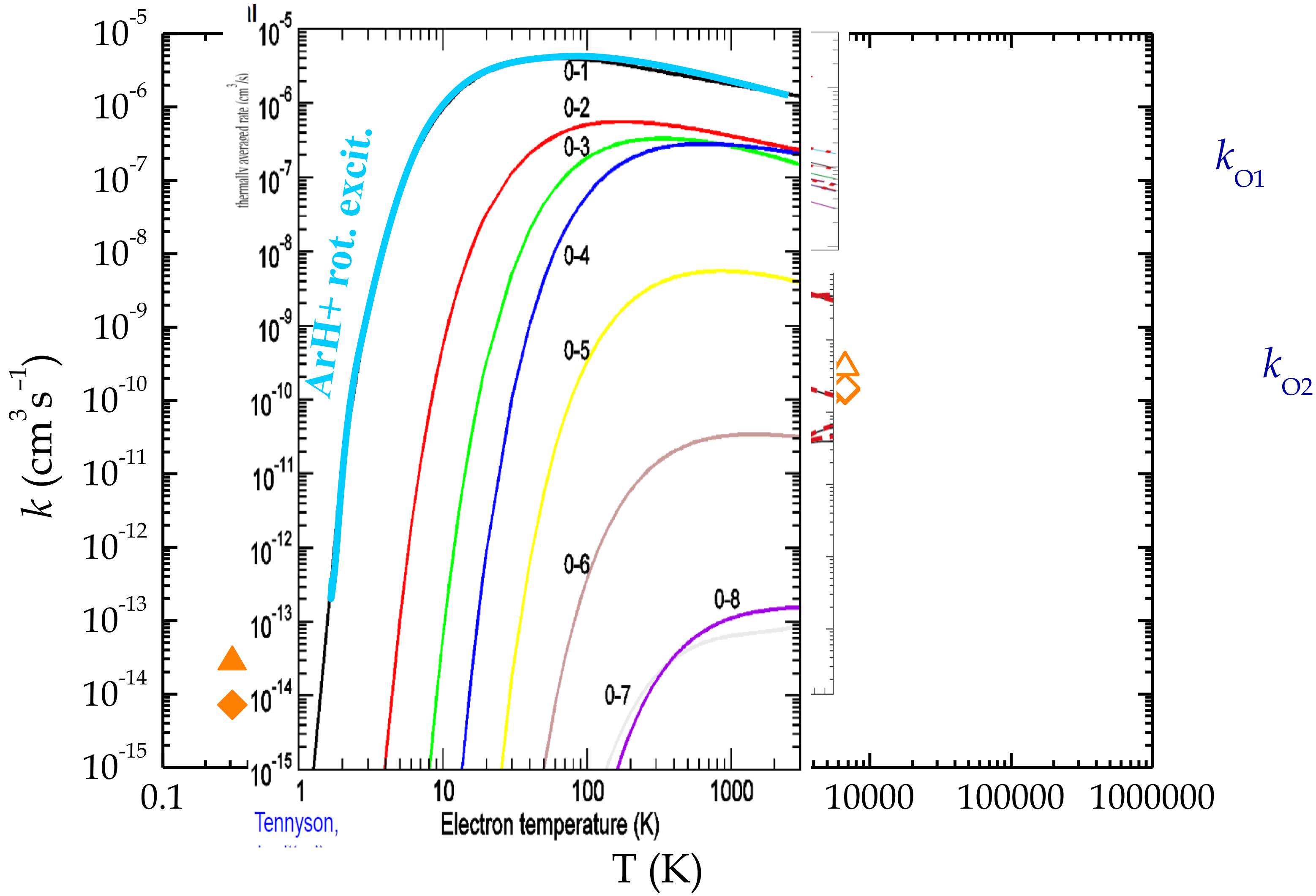

*E*/k←→T
1eV ~ 11 400 K
1K ~ 9x10$^{-5}$eV

**Electron impact rot. vibr. exciattion/deexcitation $H_3^+$**

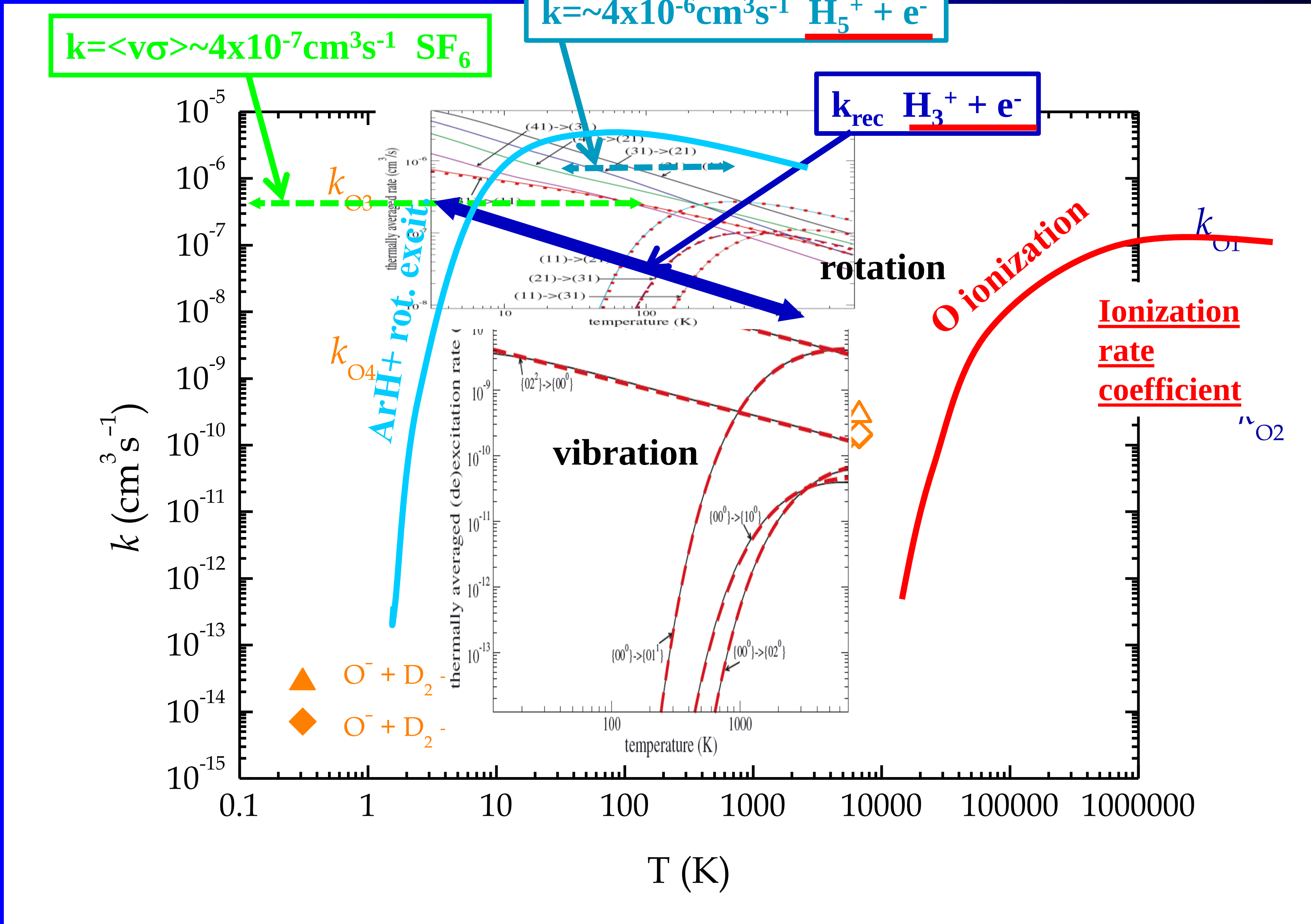

*E*/k←→T
1eV ~ 11 400 K
1K ~ 9x10$^{-5}$eV

# Electron impact rot. vibr. exciattion/deexcitation $H_3^+$

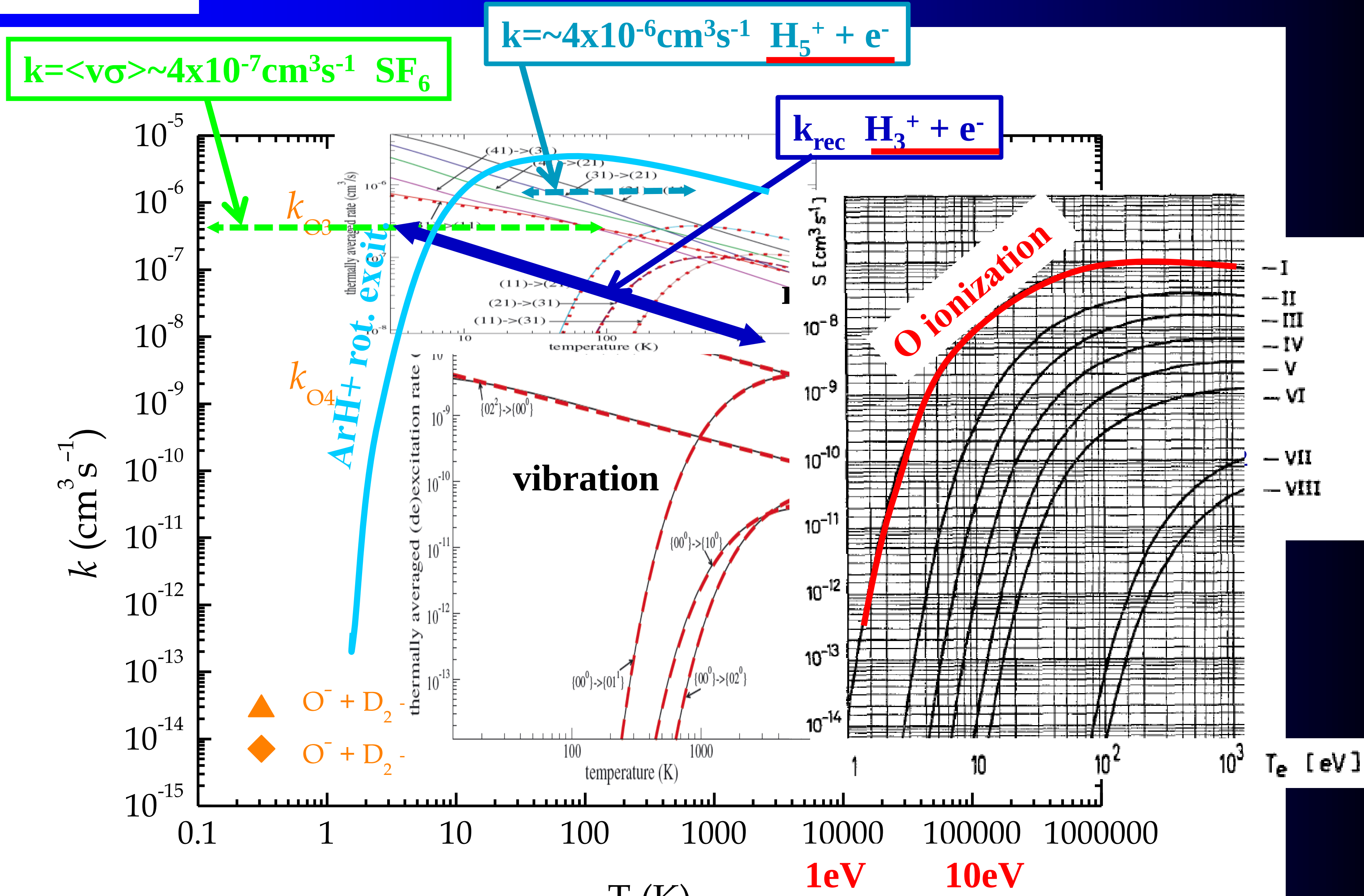


Fig. 4. Ionization rate coefficients for single ionization of oxygen atoms and ions from the ground state by electron-impact in a tenuous plasma (Maxwellian distribution, no lowering of ionization potential, no collision limit)